CZECH UNIVERSITY OF LIFE SCIENCES PRAGUE

Faculty of Tropical AgriSciences

Design and performance of a solar dryer for processing of coffee beans in Colombia

DISSERTATION THESIS

Author: Ing. et Ing. Eduardo Duque Dussán, MBA.

Department of Sustainable Technologies

Supervisor: prof. Ing. Jan Banout, Ph.D.

Co-supervisor: Ing. et Ing. Juan Rodrigo Sanz Uribe, Ph.D.

Prague, July 25th, 2023

Declaration

I hereby affirm that I have done this thesis entitled **"Design and performance of a solar dryer for processing of coffee beans in Colombia"**, except for jointly authored publications that are included. In the case of such publications, my specific contributions to each chapter have been clearly stated at their respective beginnings. Furthermore, I affirm that proper acknowledgement has been provided within this thesis for any references made to the works of others, I also ensure that this work has not been and is not being submitted for any other degree to this or any other university. All the sources have been quoted and acknowledged by means of complete references and according to Citation rules of the FTA.

In Prague July 25th, 2023.

Eduardo Duque Dussán

Acknowledgement of Funding

The research conducted was funded by project POS103010 at the National Coffee Research Center of Colombia - Cenicafé, and additionally received financial support from the IGA grants [20213101, 20223109, and 20233101] at the Faculty of Tropical AgriSciences, Czech University of Life Sciences Prague.

CZECH UNIVERSITY OF LIFE SCIENCES PRAGUE

Faculty of Tropical AgriSciences

DISSERTATION THESIS TOPIC

Author of thesis:	Ing. Eduardo Duque Dussan
Study programme:	Sustainable Rural Development
Thesis supervisor:	prof. Ing. Jan Banout, Ph.D.
Supervising department:	Department of Sustainable Technologies
Language of thesis:	English
Thesis title:	**Design and performance of a solar dryer for processing of coffee beans in Colombia**
Objectives of thesis:	The main objective of this research is to design a hybrid solar coffee drying unit for house-farm coffee growers in Colombia. The novel hybrid solar coffee dryer is expected to increase the drying efficiency compared to traditional coffee drying techniques.
Methodology:	The theoretical design is a comprehensive step that intends to have as an output, a hybrid coffee solar drying unit with all the theoretical demands to have optimal behaviour and efficiency while drying from the mathematical and physical point of view. To achieve this, the theoretical design follows the subsequent procedure. Once the foundations of the research based on the literature are settled, the CFD (Computational Fluid Dynamics) analysis of the witness dryer (Parabolic) will be done to find potential flaws or strengths in the dryer's geometry; the results will be helpful for the design of the new hybrid unit since the behaviour inside the dryer will be known. Afterwards, the ANSYS Fluent module can enter the geometry, boundary conditions and flow state information to run the simulation. During the simulation is essential to understand the relation between the described phenomena and the governing equations. The new hybrid unit will be arranged in parallel next to two typical parabolic type sun dryers, the three of them will have the same capacity and dimensions, which preliminarily will be 5 m x 2 m (length × width), at a height of ±80 cm from the floor. The drying area (10 m^2) will hold up to 140 kg of wet coffee. The assembly will be done at the National Center of Coffee Research of Colombia (CENICAFE) facilities in Chinchiná, Colombia. An expected number of 4 total experiments are intended to be executed.
The proposed extent of the thesis:	80 - 120
Keywords:	Coffea arabica L; Computational fluid dynamics; Mechanical drying; Parchment coffee; Solar drying;

Recommended information sources:

1. Burmester, K., & Eggers, R. (2010). Heat and mass transfer during the coffee drying process. J. Food Eng., 99(4), 430-436. https://doi.org/10.1016/j.jfoodeng.2009.12.021
2. Nilnont, W., Thepa, S., Janjai, S., Kasayapanand, N., Thamrongmas, C., & Bala, B. K. (2012). Finite element simulation for coffee (Coffea arabica) drying. Food Bioprod. Process., 90(2), 341-350. https://doi.org/10.1016/j.fbp.2011.06.007
3. Parra-Coronado, A., Roa-Mejía, G., & Oliveros-Tascón, C. E. (2008). SECAFÉ Parte I: Modelamiento y simulación matemática en el secado mecánico de café pergamino. Revista

Brasileira de Engenharia Agrícola e Ambiental, 12(4), 415-427. https://doi.org/10.1590/s1415-43662008000400013
4. Putranto, A., Chen, X. D., Xiao, Z., & Webley, P. A. (2011). Mathematical modeling of intermittent and convective drying of rice and coffee using the reaction engineering approach (REA). J. Food Eng., 105(4), 638-646. https://doi.org/10.1016/j.jfoodeng.2011.03.036
5. S. Phitakwinai, S. Thepa, W. Nilnont, Thin-layer drying of parchment Arabica coffee by controlling temperature and relative humidity, Food Sci. Nutr. 7 (9) (2019) 2921–2931, https://doi.org/10.1002/fsn3.1144.

Expected date:	2022/2023 (summer) - FTA - State Doctoral Examinations
Advisor of thesis:	Juan Rodrigo Sánz Uribe Ph.D.

Electronically approved: 13. 7. 2023
prof. Ing. Jan Banout, Ph.D.
Head of department

Electronically approved: 13. 7. 2023
prof. Ing. Jan Banout, Ph.D.
Chairperson of Field of Study Board

Electronically approved: 20. 7. 2023
prof. dr. ir. Patrick Van Damme
Dean

Abstract

This research aimed to provide a comprehensive set of tools to understand, simulate, predict and control the coffee drying process in different scenarios: Natural convection, forced convection and mixed. In different coffee-producing countries, the drying process poses a challenge to the coffee growers due to the complex phenomenon, considering that large amounts of water should be removed from the grain to protect it from bacteria, fungi and filamentous fungi development. However, the process must be thoroughly controlled to preserve the quality of the beans; this stands as an issue to the growers that are usually considered small because of their plot size and socio-economic conditions. In Colombia, around 96% of the 540000 coffee-growing families are considered small-scale farmers; this percentage relies mainly on sun-drying techniques to process their coffee. Nevertheless, the dependence of sun drying on the weather conditions is an issue since the harvesting times usually coincide with the rainy seasons, which are not the optimal conditions to dry coffee through natural convection due to the high ambient relative humidity and low temperatures. Therefore, mechanical dryers appeared as a solution seeing that the drying times are drastically reduced. Nonetheless, their elevated price and running costs prevent small-sized growers from acquiring these technologies. Therefore, wet coffee commercialization emerged as an answer, though the growers' selling prices dropped drastically. Hence, a solution for the coffee growers seemed to be in place, integrating the product quality of sun-dried coffee and the technologies already existing in the farms (solar parabolic and tunnel dryers) with the rapid drying dynamics of mechanical dryers: a hybrid solar dryer. However, to achieve a proper design, independent studies were carried out on natural and forced convection drying of a coffee seed to provide predictive models to stochastic processes through Finite Element Methods (FEM) on mechanical drying to obtain mathematical models that simulate and characterize deep and thin bed drying of coffee and also, the thermal and physical properties of parchment coffee of new Colombian varieties were calculated not only to sharpen the mathematical and FEM and computational fluid dynamics models but also to update the literature. With this information, a hybrid solar drying unit was designed that provides a solution to coffee growers.

Keywords: Computational fluid dynamics; Hybrid solar dryer; Parchment coffee; Solar drying; Mathematical modelling; Mechanical Drying.

Contents

List of tables

List of figures

- Figure 7. Wet processed coffee husk.

Chapter 3.

- Figure 1. Digitized geometry of the 3D scanned wet coffee grain.
- Figure 2. The effect of drying the coffee bean isothermally, as in a mechanical drying process scenario. (a) Moisture content over time in the center of the bean for three optimized mechanical drying temperatures: 40°C, 45°C, and 50°C. (b) The evolution of the diffusion coefficient as the moisture content was lost over time for the three isothermal cases. (c) The internal temperature at the center of the coffee bean.
- Figure 3. Cross sections of the coffee bean model showing the moisture concentration along the center throughout the isothermal drying process for three optimized mechanical drying temperatures: 50°C, 45°C, and 40°C.
- Figure 4. Results of a time-dependent natural convection phenomenon. (a) The moisture content in the center of the coffee bean for the dry season and wet season scenarios, where the initial moisture content of the coffee bean was again set as 53% (wb). (b) The evolution of the diffusion coefficient as the moisture content was lost over time for the two cases. (c) The internal temperature in the center of the coffee bean.
- Figure 5. Cross-sections of the coffee bean model showing the concentration of moisture content along the center throughout the natural outdoor drying process for wet season and dry season scenarios.
- Figure 6. The loss of water content and related variable behavior in the coffee bean as a result of constant natural convection. (a) The moisture content at the center of the coffee bean for the dry season and wet season scenarios, where the initial moisture content of the coffee bean was again set as 53% (wb). (b) The evolution of the diffusion coefficient as the moisture content was lost over time for the two cases. (c) The internal temperature in the center of the coffee bean.
- Figure 7. Cross-sections of the coffee bean model showing the concentration of moisture content along the center throughout the simplified outdoor drying process for wet season and dry season scenarios**.**

Chapter 4.

Chapter 5.

Chapter 6.

Introduction

Drying coffee is a complex process considering the amount of water removed from the grains. The process has been traditionally carried out using open sun drying; despite its sanitary disadvantages, its easy working principles are attractive to coffee growers. Solar dryers emerged to mitigate the issues posed by open sun drying; however, their dependence on climate conditions limits the coffee processing dynamics. Hence, mechanical dryers appeared as a solution due to their rapid processing capacity. However, their reliance on fossil fuels, risk of overheating the grain and high running costs is still a reason to consider when drying coffee.

Smallholders are the leading affected group of people due to their economic limitations; therefore, this research aimed to perform a comprehensive study of different drying processes and properties affecting it in order to provide the best available design of a hybrid solar dryer for coffee, integrating mechanical and solar drying in one unit, aiming to provide the grower with more flexibility and control to foresee the drying process to ensure the product's quality while dynamizing the moisture removal.

Solar drying technologies display a promising future for food processing and drying due to their use and transformation of sun energy, especially nowadays, with rising global warming. Efficient technologies are needed to address different postharvest processes; the transition from fossil fuels to sustainable technologies that work on a renewable energy basis is also relevant. It is also important to mention that using biomass and carbon-neutral biofuels is relevant in the above-mentioned energetic shift; therefore, the integration of both drying principles seemed to be in place, not only to help the coffee grower to increase the drying efficiency but also to offer the coffee drying technologies a carbon neutral hybrid solar drying unit which provides the tools to perform environmentally sustainable.

1. Literature Review

Sun drying has been utilized for generations, as a means to preserve food (Silva et al. 2021). This traditional method involves exposing food items to the warmth of the sun and the surrounding air effectively removing moisture and preventing spoilage (Guiné 2018). It is an employed technique for preserving foods such as fruits, vegetables, meats and even coffee beans (Hicks 2002).

Within the coffee industry sun drying is a method among coffee growers. The process begins by spreading out harvested coffee beans in layers on drying beds or patios as illustrated in Figure 1. These beans are left to bask in the sunlight for days until they reach the desired moisture level of around 10 12% (wb). One notable advantage of sun drying is its simplicity and cost effectiveness. Unlike methods that rely on machinery or specialized equipment sun drying harnesses the power of energy allowing small scale farmers to access it and reducing production costs. Besides, sun drying exhibits environmental friendliness as it relies solely on resources without the need, for fossil fuels or electricity.

Figure 1. Traditional coffee open sun drying patio (Ghosh & Venkatachalapathy 2014).

Another benefit of sun drying is its ability to enhance the flavour and aroma of coffee (Sandeep et al. 2021), since the gradual drying method allows the coffee beans to preserve their qualities resulting in an intricate and rich flavour profile (Kulapichitr et al. 2019), also, the exposure to sunlight can also add fruity or floral hints to the coffee making each cup unique and full of character (Siagian et al. 2017). Coffee enthusiasts

particularly value the attributes that come from sun-dried beans during the brewing process because of their taste (Hicks 2002).

Sun drying also grants physical control over the drying procedure, the farmers can adjust the drying duration and conditions based on their expertise and the specific characteristics of the growing coffee variety (Wahyuni et al. 2020). This adaptability allows them to achieve desired outcomes and produce high-quality coffee beans that meet the market's demands (Rueda et al. 2014). Likewise, sun drying allows farmers to monitor and sort the beans during drying ensuring quality throughout the process.

Nevertheless, sun drying does have its challenges and drawbacks, one notable downside is its reliance on weather conditions (García et al. 2014). Sun drying heavily depends on sunlight, so rainy days can significantly prolong the drying time, increasing the risk of spoilage or filamentous fungi growth (Culliao & Barcelo 2015); this poses a threat to the coffee crop in regions with weather patterns. Additionally, prolonged exposure to sunlight during the drying process can result in over drying or uneven drying of the coffee beans (Doymaz & Pala 2003), causing inconsistencies in the product, impacting its quality and flavour (Fadai et al. 2017). Coffee farmers must monitor and pay attention to ensure the beans are adequately dried without heat or prolonged exposure and avoiding crossed contamination (Rodríguez-Robles & Monroig-Saltar 2014).

Another drawback of sun drying is its susceptibility to contamination or damage from pests, insects or birds (Avelino et al. 2015; Kath et al. 2021). Without measures like nets or coverings, coffee beans become vulnerable to infestation or theft, leading to crop loss; this requires labour and resources to protect the drying coffee from threats resulting in increased production costs. Also, sun drying often takes longer than other drying methods due to their dependance on weather conditions as above mentioned (Sanghi et al. 2018; Kath et al. 2021), postharvest process and moisture content, the coffee beans can take days to weeks (Mwithiga & Kigo 2006; Duque-Dussán et al. 2022) to achieve the desired moisture content. The extended drying period impacts the production timeline, limiting the drying process and deriving the need to increase the drying area for drying beds or patios and its prediction is non reliable due to its stochastic behaviour (Richardson 1981).

Sun drying remains an adopted and spread technique for preserving food products, including coffee beans. There are benefits to sun-drying coffee, including its simplicity, cost-effectiveness, ability to enhance flavour and the physical control it allows over the drying process (Philip et al. 2022). However, there are also challenges associated with this method as susceptibility to pests, microorganism, and mycotoxin development (Culliao & Barcelo 2015), as well as longer drying times. Despite these drawbacks, sun drying continues to be a choice for coffee farmers because of its easy working setups, and quality coffee if done properly.

Due to the issues posed by open sun drying, solar drying technologies for food products emerged as a solution to the challenges displayed by drying food under the sun (Silva et al. 2021). This method uses solar energy to dry and preserve food items like fruits, vegetables, meats and coffee beans. The rise of this drying technologies is a response to the downsides associated with sun drying, although sun drying has been widely used, its effectiveness heavily relies on weather conditions as mentioned above. Solar drying involves collectors, panels, or materials concentrating, capturing, and converting solar energy into heat (Briceño-Martínez et al. 2020), which creates a proper drying environment for food products. The design of dryers allows for regulating temperature, airflow, and humidity, resulting in a more precise and efficient drying process than traditional sun drying (Silva et al. 2021; Firdissa et al. 2022).

In the context of coffee drying, solar drying brings several advantages (Duque-Dussán et al. 2022), one noteworthy benefit is the enhanced consistency and quality of the dried coffee beans since maintaining a temperature and airflow within a controlled drying environment is crucial (Banout et al. 2011). It ensures even product drying without the risk of over drying or under-drying (Tun et al. 2020; Benlioğlu et al. 2023). The most common solar dryers for coffee in Colombia are the parabolic and the tunnel dryer (Figure 2 and 3), they offer protection against elements like rain, dust, pests and insects (Oliveros-Tascón et al. 2006, 2008). Using enclosed dryers or covered drying racks shields the coffee beans from contamination, reduces the chances of spoilage and crop loss, enhancing significantly the quality and value of the dried coffee beans (Briceño-Martínez et al. 2020). Additionally, solar drying technologies gives coffee farmers to better predict the drying process even though it is still climate-dependent (Diamante & Munro 1993; Liu & Bakker-Arkema 2001), allowing them to adapt the

drying conditions according to the needs of coffee varieties and foresee an approximate drying time and quality, by adjusting factors such as drying temperature and airflow, farmers can achieve desired outcomes (Prakash & Siebenmorgen 2018; Silva et al. 2021).

Figure 2. Parabolic type dryer for coffee. (Restrepo Victoria & Burbano Jaramillo 2005).

Figure 3. Tunnel type dryer for coffee. (Oliveros-Tascón et al. 2006).

Energy efficiency is another advantage of solar drying; this method reduces dependence on energy sources like electricity or fossil fuels (Simate 2003; Udomkun et al. 2020). As a result, operating costs are minimized while decreasing the impact associated with energy consumption, also, the solar drying technologies are often built with materials that can be found on the farm (wooden) (Ramirez-Gómez et al. 2002), hence, the construction costs are reduced, aligning perfectly with practices making it a greener and environmentally friendly approach to coffee production. Nonetheless, solar drying technologies also present different downsides and challenges associated with drying. Firstly, setting up drying systems can require an upfront investment as the cost

of collectors or panels, along with the infrastructure for the dryer, may present a financial hurdle for small-scale farmers or producers with limited resources (Oliveros-Tascón et al. 2017). Additionally, the effectiveness of drying still largely relies on the availability of sunlight and other factors as air temperature and relative humidity (Duque-Dussán et al. 2022); cloudy or overcast weather impact negatively the drying efficiency, prolonging the drying time. Therefore, planning and considering climate conditions is crucial when implementing solar drying systems (Duque-Dussán et al. 2023).

Additionally, solar drying requires thorough monitoring and management, hence, farmers must understand the working principles of the technology as well as characteristics of the drying process, such as drying times, mixing patterns, moisture level tracking and storage requirements (Duque-Dussán et al. 2023), to ensure the production of high-quality coffee beans (Luna González et al. 2019). Solar drying technologies allow coffee producers to improve the drying processes and deliver top-notch coffee beans that meet market demands while embracing new practices.

Seeing the necessity to dry coffee faster, mechanical and forced convection drying occurred (Parra-Coronado et al. 2008a) and the need for a reliable and efficient drying process drove the development of machine drying technology, its use has been rising to process different agricultural products and foods (Hung et al. 2019; Gu et al. 2022). These methods provide controlled alternatives to sun and solar drying methods addressing the challenges and limitations of natural drying techniques (Philip et al. 2022). Even though mechanical drying has proven to process large amounts of coffee, offer different capacities, setups and allows for a better process control (Duque-Dussán & Banout 2022) it also presents different disadvantages in coffee drying. Mechanical drying involves using equipment such as drying chambers, conveyor dryers or fluidized bed dryers to remove moisture from food products and grains (Bakker-Arkema et al. 1974; Brooker et al. 1992; Liu & Bakker-Arkema 2001). These machines employ hot air, microwave radiation or vacuum principles to accelerate drying (Guiné 2018); unlike natural convection drying methods, mechanical drying allows for total control over drying air temperature, airflow and humidity, often including instrumentation (Banaszkiewicz et al. 1997; Oliveros-Tascón et al. 2010) leading to more efficient and predictable outcomes seeing that the mechanical drying is often considered a

deterministic process (Midilli et al. 2002; Hii et al. 2009; Prakash & Siebenmorgen 2018; Duque-Dussán & Banout 2022).

In the case of coffee drying, mechanical drying brings different advantages, one significant benefit is the reduction in drying time which helps expedite the process, reducing the drying time from 10-18 days (natural convection) (Mwithiga & Kigo 2006; Duque-Dussán et al. 2023) to few hours (Parra-Coronado et al. 2008b; Duque-Dussán & Banout 2022), boosting productivity, minimizing spoilage risk, and optimizing resource utilization. These technologies emulate the industrial coffee dryers at a smaller scale under the same working principles (Parra-Coronado et al. 2008a; Sandeep et al. 2021). The grain is usually located as a deep bed, allowing it to process a more significant amount of product. Usually, a 3-tray static vertical mechanical dryer with a capacity of 7.5 arrobas (Figure 4) processes 31.25 kg of DPC in 20-21 hours (Parra-Coronado et al. 2008a; Oliveros-Tascón et al. 2010; Coradi et al. 2014; Duque-Dussán et al. 2022); hence, in approximately 85 hours, a low-capacity mechanical dryer processes the same as one 10 m^2 tunnel dryer processes in 15 days.

Figure 4. Penagos SC Silo static mechanical coffee dryer.

Nevertheless, not only static coffee dryers are available; rotating drum and dynamic dryers are also common worldwide, however they tend to be more in the industrial because of their size, running costs and area requirements locates to be more industrial (Perazzini et al. 2021). Mechanical drying improves consistency and control

over the drying process by ensuring heat and airflow uniform distribution (Renaudo et al. 2019; Duque-Dussán & Banout 2022), preventing uneven drying. Additionally, mechanical drying protects the product to external factors that threatens its quality, reducing crop losses and guaranteeing a product of high quality (Hung et al. 2019).

Furthermore, mechanical drying enables coffee farmers to control and set the drying parameters to suit different coffee varieties, this flexibility creates opportunities for experimentation and fine-tuning, ultimately producing coffee beans with different flavour profiles and characteristics (Budiyanto et al. 2021; Tesfaye et al. 2022). Conversely, the disadvantages of mechanical drying also pose serious threats not only to the coffee grower, but also to the coffee. One significant weakness is the cost involved, drying equipment and machinery required for drying can be expensive, which might pose a barrier for small-scale coffee farmers or those with limited resources (Duque-Orrego et al. 2001; Hung et al. 2019; Duque-Dussán & Banout 2022). Additionally, it is vital to consider the maintenance expenses associated with these machines when evaluating the feasibility of mechanical drying; running costs are also a negative remark on mechanical drying, seeing that electricity and fuel is required to perform the process, not ideal for an isolated household (Hicks 2002). Also, using fossil usage (liquid petroleum gas) is not fully recommended from the environmental point of view.
Another challenge is the need for expertise and ongoing monitoring during the drying process.

Additionally, it is worth noting that mechanical drying could impact the flavour profile of coffee beans, when employing mechanical drying, the air's temperature should not surpass 50°C (Borém et al. 2008; Duque-Dussán & Banout 2022), if exceeded, there is a high chance that the embryo of the seed will die, leading to a rapid internal structure deterioration, liberating undesired compounds that compromise the coffee quality (Tarzia et al. 2010). The accelerated drying process can alter the coffee's chemical composition and aroma, resulting in an lower quality compared to beans dried using natural methods (Puerta 1999; Osorio Hernandez et al. 2018).

In summary, mechanical and machine drying technology provides controlled alternatives to drying methods for food products and grains, including coffee; they reduce the drying times, increase the processing amounts, and allow for better process

control. Nevertheless, investment cost, energy and fuel requirements and thorough process control should be considered.

Seeing the benefits of solar drying and mechanical drying *Hybrid drying* appeared as an approach that combines different drying technologies (Al-Kayiem 2016; Deeto et al. 2018), including sun, solar and mechanical drying, to enhance the drying process for food products and grains (Udomkun et al. 2020). This method has gained attention as a solution to overcome the limitations and challenges associated with drying techniques (Simate 2003; Natesan et al. 2020). The origin of hybrid drying technology derives from the realization that more than relying on one single drying method may be required to address the complexities and demands of the drying process (Duque-Dussán et al. 2023). Sun drying, although cost-effective, is heavily reliant on weather conditions and lacks control. Even though Solar drying improves control to some extent, it can be affected by days or limited sunlight. On the other hand, mechanical drying offers drying but may pose challenges regarding initial investment and potential flavour alterations.

Hybrid drying aims to optimize drying efficiency, quality and productivity by harnessing the strengths of the abovementioned drying techniques (Weigler et al. 2012; Muñoz-Neira et al. 2020). In the context of coffee drying, it displays several advantages as is the flexibility to customize the drying process according to requirements and environmental conditions (Manrique et al. 2020). Coffee farmers can utilize the advantages of sun drying during periods while incorporating mechanical drying methods during unfavorable weather conditions (Duque-Dussán et al. 2023). Furthermore, hybrid drying improves the efficiency of the drying process; using these technologies reduces the reliance on one single drying method energy, also lays a bridge between passive and active drying (Udomkun et al. 2020). Using the sun and drying taps into energy, lowering energy consumption and operational costs, mechanical drying can be employed when solar or sun drying is not feasible (nighttime), increasing productivity and reducing drying time.

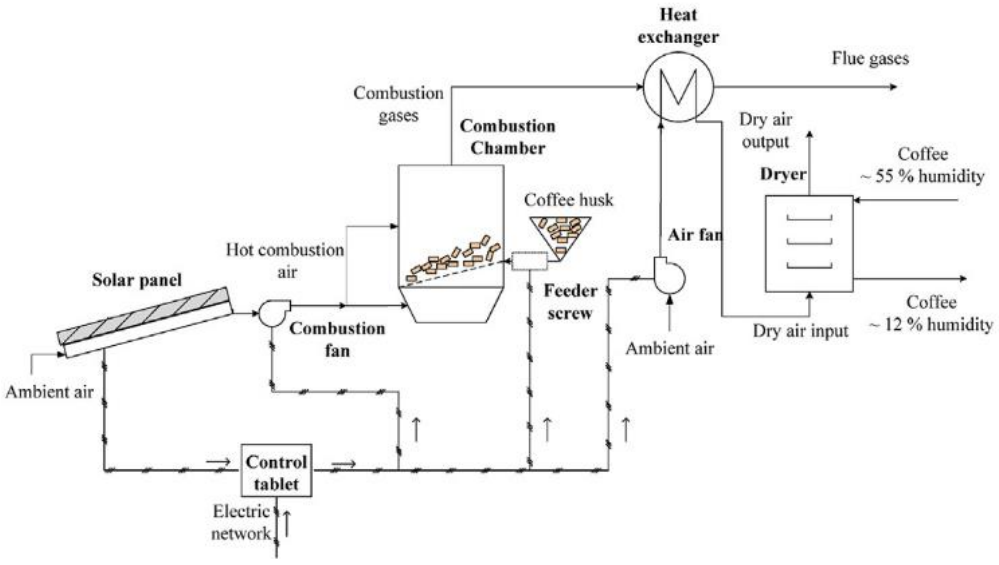

Figure 5. Hybrid dryer schematics. (Manrique et al. 2020).

In addition, hybrid drying helps minimize risks caused by different factors as do solar and mechanical dryers, but the process control allows to enhance the product's market value (Hamdani et al. 2018). One significant disadvantage of the hybrid drying is the complexity involved in implementing and managing drying systems (Kong et al. 2022), it requires an understanding of drying technologies and optimizing their use effectively. Coffee farmers or producers may need training, resources and expertise to ensure implementation (Elavarasan et al. 2017). Another issue to consider is the possibility of requiring funds for investment since hybrid drying systems involve integrating drying technologies and equipment, which can lead to high initial costs (Manrique et al. 2020; Duque-Dussán et al. 2023). Moreover, maintaining and operating hybrid drying systems can be more complex, requiring monitoring and adjustments to ensure performance.

It is crucial to consider the impact of hybrid drying on the flavour of coffee beans. The combination of drying methods and variations in drying conditions could affect the taste and aroma of the coffee product, however, in the literature there is no record on negative impact (Deeto et al. 2018; Manrique et al. 2020). Monitoring and implementing quality control measures are necessary to maintain the desired flavour profile consistently. Hybrid drying technologies offer an adaptable approach to drying food products and grains, it combines the strengths of drying methods to optimize efficiency, quality and productivity (Simate 2003). The benefits of hybrid drying include customized drying parameters, improved efficiency, risk reduction and

enhanced control (Benlioğlu et al. 2023), however, its displayed challenges must be duly addressed in order to attain its benefits. Overall hybrid drying provides an opportunity for coffee producers to achieve quality, reduce reliance on factors and optimize the drying process according to specific needs and conditions (Deeto et al. 2018; Manrique et al. 2020; Duque-Dussán et al. 2023).

Using biomass, such as coffee husks and trunks, in coffee drying processes (mechanical and hybrid) holds significant importance and benefits for coffee production (Sonthikun et al. 2016). These biomass materials provide valuable energy sources, contribute to sustainability, and offer coffee farmers and processors economic opportunities. Understanding their importance can shed light on the efficient and eco-friendly practices within the coffee industry, also it must be considered that the calorific value of these materials is high 16-20 kJ kg^{-1} (Duque-Dussán et al. 2023). Coffee husks, dry pulp, are a side product generated during coffee processing, often considered waste, discarded or left to decompose (Rodríguez Valencia et al. 2010). However, nowadays their potential as a biomass resource is recognized and used mainly in industrial dryers (Tesfaye et al. 2022).

There are advantages to using coffee husks as a biomass fuel source for drying. Firstly, they offer a renewable energy supply, they are a byproduct of coffee production, they are easily accessible (Duque-Dussán et al. 2023). It can be obtained at no cost, reducing the dependence on fuels like wood or coal for drying coffee beans (Tesfaye et al. 2022). Utilizing coffee husks as biomass helps minimize environmental impact by diverting these husks from landfills or burning them openly, coffee farmers contribute to waste reduction and to decrease air pollution (Aristizábal-Marulanda et al. 2022). The controlled combustion of coffee husks results in emissions of greenhouse gases compared to fossil fuel sources, thereby reducing the carbon footprint associated with coffee drying, as well as using carbon neutral fuels (Duque-Dussán et al. 2023).

Another type of biomass material called coffee trunks can also be repurposed of being discarded or burned. These trunks are obtained from pruning or removing branches during the maintenance or rejuvenation of coffee trees (Rendón 2021; Aguirre Cuellar et al. 2022). They can serve as a source of biomass energy. Coffee logs offer benefits to coffee husks providing a readily accessible fuel source for drying coffee.

Using biomass like coffee husks and logs also brings advantages not only to the drying process, coffee farmers and processors can generate income by selling or exchanging these biomass materials, creating revenue streams (Oliveira & Franca 2015; Tesfaye et al. 2022), improving the economic viability of coffee production, especially for small-scale farmers due to their financial limitations, and, utilizing biomass reduces the reliance on fossil fuels resulting in cost savings for coffee processors. At the same time, using biomass in coffee drying and maximizing the utilization of coffee husks and logs, the coffee industry promotes the principles of establishing an economical closed-loop system where waste materials are reused (Hamdani et al. 2018), minimizing waste generation and enhancing resource efficiency; contributing to the overall sustainability of the coffee sector.

Figure 6. Coffee trunks after pruning. Picture taken by Andrés Acosta.

An evaluated disadvantage of the biomass utilization for coffee drying is that the availability and accessibility of biomass materials may vary depending on the region where coffee is grown (Aguirre Cuellar et al. 2022), some areas may need more access to coffee husks or logs, meaning that supply of biomass materials may be required, including collection, storage and distribution infrastructure (Aristizábal-Marulanda et al. 2022). Besides, it is crucial to ensure that the equipment used for biomass combustion during drying processes is efficient and well maintained, if poorly designed or operated, biomass combustion systems can lead to burning, excessive smoke emissions and

inefficient energy usage (Hamdani et al. 2018; Manrique et al. 2020; Duque-Dussán et al. 2023). Another factor to consider is the competition for biomass resources within the community.

Figure 7. Wet processed coffee husk.

Drying coffee is extremely important for small-scale coffee farmers as it dramatically affects the quality and price and value of their product. It is a complex process, when processing coffee through the wet method (harvesting, classification, pulping, fermenting, washing, and drying), the coffee seeds hold an initial moisture content of 53% (wb) right after washing that must be reduced to the commercialization levels (equilibrium moisture content) of 10-12% (wb) (Duque-Dussán et al. 2023). The problems related to coffee drying affect many coffee growers, for instance out of the 540000 coffee growing families, 96% are classified as small-sized farmers, meaning that their plot is not bigger than 5 ha (Bravo-Monroy 2019), being 1.5 ha the average plot size (Barjolle et al. 2017). Small-sized coffee farmers rely on sun and solar drying as their primary choice to dry their coffee. However, in Colombia, the harvest peaks come together with the rain season (García et al. 2014); therefore, employing solar energy to dry coffee during this time of the year is complex due to high precipitation, high relative humidity, and cloudiness. Hence, the importance of the description of the different drying processes presented in this chapter.

In addition to preserving quality, coffee drying also plays a role in determining the value of the beans (Berhanu et al. 2014; Pires et al. 2021). The better the beans are dried, then the market price be better; the issues posed by the discussed drying techniques (mechanical, solar and hybrid) facilitated the increase of wet coffee commercialization, where the coffee grower sells its product for a significantly reduced amount of money as soon as it is washed to someone who runs a mechanical drying facility. Even though the selling price is lower, the cash flow is higher, and in rural places, this is usually weighs in more (Duque-Orrego et al. 2001). With appropriate dried coffee beans, small-scale farmers have the opportunity to sell their produce at prices leading to improved income and livelihoods. An appropriate drying process offers farmers the flexibility to handle their harvest and store their crops until they can sell them at the time (Trejos et al. 1989; Hicks 2002) in the market. This permits small-scale farmers to participate in the coffee industry without depending on intermediaries, potentially increasing their profits (Bravo-Monroy 2019).

By implementing drying techniques, farmers can enhance the unique qualities of their coffee beans as specialty coffee (Barrios-Rodríguez et al. 2021), known for its flavours and high-quality features, often leads prices in the market, improving their economic outlook.

It is crucial to prioritize the development of technology that smallholder farmers can easily access; this is essential for promoting inclusivity, increasing productivity and enhancing farmers' livelihoods in developing regions (Osorio-Arias et al. 2020; Udomkun et al. 2020). Smallholders play a role in food production and providing them with affordable and appropriate technology can have wide-ranging positive effects. Affordability is a factor in ensuring technology is accessible to smallholders and improve their acceptation (Kamal et al. 2008; Briceño-Martínez et al. 2020; Udomkun et al. 2020; Atalay et al. 2022). These farmers often need more support, limited credit options and low-profit margins. Therefore, it is vital to focus on developing cost technology within their means, seeing that making technology affordable, smallholders can embrace practices to enhance productivity and improve the quality of their products.

Accessible technology also addresses labour tasks and operational challenges faced by smallholder farmers, manual labour is often the means for activities, which can be time-consuming, physically demanding and less efficient (Avelino et al. 2015).

Smallholders can save time and effort by introducing technology that simplifies tasks like seed planting, drying, irrigation, or harvesting; this enables them to concentrate on aspects of farming and ultimately enhances productivity (Tarzia et al. 2010; Fagundes et al. 2020). Likewise, deploying technology can play a role in mitigating postharvest losses, small-scale farmers frequently need assistance storing and preserving their produce, leading to losses and diminished income. By introducing solutions such as dryers, improved storage facilities or innovative processing methods, farmers can extend the shelf life of their produce (Gutiérrez-Flórez & Copete-López 2009; Coradi et al. 2014; Oliveira & Franca 2015; Cardona et al. 2022).

2. Objectives

2.1. Main objective

Design a hybrid solar coffee drying unit for house-farm coffee growers in Colombia. The novel hybrid solar coffee dryer is expected to increase the drying efficiency compared to traditional coffee drying techniques.

2.2. Specific objectives

1. Perform a Finite Element Model that predicts natural and forced convection drying of coffee.
2. Design Computational Fluid Dynamics models that simulate the airflow distribution and behaviour of drying air in different mechanical drying applications.
3. To calculate the thermal and physical properties of newly developed coffee varieties to update not only the literature but also the thin layer and deep bed drying mathematical models.

3. Modelling of Forced and Natural Convection Drying Process of a Coffee Seed.

Adapted from: Duque-Dussán E, Villada-Dussán A, Roubík H, Banout J. Modeling of Forced and Natural Convection Drying Process of a Coffee Seed. J ASABE. 2022;65: 1061–1070. doi:10.13031/ja.15156

Abstract

Different coffee drying technologies face complex tasks in ensuring an acceptable final seed moisture content. This research performed a Finite Element Analysis (FEA) study, simulating a single coffee bean's drying process as a transient mass diffusion model under mechanical and natural convection conditions so the drying behavior and data of both case scenarios can be foreseen and controlled by a predictive Finite Element Model (FEM). A wet bean was 3D-scanned and digitized as the FEA simulation geometry; the water diffusion between the grain and the atmosphere was defined by a diffusion coefficient subject to the drying air temperature and the grain's moisture content. Three cases were studied: mechanical grain drying at three different temperatures (50, 45 and 40°C) in a forced convection environment, variable natural convection drying under environmental conditions (wet and dry season), and constant natural convection (wet and dry season) including the variation in day/night temperature and relative humidity. The results agree well with the data found in the literature, obtaining the graphical moisture distribution of the phenomena, predictive drying curves, diffusion coefficients and isotherms. Both simulated drying scenarios provide essential information for coffee growers to improve and control their drying processes, thus obtaining high-quality grains, reducing contamination by microorganisms, and ensuring their products' integrity.

Keywords: Coffee Drying; Coffea arabica; Coffee Seed; Finite Element Model; Moisture Diffusion.

3.1. Introduction

Drying is one of the most critical steps in the post-harvesting stages when processing coffee using the wet method. Once the berry has been pulped, demucilaginated and washed, it usually has a moisture content between 60-50% (wb) [1,2] and must be dried until it reaches 10-12% (wb) [3,4]. After washing, due to its high water content, the coffee grain is host to an elevated biological activity. Hence, the drying process should be performed as quickly as possible in order to reduce the probabilities of spoilage and to inhibit the development of microorganisms, bacteria, and mycotoxins within the grain [5]. As well as to preserve its characteristics so that high-quality dry parchment coffee is obtained at the end of the process [6] that meets the proper commercialization and storage requirements.

To achieve proper grain dryness, the coffee growers usually select between mechanical or sun drying methods to process their product [7]. The decision is based on the amount of coffee to be dried, the climate conditions and their economic situation. Sun drying methods are quite helpful for a reduced amount of grain to dry since it is a rather time-intensive process [8]. Therefore, several technologies have been developed to accelerate it, ranging from open sun dryers, parabolic and tunnel sun-drying technologies [9], as well as hybrid systems [3,8,10]. Sun drying also provides a cheap and environmentally friendly solution, being an attractive option for smallholders, such as the case of the 563000 Colombian coffee farming families, where 95% of them have a plot smaller than 5 ha [11]. Despite their advantages, sun drying technologies, often considered a stochastic process, face many complications due to their direct dependence on climate conditions [12] that can rapidly change over time, limiting the drying behavior predictions and control. For example, in Colombia, the harvest peak periods overlap with the wet seasons [13], depicted by high cloudiness, pluviosity, and air dampness; evidently not the best terms for sun-drying coffee.

In contrast, mechanical drying is not entirely dependent on weather conditions. Once the applied heat defines the drying air psychrometric properties to reach specific air temperature and moisture characteristics, the grain drying can be accurately predicted. Thus, mechanical coffee drying is usually defined as a deterministic process [14], and its working principles allow it to dry higher amounts of grain at a faster rate

[1,15]. Nevertheless, mechanical drying processes usually require large equipment and more complicated working setups compared to sun drying technologies [16]. Moreover, even though reduced versions of the drying silos and general mechanical dryers are available, there is still a considerable energy demand and fuel consumption to heat and blow air into the dryer. At the same time, the literature indicates that sun-dried coffee holds higher quality values than mechanical-dried one [17,18]. Therefore, a balance between drying efficiency, product quality, and energy requirements of the system should be considered before performing the process itself.

Many studies have been carried out to describe, predict, and simulate the drying process of coffee, corn, soybean, and other types of seeds using numerical methods [12,19–21]. Still, most simulation models aim to approximate the drying solution for a thin or deep bed of the product [22–24]. There are also records in the literature on the simulation of single grain and food using finite element methods [25–27], which allow for control over the occurring heat and mass transfer phenomena and predict the change in moisture and temperature over time within the geometry boundaries [28,29]. There are, however, no finite element models that include the temperature and moisture profile variation in time along with the diffusion of water behavior in a single coffee grain.

In order to preserve the quality of coffee seeds during drying, it is essential to consider the perishable nature of the coffee grain after harvesting. Identifying and understanding how moisture and temperature change within the grain structure during heat and mass transfer throughout the drying process is necessary; this is so the overall process can be clearly described. Therefore, the primary purpose of this study was to perform a set of Finite Element Method (FEM) simulations based on an actual 3D body model of a single coffee grain under mechanical and sun-drying conditions, from an initial grain moisture content of 53% (wb) until reaching 12% (wb), intending to supply both drying methods their correspondent prediction of the internal drying process of the grain under different circumstances where microorganisms and mycotoxins can grow. Thus, control measures can be applied, especially when the drying predictions are unfavorable, allowing the coffee grower to plan the drying procedures to keep the product safe, moving from a stochastic scenario to a deterministic one.

3.2. Methodology

The drying process of the coffee bean was simulated using Abaqus Finite Element Analysis (FEA) software (*Dassault Systemes*) as a transient mass diffusion model. While wet, a real coffee grain (*Coffea arabica L.*) was 3-D scanned and digitized. The resulting CAD file was used as the basis for the Finite Element Model (FEM), the orthogonal dimensions (length L = 0.0117 m, width W = 0.0081 m and thickness S = 0.0050 m) of the grain agree accurately with those previously calculated and published in the literature for such specie [30,31].

The diffusion of water molecules through the coffee bean and into the environment was incorporated into the FEM by defining the drying coffee bean's temperature and humidity-dependent diffusion coefficient. Beginning with a definition for normalized mass concentration of water *M*:

$$M = \frac{c}{s} \tag{1}$$

where *c* is the mass concentration and s is the solubility. A mass balance to steady state yields the chemical potential equation:

$$\vec{J} = -s\vec{D} \cdot \left[\frac{\partial M}{\partial \vec{x}} + k_s \frac{\partial}{\partial \vec{x}}\left(ln(T - T^z)\right) + k_p \frac{\partial p}{\partial x}\right] \tag{2}$$

where *J* is the concentration flux vector, *D* is the diffusivity vector, k_s is a temperature-dependent diffusion constant, k_p is a pressure-dependent diffusion constant, *T* is the temperature (*z* denotes the temperature at absolute zero), and *p* is the pressure stress, which is defined as one third of the negative trace of the normal stresses. The relationship between concentration flux and diffusion is also conveniently provided by Fick's first law of diffusion [22,32]:

$$\vec{J} = -\vec{D} \cdot \frac{dc}{d\vec{x}} \tag{3}$$

where c is the mass concentration. Putting together equations (1), (2) and (3), and making the generalized assumption that solubility is equal to unity and that the material is isotropic, having the same boundary conditions in all directions, yields a specific case of the diffusion equation for a grain of coffee with an initial moisture less than or equal to ~50% (wb) [1,33] defined as:

$$D = (4.1582 \times 10^{-8}) e^{\left[(0.1346T + 2.2055)M - \frac{1184}{T + 273.15}\right]}$$

(4)

The evolution of the water diffusion process in the FEM is thus simplified to be a function of the temperature and mass concentration of water throughout the body of the coffee bean as indicated by [34], it is assumed that they are initially homogeneously distributed. This diffusion relationship was defined as a heat transfer material property for the coffee bean, along with its density, which is also a factor of the mass concentration of water M and provided by [1] and [33] as:

$$\rho = 365.884 + 2.707M$$

(5)

To simplify the analysis, the volumetric shrinking of the coffee bean as it loses water content was not considered. The initial temperature was based on the different analysis cases, and the initial mass concentration of water was defined as 53% (wb) (but input into Abaqus as parts per million). Boundary conditions were defined solely as temperature-dependent convective heat transfer, with a general grain heat transfer coefficient based on [14] defined as follows:

$$h = AC_a G_a \left(\frac{2r_0 G_a}{C + DT}\right)^B$$

(6)

Where A = 0.2755, B = -0.34, C = 0.06175, D = 0.000165 are constants that were fitted to the grain drying models; C_a is the specific heat of air, defined as approximately 1005 J kg^{-1} K^{-1} for the temperature range of interest; G_a is the mass

transfer per unit area per time, set as 0.63 kg s^{-1} m^{-2}; and r_0 is the longest dimension of the wet coffee bean, simplified as 0.02 m. This empirical equation (6) for the heat transfer coefficient of forced convection was created using nonlinear regressions to fit experimental data and corresponds to an air velocity of 10 m s^{-1}. The natural convection heat transfer coefficient corresponds to air velocities of 1 m s^{-1}. For all cases, the coffee seed was assumed to be exposed to equal convective boundary conditions on all surfaces as if resting on a fine mesh surface, diffusing homogeneously in all directions. For the idealized case of a single seed drying, this restriction allows for a study of the direct effects of air temperature, surrounding humidity, and solar radiation without the introduction of such variables as the packed location of the coffee bean among others or the temperature and material properties of the surface on which the seed lies. The heat transfer coefficient values used for the study are shown in Table 1.

Table 1. Convective heat transfer coefficients and air temperature. DS: Dry season, WS: Wet season.

Case		Convective heat transfer coefficient [W m^{-2} K^{-1}]	Air Temperature [°C]
Forced convection		292.33	50
		291.62	45
		290.90	40
Natural convection (fluctuating)	DS (day)	218.90	21.5
	DS (night)	18.50	18.5
	WS (day)	220.02	20
	WS (night)	16.00	16
Natural convection (constant)	DS	120.11	21.5
	WS	119.68	20

Mechanical drying simulations were performed at three different air temperatures 50, 45, and 40°C with a relative humidity of 16.88, 21.75 and 28.28% respectively in a forced convection scenario. The weather data was taken from the records of the municipality of Chinchiná, Caldas Colombia (4.9827° N, 75.6053° W; 1382 m.a.s.l.), considering that it is located in the coffee producing region of Colombia, the so-called coffee axis, and its meteorological conditions are registered in full by the Colombian National Coffee Research Centre. In the case of evolving day and night

cycles, the heat transfer coefficient and temperature were alternated using a simplified step-shaped amplitude between their respective values every 12 hours.

To simulate the outdoor sun-drying process, which is still very prevalent in coffee-growing regions, the effects of sunlight and relative ambient humidity have been included into the model to understand their effect on the time it takes the coffee bean to reach the required internal moisture. A time-dependent natural convection heat transfer coefficient was used instead of a constant forced convection coefficient in order to model the effect of sunlight throughout the 12-hour day and 12-hour night cycle. The equation for the altered heat transfer coefficient was the same as in (6) but also included a constant solar radiation term indicating the average flux of radiation from the Sun that reaches the Earth [35]:

$$h_{radiation} = \frac{flux \odot}{area \oplus} = \frac{3.6 \times 10^{26}\ W}{4\pi(149 \times 10^{9} m)^2} = 1290\ W\, m^{-2} K^{-1} \quad (7)$$

The radiation heat transfer of the coffee bean itself and of whatever surface it may be drying upon are important factors to consider for applications of this model to coffee drying techniques in the field, but these variables were not included in this model in order to focus on the effects of introducing the sun-drying process. For the relatively low temperatures and wind speeds being studied in this scenario, the heat transfer radiation from the Sun was modeled to be the primary mode of energy transfer.

The scanned coffee bean was meshed into approximately 340000 tetrahedral elements throughout its entire volume, following the resolution dimensions of the 3D scan, and is shown in Figure 1. Because the FEA elements had a pre-existing geometrical relationship with the scanned model, the skewness of the mesh was on the order of 0.2 with negligible non-orthogonality. The elements were defined as standard linear heat transfer elements for the simulation.

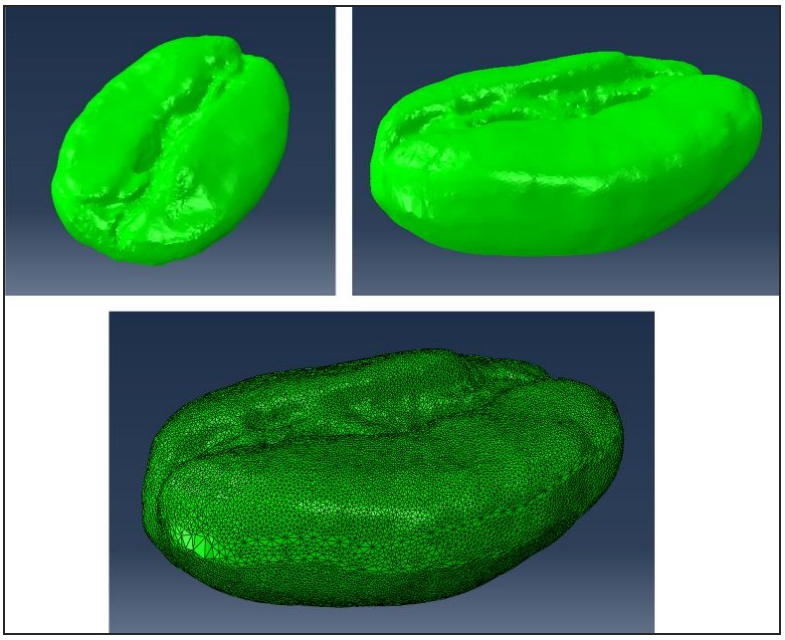

Figure 1. Digitized geometry of the 3D scanned wet coffee grain.

3.3. Results and Discussion

The primary range of moisture that was studied was the average percentage of water content of coffee beans after washing and draining approximately 53% (wb) to the requisite moisture content of the beans to be hulled, shipped, and roasted just about 12% (wb). The effects of forced convection at specific temperatures in a mechanical process dryer were compared, as well as the effects of temperature and environmental humidity for outdoor drying. The temperature profile of a coffee bean as it dries can also be extracted from the simulation's results. The effects of sunlight and environmental humidity were incorporated into the model by altering the heat transfer convection coefficient, and the effects of temperature and the internal moisture content of the coffee bean were incorporated by altering the bulk diffusivity of the material [36].

The effect of drying the coffee bean isothermally is shown as the moisture concentration in the center of the bean over time in Figure 2a for three optimized mechanical drying temperatures: 40, 45, and 50°C. A constant heat transfer convection coefficient was used to model the forced drying process, meaning that the effects of wind and sunlight are not factored into the time it takes the coffee bean to reach an adequate level of internal moisture for shipping and roasting. At a constant 40°C, it

takes about 29 hours for the bean to reach ~12% (wb) moisture, beginning at 53% (wb). This same process takes approximately 26 hours at 45°C and nearly 23 hours at 50°C, however, it is important to mention that drying at 50°C and above could damage the seed's endosperm, threatening its structure during the storage period [37]. The results of the various simulations agree well with the experimental values found in the literature.

The evaluated behavior of the mechanical drying time at the three different temperatures displayed a substantial similarity to the data published [26,38]; a few minutes differ from the findings at the same temperatures. However, it is essential to mention that the simulation conditions are idealized, and although the process can be considered deterministic, the initial conditions, such as relative humidity, height above sea level, and others, as explained by [39], play a relevant role in the drying process, as well as the airflow and air resistance of the parchment [40]. For the given temperatures, [2,8,41] also achieved similar drying times; nevertheless, the available records are generally for a thin layer or a deep grain bed.

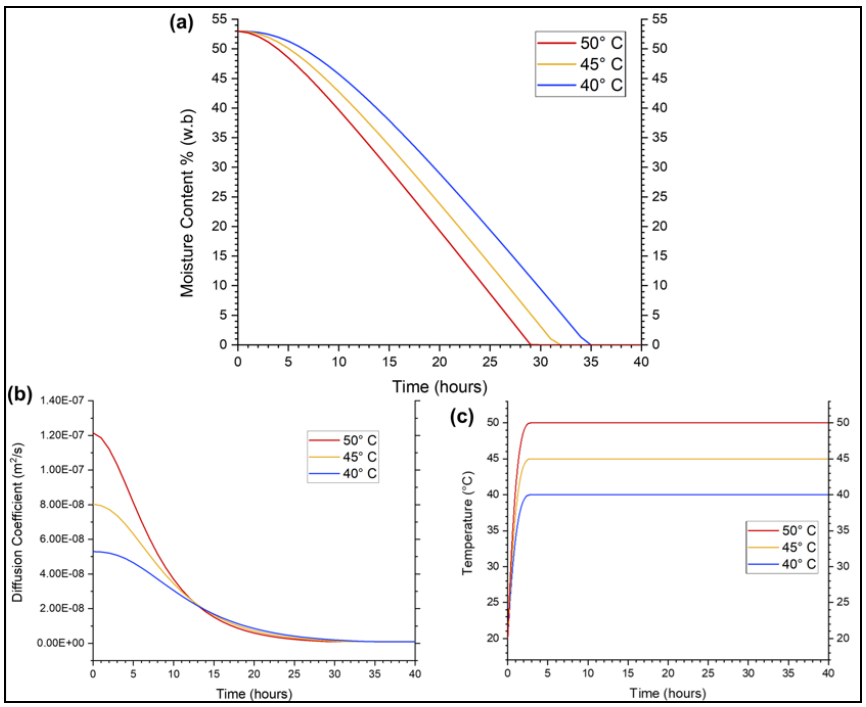

Figure 2. The effect of drying the coffee bean isothermally, as in a mechanical drying process scenario. (a) Moisture content over time in the center of the bean for three optimized mechanical drying temperatures: 40°C, 45°C, and 50°C. (b) The evolution of the diffusion coefficient as the moisture content was lost over time for the three isothermal cases. (c) The internal temperature at the center of the coffee bean.

The evolution of the diffusion coefficient as moisture was lost over time for these three isothermal cases is shown in Figure 2b, after 13 hours of drying, the lines overlap and change positions, reflecting that water is being removed, and seeing that the diffusion coefficient depends on the moisture content of the grain and drying air temperature (Equation 4), a higher diffusion coefficient is expected at high drying temperatures. However, the rapid diffusion of water will also lower the diffusion coefficient tending to steadiness which happens after 15 hours; therefore, the recorded depiction is logical and expected, sharing a similar behavior with the results pronounced by [26]. The internal temperature in the center of the coffee bean reached the drying temperature in less than three hours for the isothermal models, as shown in Figure 2c. The cross-sections of the coffee bean model depict the moisture concentration in parts per million of water throughout the isothermal drying process shown in Figure 3. Although a similar moisture distribution is observed, it is evident that moisture diffusion occurs faster at higher temperatures. Water removal occurs radially, considering that the bean has an approximate ellipsoidal shape. Nevertheless, it is not a regular geometry; hence, an asymmetric moisture distribution is seen when drying at lower temperatures (40°C) for 5 h.

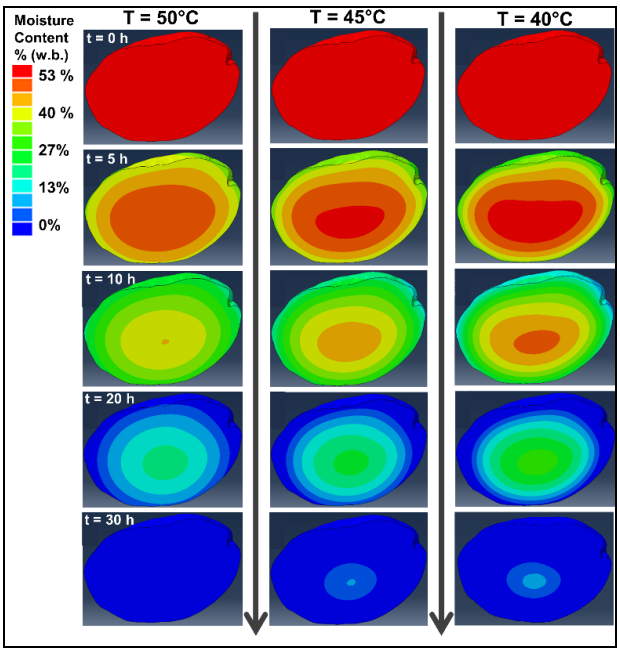

Figure 3. Cross sections of the coffee bean model showing the moisture concentration along the center throughout the isothermal drying process for three optimized mechanical drying temperatures: 50°C, 45°C, and 40°C.

Figure 4a shows the drying process of the coffee bean under forced conditions, again with an initial humidity of 53% (wb), for a "dry season" scenario, during which the ambient temperature was assumed to be constant at 21.5°C during the day and 18.5°C at night, with relative humidity during the day and during the night of 74.5% and 76%, respectively. The same situation occurred for the "wet season" scenario during which the ambient temperature was assumed to be constant at 20°C during the day and 16°C at night, with relative humidity during the day and night of 80.5% and 83%, respectively. The natural convection coefficient also changed according to the average number of daylight hours during this region's wet and dry seasons, simplified as 12 hours of daytime and 12 hours of night-time for both cases as the region in question lies near the Earth's equator.

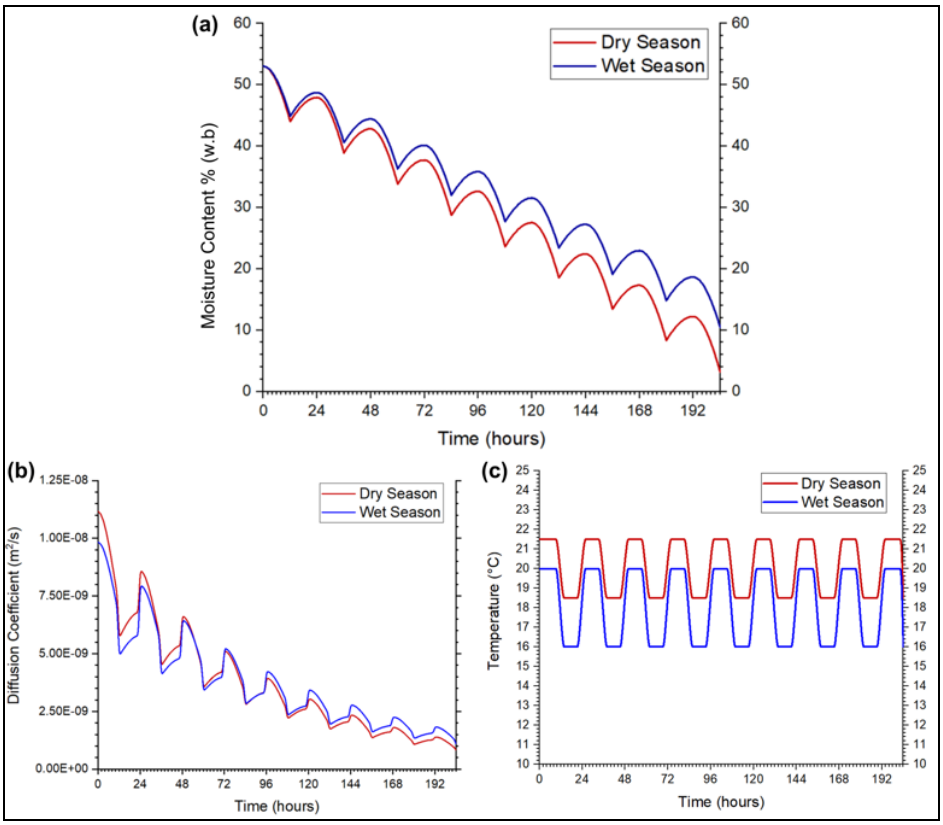

Figure 4. Results of a time-dependent natural convection phenomenon. (a) The moisture content in the center of the coffee bean for the dry season and wet season scenarios, where the initial moisture content of the coffee bean was again set as 53% (wb). (b) The evolution of the diffusion coefficient as the moisture content was lost over time for the two cases. (c) The internal temperature in the center of the coffee bean.

When including the fluctuation between day and night convection, temperature, and relative humidity for both dry and wet seasons, it is seen that humidification occurs during the night due to the temperature and relative humidity change, such as in Figure 4a. This phenomenon is explained by [42], yet it should occur at a lower rate in the field, seeing that the simulation conditions are ideal and the seed hardening that occurs when drying, as described by [43], is not considered. Given that the weather fluctuations variate enormously over time, obtaining a general predictive model for every natural convection case is nearly impossible [44]. However, the obtained drying time (Figure 4a) is within the standard drying time for natural convection and open-sun coffee drying as reported by [45], validating the accuracy of the model.

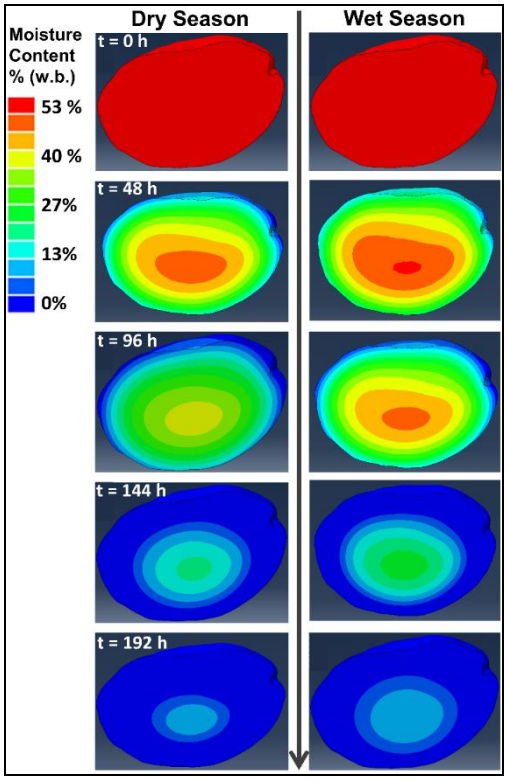

Figure 5. Cross-sections of the coffee bean model showing the concentration of moisture content along the center throughout the natural outdoor drying process for wet season and dry season scenarios.

The change of the diffusion coefficient throughout this cycle is shown in Figure 4b which displays a more complicated behavior, the valley-peak conduct occurs due to the fluctuation of temperature and humidity included in the model. It is also seen that after 84 hours of drying, the lines shift their position as expected due to the decrease in moisture within the grain domain as explained in Figure 2b. The humidification

happening during night-time also momentarily raises the diffusion coefficient because of its dependence on moisture content. The internal temperature change at the center of the coffee bean is exhibited in Figure 4c is also marked by the fluctuation. The cross sections of the coffee bean model depict the moisture concentration in parts per million of water throughout the outdoor drying process in 12-hour cycles in Figure 5, the moisture removal is shown to occur similarly to the one displayed in Figure 3, but it happens slower due to the lower drying temperatures and their oscillation along with the relative humidity. This process is shown to be far more time-intensive than its forced convection counterpart due to a fluctuating humidity gain during the night-time hours. On average, it takes a coffee bean approximately 7 days to reach the desired humidity during the dry season and 8 days during the more humid wet season under the described conditions.

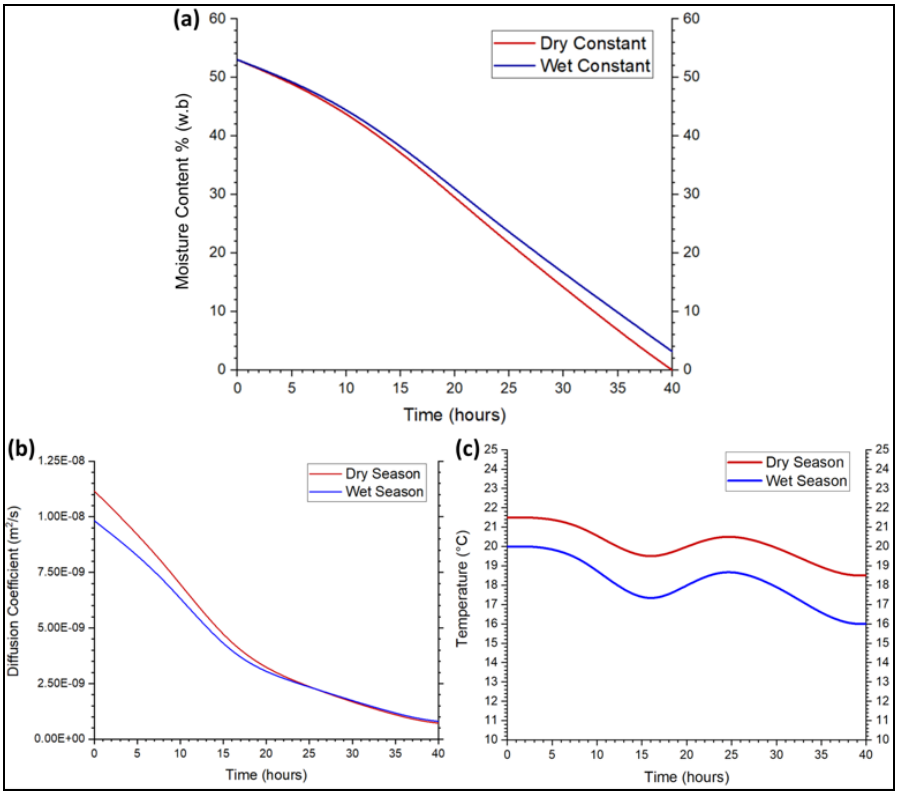

Figure 6. The loss of water content and related variable behavior in the coffee bean as a result of constant natural convection. (a) The moisture content at the center of the coffee bean for the dry season and wet season scenarios, where the initial moisture content of the coffee bean was again set as 53% (wb). (b) The evolution of the diffusion coefficient as the moisture content was lost over time for the two cases. (c) The internal temperature in the center of the coffee bean.

The loss of water content throughout the coffee bean due to constant natural convection is shown in Figure 6a. The aforementioned wet or dry season ambient humidity and temperature are implemented throughout the drying process in this scenario, but all other factors are neglected. The evolution of the diffusion coefficient during this process is illustrated in Figure 6b, unsurprisingly, the constant natural convection affects the diffusion coefficient, as seen, noticing that the line is smoother than when the effects of the sun and rain are introduced. 26 hours after starting the process, the line overlapping occurs, following each other closely until the end of the process. The internal temperature change in the center of the coffee bean is shown in Figure 6c.

The cross sections of the coffee bean model display the moisture concentration in parts per million of water throughout the simplified outdoor drying process in Figure 7, where a similar situation to the one shown in Figure 3 and Figure 5 is seen, uneven moisture removal happens but still keeping a dependence on the shape of the grain. This situation would relate, for example, to drying the coffee beans outdoors but covered from the effects of both rain and sunshine with a tarp. This is another common means through which people in coffee-growing regions dry their product; also, the so-called hybrid solar dryers could be described likewise since they can operate at certain constant temperatures [3,8]. As shown in the figures, this approach to drying coffee is less efficient than mechanically drying the grain but can be significantly faster than allowing the beans to be fully exposed to the elements. For this model, a bean could reach a moisture content of 12% (wb) in 31 hours during the dry season and 34 hours when it would rain more.

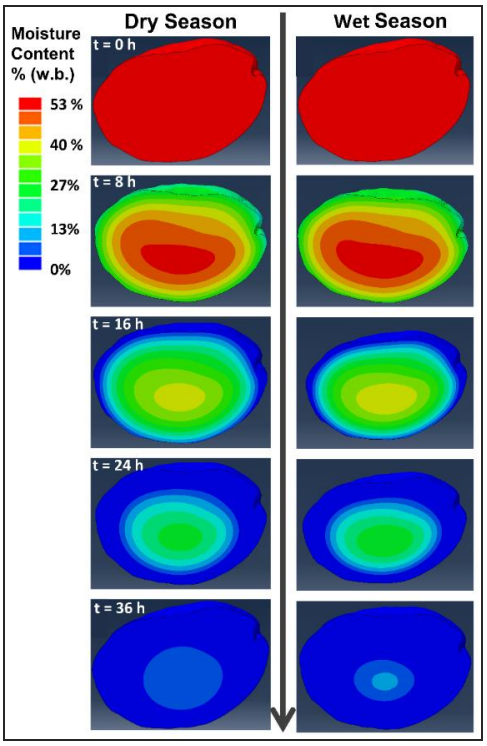

Figure 7. Cross-sections of the coffee bean model showing the concentration of moisture content along the center throughout the simplified outdoor drying process for wet season and dry season scenarios.

Figures 3, 5 and 7 illustrate the water distribution inside the coffee grain during the drying process at different moments. The moisture concentration is represented by the different colors shown in the figures. The kernel initially has a moisture content of 53% (wb) throughout all its domain, and it is pictured how the distribution changes over time as a result of the water diffusion. These images provide relevant information about the problematic points inside the grain, from which the water is more difficult to remove, generating zones vulnerable to contamination [46]. Once revealed and established, these can be further analyzed to ensure a proper grain moisture content. The change over time in the moisture distribution is similar in all simulations; still, when drying by natural convection, the moisture profiles denote higher contours, which means that the moisture removal occurs slower, hence, extra care should be taken when using these drying methods to preserve the grain quality.

Although the diffusion coefficient curves were quite different between the simulations performed due to the different model parameters, the interval of values obtained varying between 1.20×10^{-7} to 1.0×10^{-9} m^2 s^{-1} match adequately with the results achieved by [24]. Additionally, the diffusion coefficients at the desired moisture

contents fit within the diffusivity values of different crops [47]. Also, the diffusion coefficient of all simulations is greatly affected by the material assumptions and inner structure definitions [27,48], nevertheless all the simulations showed a similar behaviour occurring at different rates.

The temperature in the centre of the grain widely varied depending on the temperature of the drying air and the simulation boundary conditions. A homogeneous internal grain temperature is reached 3 hours after starting the process during mechanical drying. The internal temperature at the drying air temperature is maintained afterwards for all the three evaluated temperatures until the end of the drying process, as seen in Figure 2c. [27] shared analogous results when simulating the drying process of a corn kernel. For these simplified cases, it was assumed that the grain had isotropic material properties, so, in reality, a slightly different behaviour should occur [49,50]. Figure 4c exhibits the same behaviour, but the process includes the relative humidity and temperature fluctuation, as well as the convection boundary condition, which changes throughout the day and night, resulting in a steady-decrease and steady-rise curve description. The inner temperature of the grain is held during the day and the night for 10 hours, and the escalation or decrease of the temperature occurs in 2 hours.

Examining the drying simulations at constant natural convection without including any convection fluctuation shows a drying rate that is faster than expected. Even as the internal temperature oscillates slightly, the effects due to the convection boundary conditions dominate the drying process, as was seen for the other results. The drying time performance shows a similarity to the conduct shared by [1]. However, the situation above-mentioned applies again; under the given conditions, the simulation displayed reliable results, yet it must be highlighted that natural convection drying usually operates with varying conditions. Consequently, a slight difference would be expected in reality.

Although the model agrees with previous experimental and numerical measurements, the use of idealized boundary conditions and the omission of volumetric shrinkage [26,51,52] due to water loss limit the application of the model in certain circumstances. The most significant factor that contributes to variability is the heat

transfer convection coefficient at the edge of the coffee bean, which is highly dependent on environmental conditions.

3.4. Conclusions

Much of the world's coffee is grown on small farms by people with limited means, so the approach of using natural convection to dry coffee beans remains relevant. A model that depicts and predicts this process can be used to help optimize it. The finite element model from this work can be used to simulate the drying characteristics of parchment coffee and for the optimal design of parchment coffee dryers. Furthermore, the model provides a better understanding of the transport processes in the different components of the parchment coffee and the areas of moisture concentration where the growth of microorganisms, mycotoxins, bacteria, or moulds is a concern. Studying the phenomenon at the level of a single grain provides new insight into the specific processes and effects of forced and natural convection drying methods and even estimate the lead times on production from harvesting to shipping.

It is evident from the results that the convection and the radiation heat transfer boundary condition is the most critical determinant of how long the coffee will take to dry, thus putting its optimization (through increasing airflow and surface area) at the forefront of maximizing efficiency. Variables such as the proximity between beans, the amount and intensity of sunshine or wind, and the humidification effects of rain will play a significant role in the drying process and continue to be a concern for small-scale growers. The trade-off between pre-emptively covering the beans from the rain and the resulting loss of direct sunshine, for example, would have to be modelled on a case-by-case basis.

Prospective simulations could also introduce more minor scale fluctuations in the heat transfer coefficient to model these phenomena, but these would necessarily be averaged local experimental values at best and beyond the scope of this study. Future iterations of the model could incorporate multiple coffee beans in different stacked patterns to predict shelf time as a factor of coffee volume and have broader applications for real-world drying processes or even adapted to another food materials.

Acknowledgments

The authors would like to thank Dr. Jianliang Xiao, Associate Professor in the Mechanical Engineering Department of the University of Colorado, Boulder, for his ongoing guidance and support during the development of this study. This research was funded by the Internal Grant Agency of the Faculty of Tropical AgriSciences, Czech University of Life Sciences Prague, Grant number 20213101.

Contribution Statement

Eduardo Duque-Dussán: Conceptualization, Investigation, Methodology, Software, Writing – original draft. **Andres Villada-Dussán:** Data curation, Methodology, Software, Formal analysis. **Hynek Roubík:** Writing-Review, Conceptualization. **Jan Banout:** Conceptualization, Supervision, Writing-review & editing, Funding acquisition.

List of Symbols and Abbreviations

Symbol/Abbreviation	Meaning	Unit
C_a	Air specific heat	J kg^{-1} K^{-1}
D	Diffusivity	m^2 s^{-1}
FEA	Finite Element Analysis	-
FEM	Finite Element Method	-
G_a	Mass transfer per unit area per time	kg s^{-1} m^{-2}
h	Convective heat transfer coefficient	W m^{-2} K^{-1}
$h_{radiation}$	solar radiation term	W m^{-2} K^{-1}
L	Grain length	m
m.a.s.l	Meters above sea level	m
R_0	Largest grain orthogonal dimension	m
ρ	Kernel density	kg m^3
S	Grain thickness	m
T	Temperature	°C
W	Grain width	m
(wb)	Wet basis moisture content	%

References

1. Parra-Coronado A, Roa-Mejía G, Oliveros-Tascón CE. SECAFÉ Parte I: modelamiento y simulación matemática en el secado mecánico de café pergamino. Rev Bras Eng Agrícola e Ambient. 2008;12: 415–427. doi:10.1590/s1415-43662008000400013

2. Sfredo MA, Finzer JRD, Limaverde JR. Heat and mass transfer in coffee fruits drying. J Food Eng. 2005;70: 15–25. doi:10.1016/j.jfoodeng.2004.09.008

3. Manrique R, Vásquez D, Chejne F, Pinzón A. Energy analysis of a proposed hybrid solar–biomass coffee bean drying system. Energy. 2020;202: 1–8. doi:10.1016/j.energy.2020.117720

4. Rodríguez-Robles F, Monroig-Saltar F. Parametric Thermodynamic Models of Parchment Coffee Beans during HARC2S Dehydration. J Food Process Technol. 2014;05: 1–7. doi:10.4172/2157-7110.1000322

5. Batista LR, Chalfoun SM, Silva CF, Cirillo M, Varga EA, Schwan RF. Ochratoxin A in coffee beans (Coffea arabica L.) processed by dry and wet methods. Food Control. 2009;20: 784–790. doi:10.1016/j.foodcont.2008.10.003

6. Elhalis H, Cox J, Frank D, Zhao J. The role of wet fermentation in enhancing coffee flavor, aroma and sensory quality. Eur Food Res Technol. 2021;247: 485–498. doi:10.1007/s00217-020-03641-6

7. Sandeep TN, Channabasamma BB, Gopinandhan TN, Nagaraja JS. The effect of drying temperature on cup quality of coffee subjected to mechanical drying. J Plant Crop. 2021;49: 35–41. doi:10.25081/jpc.2021.v49.i1.7059

8. Deeto S, Thepa S, Monyakul V, Songprakorp R. The experimental new hybrid solar dryer and hot water storage system of thin layer coffee bean dehumidification. Renew Energy. 2018;115: 954–968. doi:10.1016/j.renene.2017.09.009

9. Oliveros-Tascón CE, Ramírez-Gómez CA, Tibaduiza-Vianchá CA, Sanz-Uribe JR. Construcción de secadores solares tipo túnel con nuevos materiales. Cenicafé - Cent Nac Investig Café, Av Técnicos. 2017;482: 8.

10. Udomkun P, Romuli S, Schock S, Mahayothee B, Sartas M, Wossen T, et al. Review of solar dryers for agricultural products in Asia and Africa: An innovation landscape approach. J Environ Manage. 2020;268: 110730. doi:10.1016/j.jenvman.2020.110730

11. Bravo-Monroy L. A Network behind Coffee. J Rice Res Dev. 2019;2: 61–65. doi:10.36959/973/421

12. Liu Q, Bakker-Arkema FW. A model-predictive controller for grain drying. J Food Eng. 2001;49: 321–326. doi:10.1016/S0260-8774(00)00229-6

13. García JC, Posada-Suárez H, Läderach P. Recommendations for the regionalizing of coffee cultivation in Colombia: A methodological proposal based on agro-climatic indices. PLoS One. 2014;9: 1–22. doi:10.1371/journal.pone.0113510

14. Brooker DB, Bakker-Arkema FW, Hall CW. Drying and storage of grains and oilseeds. 2nd Revise. New York, NY, United States: Van Nostrand Reinhold, New York; 1992.

15. Sampaio CP, Nogueira RM, Roberto CD, Silva JS. Development of a dryer with airflow reversal and a pneumatic system for grain movement. Biosyst Eng. 2007;98: 33–38. doi:10.1016/j.biosystemseng.2007.02.014

16. Osorio Hernandez R, Ferreira Tinoco IDF, Correna Carlo J, Osorio Saraz JA, Aristizábal Torres ID. Bioclimatic analysis of three buildings for wet processing of coffee in Colombia. Rev Fac Nac Agron Medellín. 2018;71: 8609–8616. doi:10.15446/rfnam.v71n3.64566

17. Berhanu T, Ali M, Essubalew G. Impact of Sun Drying Methods and Layer Thickness on the Quality of Highland Arabica Coffee Varieties at Limmu, Southwestern Ethiopia. J Hortic. 2014;01: 1–7. doi:10.4172/2376-0354.1000117

18. Kleinwächter M, Selmar D. Influence of drying on the content of sugars in wet processed green Arabica coffees. Food Chem. 2010;119: 500–504. doi:10.1016/j.foodchem.2009.06.048

19. Bakker-Arkema FW, Lerew LE, De Boer SF, Roth MG. Grain dryer simulation. Agricultural Experiment Station, Res. Rep 224, Michigan State University, East Lansing, USA; 1974.

20. Cenkowski S, Jayas DS, Pabis S. Deep-Bed Grain Drying - A Review of Particular Theories. Dry Technol. 1993;11: 1553–1582. doi:10.1080/07373939308916919

21. Kim D, Son G, Kim S. Numerical analysis of convective drying of a moving moist object. Int J Heat Mass Transf. 2016;99: 86–94. doi:10.1016/j.ijheatmasstransfer.2016.03.025

22. Cavalcanti-Mata MERM, Duarte MEM, Lira VV, de Oliveira RF, Costa NL, Oliveira HML. A new approach to the traditional drying models for the thin-layer drying kinetics of chickpeas. J Food Process Eng. 2020. doi:10.1111/jfpe.13569

23. Dalpasquale VA, Sperandio D, Silva LHM. Fixed-bed drying simulation with constant enthalpy, using the improved Michigan State University model. Acta Sci - Technol. 2012;34: 137–140. doi:10.4025/actascitechnol.v34i2.7812

24. Phitakwinai S, Thepa S, Nilnont W. Thin-layer drying of parchment Arabica coffee by controlling temperature and relative humidity. Food Sci Nutr. 2019;7: 2921–2931. doi:10.1002/fsn3.1144

25. Choudhary A, Gopirajah R. Computational modeling of dehydration of mushroom. MOJ Food Process Technol. 2018;6: 264–270. doi:10.15406/mojfpt.2018.06.00174

26. Nilnont W, Thepa S, Janjai S, Kasayapanand N, Thamrongmas C, Bala BK. Finite element simulation for coffee (Coffea arabica) drying. Food Bioprod Process. 2012;90: 341–350. doi:10.1016/j.fbp.2011.06.007

27. Zhang S, Kong N, Zhu Y, Zhang Z, Xu C. 3D model-based simulation analysis of energy consumption in hot air drying of corn kernels. Math Probl Eng. 2013;2013. doi:10.1155/2013/579452

28. Dutta SK, Nema VK, Bhardwaj RK. Drying behaviour of spherical grains. Int J Heat Mass Transf. 1988;31: 855–861. doi:10.1016/0017-9310(88)90142-1

29. Perazzini H, Leonel A, Perazzini MTB. Energy of activation, instantaneous energy consumption, and coupled heat and mass transfer modeling in drying of sorghum grains. Biosyst Eng. 2021;210: 181–192. doi:10.1016/j.biosystemseng.2021.08.025

30. Pérez-Alegría LR, Ciro VHJ, Abud LC. Physical and thermal properties of parchment coffee bean. Trans Am Soc Agric Eng. 2001;44: 1721–1726. doi:10.13031/2013.6983

31. Severa L, Buchar J, Nedomová Š. Shape and size variability of roasted Arabica coffee beans. Int J Food Prop. 2012;15: 426–437. doi:10.1080/10942912.2010.487967

32. Tian Y, Lin G, Guo J. Analysis of mass diffusion theory and models for high-temperature multi-component gases. Int J Heat Mass Transf. 2021;181: 121994. doi:10.1016/j.ijheatmasstransfer.2021.121994

33. Montoya-Restrepo EC, Oliveros-Tascón CE, Roa-Mejía G. Optimización Operacional del Secador Intermitente de Flujos Concurrentes para Café Pergamino. Rev Cenicafé. 1990;41: 19–33. Available: http://hdl.handle.net/10778/939

34. Putranto A, Chen XD, Xiao Z, Webley PA. Mathematical modeling of intermittent and convective drying of rice and coffee using the reaction engineering approach (REA). J Food Eng. 2011;105: 638–646. doi:10.1016/j.jfoodeng.2011.03.036

35. Nellis G, Klein S. Heat Transfer. Cambridge: Cambridge University Press; 2009. doi:10.1017/CBO9780511841606

36. Felizardo MP, Merlo GRF, Maia GD. Modeling drying kinetics of Jacaranda mimosifolia seeds with variable effective diffusivity via diffusion model. Biosyst Eng. 2021;205: 234–245. doi:10.1016/j.biosystemseng.2021.03.008

37. Borém FM, Marques ER, Alves E. Ultrastructural analysis of drying damage in parchment Arabica coffee endosperm cells. Biosyst Eng. 2008;99: 62–66. doi:10.1016/j.biosystemseng.2007.09.027

38. Burmester K, Eggers R. Heat and mass transfer during the coffee drying process. J Food Eng. 2010;99: 430–436. doi:10.1016/j.jfoodeng.2009.12.021

39. Guiné RPF. The Drying of Foods and Its Effect on the Physical-Chemical, Sensorial and Nutritional Properties. ETP Int J Food Eng. 2018;4: 93–100. doi:10.18178/ijfe.4.2.93-100

40. Agullo JO, Marenya MO. Airflow resistance of parchment arabica coffee. Biosyst Eng. 2005;91: 149–156. doi:10.1016/j.biosystemseng.2005.02.008

41. Mizera, Herák D, Hrabě P, Kabutey A, Wasserbauer M, Pouzarová H. Describing of drying curves of green coffee beans using mathematical model. IOP Conf Ser Mater Sci Eng. 2018;420. doi:10.1088/1757-899X/420/1/012075

42. Kath J, Mittahalli Byrareddy V, Mushtaq S, Craparo A, Porcel M. Temperature and rainfall impacts on robusta coffee bean characteristics. Clim Risk Manag. 2021;32: 100281. doi:10.1016/j.crm.2021.100281

43. Lee SS, Kim JH, Hong SB, Yun SH. Effect of humidification and hardening treatment on seed germination of rice. Korean J Crop Sci. 1998;43: 157–160.

44. Mhimid A, Ben Nasrallah S, Fohr JP. Heat and mass transfer during drying of granular products - simulation with convective and conductive boundary conditions. Int J Heat Mass Transf. 2000;43: 2779–2791. doi:10.1016/S0017-9310(99)00286-0

45. Mwithiga G, Kigo SN. Performance of a solar dryer with limited sun tracking capability. J Food Eng. 2006;74: 247–252. doi:10.1016/j.jfoodeng.2005.03.018

46. Hernández-Díaz WN, Ruiz-López II, Salgado-Cervantes MA, Rodríguez-Jimenes GC, García-Alvarado MA. Modeling heat and mass transfer during drying of green coffee beans using prolate spheroidal geometry. J Food Eng. 2008;86: 1–9. doi:10.1016/j.jfoodeng.2007.08.025

47. McMinn WAM, Magee TRA. Principles, methods and applications of the convective drying of foodstuffs. Food Bioprod Process Trans Inst Chem Eng Part C. 1999;77: 175–193. doi:10.1205/096030899532466

48. Ramirez-Martinez A, Benet J-C, Cherblanc F, García-Alvarado MA, Rodriguez-Jimenes G. Internal structure and water transport in the coffee bean. 17th Int Dry Symp (IDS 2010), Magdeburg, Ger. 2010; 1–8.

49. Fadai NT, Melrose J, Please CP, Schulman A, Van Gorder RA. A heat and mass transfer study of coffee bean roasting. Int J Heat Mass Transf. 2017;104: 787–799. doi:10.1016/j.ijheatmasstransfer.2016.08.083

50. Ramírez-Martínez A, Salgado-Cervantes MA, Rodríguez-Jimenes GC, García-Alvarado MA, Cherblanc F, Bénet JC. Water transport in parchment and endosperm of coffee bean. J Food Eng. 2013;114: 375–383. doi:10.1016/j.jfoodeng.2012.08.028

51. Afonso PC, Corrêa PC, Pinto FAC, Sampaio CP. Shrinkage Evaluation of Five Different Varieties of Coffee Berries during the Drying Process. Biosyst Eng. 2003;86: 481–485. doi:10.1016/j.biosystemseng.2003.08.012

52. Azmir J, Hou Q, Yu A. CFD-DEM simulation of drying of food grains with particle shrinkage. Powder Technol. 2019;343: 792–802. doi:10.1016/j.powtec.2018.11.097

4. Improving the Drying Performance of Parchment Coffee Due to the Newly Redesigned Drying Chamber.

Adapted from: Duque-Dussán E, Banout J. Improving the drying performance of parchment coffee due to the newly redesigned drying chamber. J Food Process Eng. 2022;45. doi:10.1111/jfpe.14161

Abstract

The Colombian coffee growers face many complications when using traditional open-sun drying techniques such as post-harvest processes delays or incomplete grain dryness because of climate conditions. Therefore, local workshops began fabricating low-capacity dryers simulating the industrial equipment working principles. One of the most commercialized units is a triple tray rectangular-shaped dryer with a 31.25kg capacity of dry parchment coffee per batch, providing the issue with an acceptable solution. However, it was redesigned into a circular shape holding a lower grain bed thickness and a vertical air inlet with a diffusive tray. Both units were simulated using the Thompson and the MSU grain drying mathematical models to obtain their theoretical drying time. Then, a computational fluid dynamics simulation was conducted, attaining the unit's drying air behaviour, the circular dryer exhibited notable drying times reduction and even air distribution, optimizing the dryer's performance, representing a benefit for the coffee-growing farmers.

Keywords: CFD Simulation; Coffea arabica; Deep bed dryer; Mechanical dryer; Moisture removal.

Practical applications

A cylindrical arranged coffee dryer with a vertical air inlet reduces the drying time of the grain, allowing a better rentability of the grower and improves the air distribution inside the equipment, meaning that the moisture removal will occur uniformly, safeguarding that the product’s final moisture content meets the required conditions for a safe storage.

4.1. Introduction

One of the reasons why Colombia has one of the top-quality coffees in the world is due to its post-harvest wet processing technique. The coffee processing consists of a set of operations to transform the coffee fruits into high physical quality parchment coffee [1]. By doing so, the dry grains will hold up their physical quality, organoleptic properties, nutrition contents and preserve the safety and innocuousness of the grains [2]. The process is further divided into the following stages: pulping (removal of the pulp), removal of the mucilage (by natural fermentation or mechanical means), washing and drying [3]. After harvesting, the coffee fruit has around 65% of its weight represented by water, having a strong physiological activity which can be translated as a threat for the grain, which, in this point, is already considered as a perishable product [4]. This is why the grain's transformation process occurs typically in the farm facilities right after picking the beans. During the wet process, the drying stage is probably one of the most delicate and essential step to ensure top quality and safe coffee production. After washing and draining the coffee, it usually has a 52-53% moisture content on a wet basis (wb), and it must be dried until reaching a moisture content between 10-12% (wb) [5,6]. The rules for commercialization of coffee demand that the final moisture fits in the range to inhibit the development of microorganisms, mycotoxins and/or fungi [7,8].

In Colombia, 563000 families depend on this crop as their primary source of income, from which 95% are considered small coffee growers, having less than five hectares (ha) sown in coffee [9], being 1.6 ha the average plot size [10]. These coffee growers face two big problems when it comes to dry their goods. The first one is related to the harvest peak since it comes twice per year in most of all the country, in April-May and November-October [11]; since they are coincident with the wet seasons, and these meteorological conditions come accompanied by high cloudiness and low direct sun radiation [12]. Hence, the open-sun drying technologies face an overly complex affair, and usually, because of the small farm owner's socioeconomic condition, they tend to open-sun dry their harvest because it is an economical and environmentally friendly method [13]. This issue will lead the growers to sell their coffee wet for less price or pay somebody who owns a mechanical dryer to dry their stock to avoid its

spoilage [14]. In any of the options, the producer is at an economic disadvantage regarding its profit.

The second problem follows the lack of infrastructure for drying even in the dry season. The traditional open air drying has a limited capacity due to the importance of reaching the final moisture requirement. To achieve a decent drying time and final product moisture to avoid spoilage, the literature suggests keeping a coffee layer height between 20 mm and 30 mm [15]. If this condition is kept, one square meter may well hold up to 14 kg of wet coffee, obtaining at the end of the process approximately 7.25 kg of dry parchment coffee (DPC) according to the wet/dry coffee ratio of 1.93 [16]. Considering that the open-air drying is rather a time-demanding process, acquiring the final moisture will take 5-7 days [17]. The mass coffee flow within the dryer is relatively static since the beans are still harvested on the field, but they must wait for the dry batches to leave the dryer, happening after five days in the best-case scenario. Responding to the needs derived from the problems related to the open-air coffee drying, local manufacturers began to produce a reduced version of the mechanical coffee dryers, trying to recreate their operating settings, seeking to reduce drying times and increase the speed of the drying process while maintaining the required moisture conditions [18]. The most common dryer that fulfils these needs is a vertical rectangular-shaped silo type convective dryer manually operated, with a net capacity of 93.75 kg – 7.5 *a* (3 batches), its commercialization grew rapidly between the farmers since the drying time was reduced to 21 h per batch representing a mass of 31.25 kg of DPC with an acceptable final product's quality. However, there are no studies in the scientific literature investigating the drying kinetics and modelling of the drying process including the computational simulations of the above-mentioned coffee dryer nor using different geometries or working principles to make the process more efficient, as is the case of the spouted beds, where a conical bottom gas inlet is used to avoid dead zones in different drying applications with high efficiencies and working versatility [19,20].

Considering that it is essential to understand the transport processes occurring during the drying stage since they play a critical role in the conservation of the product's quality, and at the same time, foreseeing and controlling the drying behaviour is also likewise significant in setting an improved system for the drying phase, it is mandatory to obtain a precise description of the occurring phenomena [21]. Therefore,

the main objective of this study was to design an efficient drying unit for coffee beans with improved drying capacity based on an existing technology, afterwards the mathematical and computational fluid dynamics simulation were performed in order to compare both processes to obtain relevant information about the occurring phenomenona in both units.

4.2. Materials and Methods

4.2.1. Drying facilities

The dryer to improve is designed keeping in mind a simple manufacturing process, foreseeing low construction costs. It has a rectangular-shaped body divided into three chambers I, II and III (Figure 1), by three perforated trays, which support the coffee and, at the same time, allow the drying air to flow through the product; the trays I and II have a small gate (also perforated) in the centre of its surface to allow the coffee grain transition between the compartments I-II and II-III that should be done by the operator of the dryer. The drying air is vented into the system through the right-side bottom of the equipment, flowing upwards after being heated directly by a liquefied petroleum gas (LPG) flame.

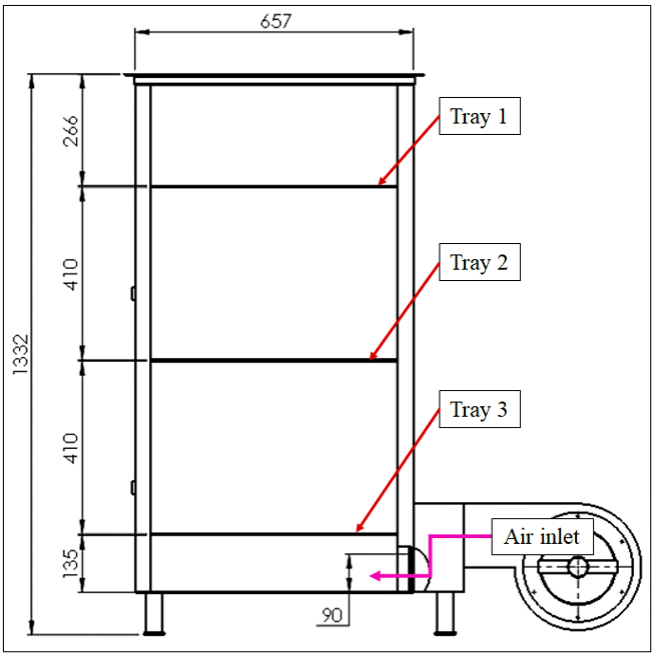

Figure 1. General dimensions of the 7.5*a* rectangular-shaped coffee dryer.

The drying process is started by fully loading the chamber I with washed coffee (A) with an average moisture of 53% (wb). The chamber I holds a capacity of VIR = 0.657 m × 0.266 m × 0.495 m = 0.0865 m^3 and a cross-sectional area of AR = 0.325 m^2. The full load of this chamber aims to obtain approximately 2.5 a (31.25 kg) of DPC at the end of the drying process; this statement was verified considering the bulk density of the wet parchment is $\rho_b \approx 687.17$ kg m^{-3} [22]. Considering that the chamber I holds up to 58.67 kg of wet coffee, a theoretical output of 30.40 kg of DPC is expected given the wet/dry parchment correlation of 1.93.

After loading, the fan is turned on together with the LPG burner; the drying air enters the apparatus at an un-exceedable temperature T = 50°C, travelling with an initial velocity u = 1. 3m s^{-1} at a rate of $Q \approx 0.163$ m^3 s^{-1}, the airflow rate was verified multiplying the air velocity after the fan, determined with a testo 425 thermal anemometer times the cross-sectional area (400 × 310 mm). The LPG burner had a diameter of 40 mm and a mean gas consumption of 0.19 m^3 h^{-1}, located perpendicularly to the fan (0.249 kW) (Figure 2), the air temperature control is done by a high precision testo 905-T2 surface thermometer located in the fan exhaust and by flame regulation, setting a uniform and stable blue flame. The process was also studied at 45°C and 40°C to provide a wider prediction of the occurring phenomenon in the event that the operator would like to dry below the 50°C temperature as recommended [23].

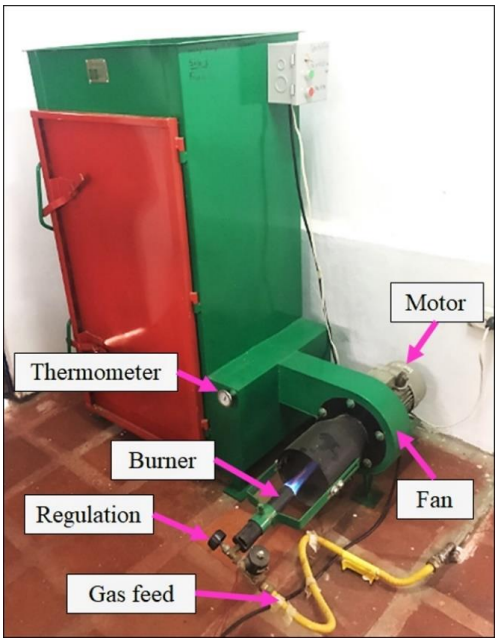

Figure 2. Rectangular dryer working set-up.

When starting the process, the chambers II and III are empty, however, after 7 hours, the initial coffee load A is moved to the chamber II, and a new batch of wet coffee (B) is placed in the chamber number I, consequently, 14 hours after starting the process, the initial load A is moved from the chamber II to the chamber III, the second load B from the chamber I to the chamber II and fresh washed coffee (C) is loaded into the compartment I (Figure 5). Finally, after 21 hours, the first batch can be removed since it must have acquired the necessary moisture content of 10-12% (wb). From this moment on, every 7 hours, a 2.5 *a* DPC batch is withdrawn from the equipment, having reached a continuous process. Each batch undergoes a net drying time of 21 hours, three replications of the drying process were done to find the average experimental drying time (DTE) and to verify the 21 h value given by the manufacturer, where DTE1: 21.083 h; DTE2: 21.016 h and DTE3: 21.05 h. $DTE_{average}$: 21.049 h; if compared with the open-air drying behaviour tendencies, it can be seen that this dryer significantly reduces the drying time in addition to having a capacity greater than four times than the one offered by an open-air dryer per square meter. A few details regarding the dryer's geometry and general working principles can be mentioned. In the first place, it was foreseen that achieving a homogeneous drying air distribution over the unit's geometry might be difficult since the location of the air inlet is not aligned with the vertical axis of the equipment [24]. At the same time the inlet geometry includes a sudden geometrical step between the fan and the bottom of the drying chamber III (Figure 1), this will perhaps reduce the air velocity, and taking into account that the rectangular nature of the dryer contains corners, it is uncertain if a low-velocity air will run properly through them or possibly filled with air gaps or undesired vortexes [25], diminishing the drying efficiency.

To improve the drying performance, the rectangular-shaped coffee dryer was re-designed into a circular shaped unit with a conical configured air inlet as in the spouted bed operations to improve the air transit into the dryer and its interaction with the particles as suggested by [26–28]. The overall height of drying chamber did not exceed 1.6 m for easy access during the dryer loading. The volume of the chamber I needed to be approximately the same as the one in the rectangular-shaped dryer to obtain the same amount of DPC at the end of the process when fully loaded $V_{IR} \approx V_{IC}$. Easy verifiable with the dimensions of the circular shaped dryer (Figure 3), it had a diameter $\emptyset$ = 0.74

m, and the chamber I height was 0.2 m. It is also important to mention that the new design kept an easy manufacturing process to maintain a low construction cost. The new design had a grain layer 0.066 m lower than the previous one; this fact is quite relevant since both drying models perform the simulation with reduced increments in the layer. Therefore, a direct relationship between the layer thickness, the drying time, drying air temperature and moisture removal was expected. Searching to ensure a homogeneous air velocity and distribution across the dryer's geometry, an extra diffusive tray was located between the air inlet and the tray number 3. The cross-section area of the circular dryer was A_C = 0.43 m^2, evidently larger than the rectangular one.

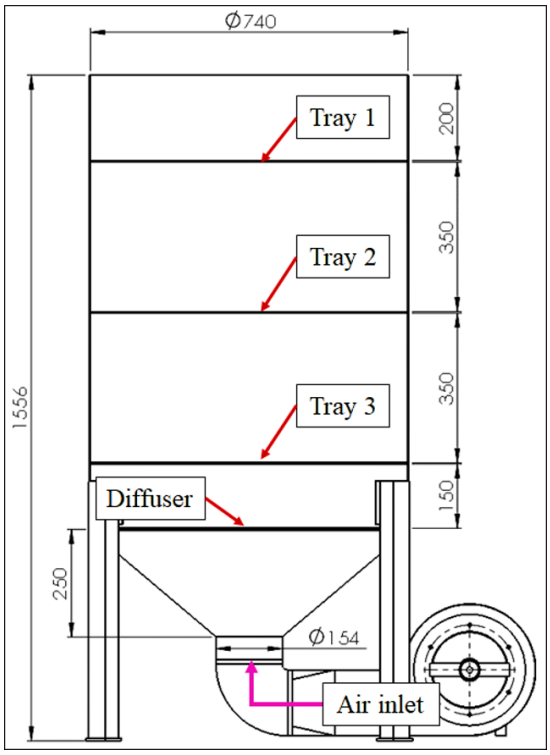

Figure 3. General dimensions of the 7.5*a* circular-shaped dryer.

4.2.2. Mathematical description

The phenomena occurring in the dryer was simulated by using a non-equilibrium, equilibrium, or logarithmic model [29]. There are plenty of models which estimate the behaviour of grain drying; however, during the coffee drying process, the semiempirical equilibrium Thompson model [30] and the theoretical non-equilibrium Michigan State University MSU model [31] seemed to be the most used since they

provide flexible and accurate equations based on deep mass and heat balance foundations [32].

4.2.2.1. Thompson Model

This model considers several thin grain layers, one placed on top of another [33], in this case each with a thickness of 0.025 m. The simulation calculates the first layer drying process, and afterwards, through an iterative process, the calculation is protracted to the other layers until the total layer height of the product of interest is reached.

The Thompson model suggests performing a sensible heat balance prior to the start of the process (Figure 4), by doing so, the T_e between the grain and the air can be estimated from the drying air's humidity H and temperature T, and the grain's specific heat capacity c_p and temperature T_g, as reads Equation 1.

$$T_e = \frac{(0.24 + 0.45H)T + c_p T_g}{0.24 + 0.45H + c_p} \quad (1)$$

The first layer drying simulation ran through a time interval Δt; afterwards, the final grain and air temperature were calculated as an output of the after-drying heat balance. For this effect, the latent heat of vaporization L was considered since there is still water within the grain.

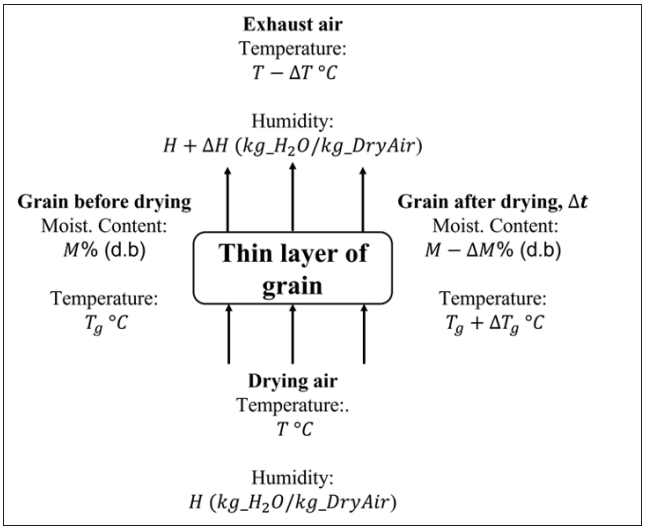

Figure 4. Schematic of Thompson, Peart, and Foster (1968) thin film drying simulation model.

Also, the air had an increased humidity ratio since it removed a fraction of the moisture contained in the grain, hence the removed moisture from the grain raised the air's humidity ratio from an initial state H_0 to a final state H_f.

$$T_f = \frac{(0.24 + 0.45H_0)T_e - \Delta H(587.9 + L - T_e) + c_p T_e}{0.24 + 0.45H_f + c_p}$$

(2)

The Thompson model provided an adjustable solution during the calculation of the exhaust air temperature and humidity stage data [34], the constants displayed are fully explained by [30].

4.2.2.2. Michigan State University MSU Model

The MSU model bears a similar structure as the Thompson model; the drying process simulation is divided into reduced increments of time and thin grain thicknesses, adopting the output drying air conditions from one layer as the input conditions for the following one [35]. It is a theoretical non-equilibrium model rigidly based on the heat and mass transfer laws; therefore, a precise and exact result was expected [36].

This model was developed by [31], where a mass and energy balance is performed upon a differential volume *S dx*, located at a random location within the grain bed divided into several thin layers [37]. The system has unknown variables as the moisture content, the grain layer temperature, the drying air humidity ratio, and the temperature. These balances originate a set of four partial differential equations which must be solved together by numerical integration [38], using in our case finite differences as performed by [36], having defined the initial and boundary conditions in section 2.4 as starting point. The equations describing the fixed bed drying phenomena proposed [31], are further explained as follow:

– The energy leaving the layer equals the incoming energy minus the energy transferred by convection (balance for the enthalpy of the air):

$$\frac{\partial T}{\partial x} = \frac{-h\, a_s}{G_a c_a + G_a c_v H}\left(T - T_g\right)$$

(3)

– The grain's enthalpy balance is stated as the internal energy change of the product minus the evaporation energy:

$$\frac{\partial T}{\partial t} = \frac{h\, a_s}{\rho_p c_p + \rho_p c_w M}\left(T - T_g\right) + \frac{L + c_v\left(T - T_g\right)}{\rho_p c_p + \rho_p c_w M} G_a \frac{\partial M}{\partial x}$$

(4)

– The air humidity ratio balance is defined as the entering humidity minus the leaving humidity:

$$\frac{\partial H}{\partial x} = -\frac{\rho_p}{G_a}\frac{\partial M}{\partial t}$$

(5)

– The product's moisture content can be expressed as a function of a suitable thin layer drying equation:

$$\frac{\partial M}{\partial t} = f\left(M, M_e, M_o, T_g, \ldots t\right)$$

(6)

These equations establish the simulation set for the static layer drying. Nevertheless, there is no analytical solution for the system; hence, an approximate method must be used to provide a solution to the problem [39].

4.2.3. Coffee parameters for simulation

To obtain an accurate and precise drying simulation, the grain's physical properties and the drying air attributes were carefully considered. Therefore, the equations describing the required grain properties and parameters are explained in the following section, these characteristics were mostly determined over the time by the National Coffee Research Center of Colombia (Cenicafe) in different research activities.

4.2.3.1. Grain-Air convective heat transfer coefficient

The convective heat transfer coefficient in grains was estimated as shown in Equation 7. This equation and its constants A=0.2755, B=-0.34, C=0.006175 and D=0.000165 were defined by [38].

$$h_c = Ac_a G_a \left(\frac{2r_0 G_a}{C + DT_g} \right)^B \tag{7}$$

4.2.3.2. Parchment coffee specific heat capacity

The parchment coffee specific heat capacity estimating equation for grain with moisture within 11% - 45% (wb) was obtained by the method of mixtures [40], where *M* is the dry basis (db) moisture content in decimal notation:

$$c_p = 1.3556 + 5.7859M \tag{8}$$

4.2.3.3. Parchment coffee equilibrium moisture content

The balance moisture content of parchment coffee M_e was achieved using Equation 9, adapted from the dynamic method [41]. It considers the relative humidity of the air H_R in decimal units, the air temperature *T*, and the constants: P_1 = 61.0309, P_2 = -108.3714, P_3 = 74.4611, Q_1 = -0.03049, Q_2 = 0.070114, and Q_3 = -0.035177.

$$M_e = \left(P_1 H_R + P_2 {H_R}^2 + P_3 {H_R}^3 \right) e^{\left(Q_1 H_R + Q_2 {H_R}^2 + Q_3 {H_R}^3 \right) T} \tag{9}$$

4.2.3.4. Parchment coffee latent heat of vaporization

[42] described the coffee parchment's latent heat of vaporization *L* as reads the Equation 10, where *M* should be considered in decimal notation (db). *L* was defined as a function of the latent heat of free water vaporization, verified by [43,44] when attaining the coffee isotherms.

$$L = (2502.4 - 2.42958T_g)(1 + 1.44408e^{-21.5011M})$$

(10)

4.2.3.5. Thin-layer drying equation

[45] established the thin layer drying formula, Equation 11, and its parameters m = 0.0143, n = 0.87898 and q = 1.06439. Valid for moisture content and temperature between 5-55% (db) and 10:70°C. The equilibrium moisture M_e and the grain's moisture M must be considered in decimal notation and dry basis (db).

$$\frac{\partial M}{\partial t} = -mq(M - M_e)(P_{vs} - P_v)^n t^{(q-1)}$$

(11)

Equation 11 has relevant importance since it involves the saturation vapour pressure P_{vs} and the partial vapour pressure P_v, improving the accuracy of the model [46].

4.2.3.6. Humidity diffusion coefficient

The humidity diffusion coefficient is expressed as a function of the grain's temperature and dry basis moisture in decimal notation [40].

$$D = 4.1582 \times 10^{-8} e^{\left[(0.1346\, T_g + 2.2055)M - \frac{1184}{T_g + 273.15}\right]}$$

(12)

4.2.3.7. Bulk density

The coffee's bulk density can change since the grain shrinks depending on the drying stage [47]. However, an estimated value was calculated from Equation 13, defining the bulk density in function of the moisture content in dry basis [40].

$$\rho_b = 365.884 + 270.67M$$

(13)

4.2.4. Mathematical Simulation

The numerical simulation was done in MATLAB based on the Thompson and MSU models for grain drying; the coffee parameters were also included in the solution scheme. Numerical discretization was established by dividing the grain bed into individual control volumes with dimensions $S \times 0.025$ m, put upon one another until reaching the total coffee layer height. Each coffee bed was treated independently and subjected to two consecutive iteration processes. The first iteration starts on the first control volume for which the initial drying air temperature, humidity and the grain moisture are known, the program iterates until convergence is reached.

The obtained outputs ΔT and ΔH defined the following control element's initial values, running likewise until the final load height has been simulated. Consequently, the final temperature and humidity values of the last control element of the first load set the initial conditions for the first control element of the following grain bed (Figure 5). This process was repeated across the entire domain until the drying simulation was completed. The second iterative process calculated the grain moisture over certain elapsed time (drying time) for each drying stage. The first phase is described in red (Figure 5), where only the I tray is loaded with coffee (A), after seven hours this load was transferred to the tray II and a wet coffee batch was loaded into the tray I (B), described in the Figure 5 as the blue box (second phase). Seven hours after the load in tray II was moved to tray III, the batch in the tray I was changed to the tray II and the final wet batch (C) was loaded into the dryer, this last phase is represented in pink in the Figure 5. After the dryer is completely loaded the air between the coffee batches relate to the drying stage air, where T1 = 40, 45 and 50°C, and T2, T3 and T4 were to be calculated. T4 represents the air when leaving the dryer to the atmosphere, the stage drying air’s temperature behaviour was predicted as T1>T2>T3>T4.

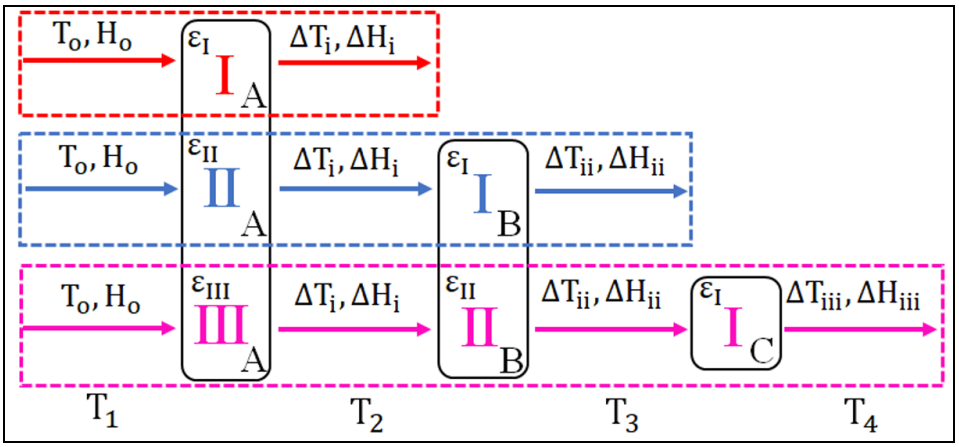

Figure 5. Box diagram of the simulation considerations.

The boundary conditions for the simulations were defined as: T (0, t) = T_0, T_g (x, 0) = T_{g0}, H (0, t) = H_0, M (x,0) = M_0. Considering that, the initial grain temperature and moisture content must be known along with the initial drying air temperature and humidity at the start of the drying stage. The initial conditions for the simulation were: Drying air temperature at the inlet: T_0 = 50°C, air humidity ratio H_0 = 0.015 kg kg^{-1}, relative air humidity HR = 0.17, air flow Q = 0.163 m^3 s^{-1}, air velocity u = 1.3 m s^{-1}, initial grain moisture M_0 = 53% (wb) and grain temperature T_{g0} = 21°C. All dependent variables were evaluated at the time $t + \Delta t$. The simulation assumptions follow those proposed by [31] for static bed dryers: i) The grain-volume shrinkage occurring during the drying simulation was assumed to be negligible since it can represent a reduction in the grain bed height. ii) Temperature gradients between particles are non-existent. iii) Particle to particle conduction is neglected. iv) Air and grain flow is plug type. v) The dryer's walls are adiabatic holding a negligible heat capacity.

4.2.5. Computational Fluid Dynamics Simulation

Both dryers were simulated in ANSYS Fluent 16.0 to observe how the geometrical arrangement affected the air distribution, flow, and velocity inside them. It was intended as well to compare both air behaviours to prove if the circular-shaped dryer described a better airflow across its domain. The simulations were performed with the drying units fully loaded; considering this, the coffee volumes and the holding trays were defined as fluid volumes with a certain porosity.

4.2.5.1. Porosity calculation

The porosity ε was calculated according to Equation 18 [48], where the V_{void} represents the air volume within the coffee mass, and the V_{total} stands for the total volume occupied by the grain. In this simulation, the porosity of each grain bed was calculated since the coffee undergoes a dimension shrinkage of approximately 7% after drying [47]. Therefore, the porosity values varied depending on the drying stage [49].

$$\varepsilon = \frac{V_{void}}{V_{total}} \tag{18}$$

1 kg of Coffea Arabica DPC contains roughly 4540 coffee seeds since one seed of DPC has a mass of 2.2×10^{-4} kg [16]. Therefore, the 31.25 kg of DPC per dried batch provided by the dryers contains approximately 141875 seeds.

The average arabica coffee seed dimensions (Figure 6), D1=1.15×10^{-2} m, D2=8×10^{-3} m and D3=5×10^{-3} m [50].

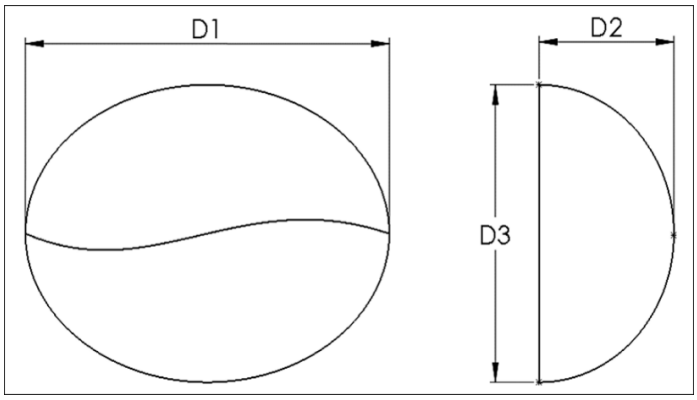

Figure 6. General average coffee seed dimensions.

Now, to simplify the calculations, two seeds were put on top of each other forming an ellipsoid with volume V_{seed} = 4.82×10-7 m^3, times the number of seeds halved due to the geometrical assumption, the total volume occupied by the seeds is V_{T_Seeds} = 0.0345m^3.

Hence, the air volume located in-between the coffee bed in the chamber III was expressed as the total volume occupied by the coffee minus the volume occupied by the seeds and applying the seed shrinkage factor, calculated as V_{void_III} = ((0.93) ×

$0.0865m^3$) – $0.0345m^3$) = $0.0459m^3$. Now, applying Equation 18, the porosity of the grain bed in the chamber III was:

$$\varepsilon_{III} = \frac{0.0459m^3}{0.0804m^3} = 0.57$$

Table 1. Coffee porosities for the different chambers.

Chamber	V_{void} [m^3]	V_{total} [m^3]	ε
I	0.0445	0.0865	0.514
II	0.0456	0.0835	0.546
III	0.0459	0.0804	0.571

A similar procedure was performed with the trays; their interaction with the drying air was described by defining their volume with a certain porosity; the void volume of the tray was represented by the volume of the perforations, which, divided by the total volume of the sheet (considering the void volume) gave as a result, the tray porosity. The tray's thickness was 0.003 m, and the perforations had a 0.005 m diameter, diagonally squared arranged.

Table 2. Tray porosities.

Tray	Rectangular	Circular
No. of perforations	6370	8480
V_{sheet}	9.756E-4m^3	1.290E-3m^3
V_{holes}	3.752E-4m^3	4.995E-4m^3
ε	0.3844	0.3872

4.2.5.2. Mesh setup

The mesh geometry was described with a hard behaviour, high smoothing, and slow transition 8 mm sized elements; considering that the flow from volume to volume plays a critical role, a high a high node match was established in the contact regions between bodies so the volumes, 8 contact regions were defined:

a) Between the inlet air and the tray 3.

b) Between tray 3 and the coffee in chamber 3.

c) Between the coffee in chamber 3 and the air above it.

d) Between the air above the coffee in chamber 3 and tray 2.

e) Between tray 2 and the coffee in chamber 2.

f) Between the coffee in chamber 2 and the air above it.

g) Between the air above the coffee in chamber 2 and tray 1.

h) Between tray 1 and the coffee in chamber 1.

In this step, the walls, inlet, and outlet were also indicated. The final mesh was specified by 9 volumes corresponding to 3 volumes of air, 3 of coffee and 3 of trays.

Table 3. Mesh metrics for both geometries.

Property		**Rectangular**	**Circular**
No. Elements		1801651	1894049
No. Nodes		1937259	2023310
Orthogonal Quality	Min	0.9998	0.3544
	Avg	1	0.9538
	Max	1	0.9999
Skewness	Min	1.31E-10	5.1E-4
	Avg	7E-4	0.1291
	Max	3.20E-3	0.841

4.2.5.3. Simulation definition

Once the mesh was properly defined (Table 3) a steady double-precision/pressure-based study was specified along with an absolute velocity formulation. A standard k-epsilon model was chosen for the simulation considering the air's turbulent flow conditions in the drying stages, verified by calculating the Reynolds number in such. The near-wall treatment followed the standard wall functions, and the air was selected as the simulation material. The porosity of the coffee was defined in the

cell zone conditions panel; simultaneously, the inertial and viscous resistances were filled in this section for each porous bed calculated from Ergun's Equation [51]. In the air inlet section, its velocity and direction were settled along with the static (gauge) pressure outlet. The spatial discretization was selected as pressure-velocity coupling. The convergence boxes in the residual sections were unselected since the simulation was carried out rather on iterations, the hybrid initialization was executed successfully, and 2000 iterations were settled before running the simulation.

4.3. Results and Discussion

4.3.1. Drying time

The drying time calculation stopped when attaining a grain moisture content under 12% (wb). After 21.3 hours of drying at 50°C, the rectangular-shaped dryer reached a grain moisture content of 11.87% (wb), which seems logical and accurate when comparing it against the process parameters where 21 hours of drying are expected. A possible explanation for the 0.3 h difference might be due to the limitations of the model because as the assumptions made and the simplification of the simulation parameters, might not precisely describe the experimental conditions. Although these variables cannot be fully described in this simulation, the obtained results fulfil the process description.

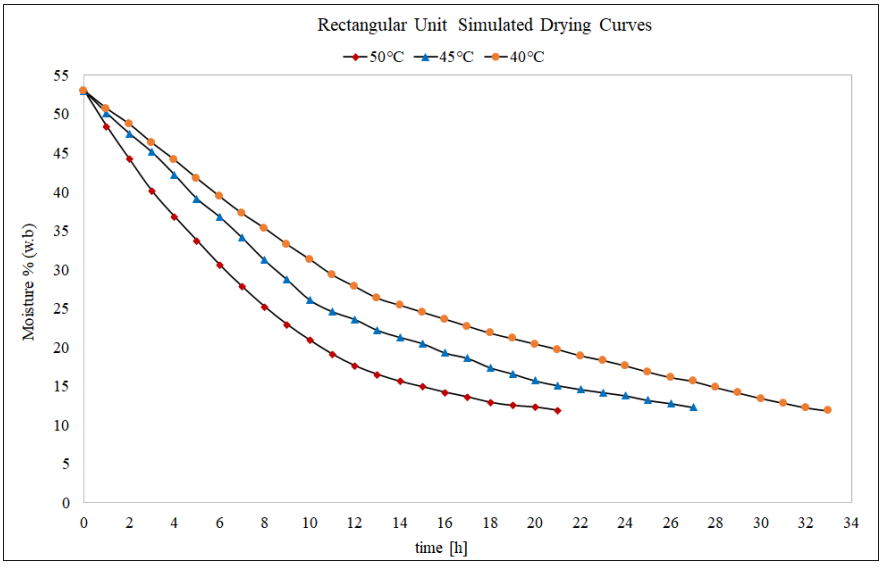

Figure 7. Rectangular unit comparative drying time plot at different drying air temperatures.

As shown in Figure 7, the drying curves at different temperatures describe logical behaviour and values. These findings are consistent with those published by [52]. The moisture remotion occurs fast in the first half of the process, afterwards, it is slower since the diffusion of the water in the grain's inner geometry is more difficult to happen as explained by [53]. Even though the process parameters require an air temperature of 50°C to obtain a faster drying, the literature recommends drying slightly under this temperature because if exceeded, the embryo might be damaged as mentioned by [23], negatively affecting the grain's structure leading to an undesired decomposition of the seed [54,55].

When drying at 45°C the required moisture will be reached after 27.6 hours. If the process is executed at 40°C the mandatory moisture was reached after 32.5 hours, which is in agreement with similar drying times as those attained by [47] under similar drying temperature conditions.

The circular-shaped dryer depicted a similar drying curve to the rectangular-shaped one, however, it reached grain moisture of 11.93% (wb) after 17.4 hours when drying at 50°C. Hence, the drying time compared with the rectangular-shaped dryer was shortened by 3.9 hours, meaning that the coffee will be dried faster, ensuring its preservation against biological threats. The gas utilization was therefore reduced by 0.74 m^3, represented as approximately 1.39 kg in the liquid phase. Also, the fan's energy consumption decreased by approximately 1 kWh, representing an extra economical advantage.

When drying at 45°C and 40°C, the circular-shaped dryer takes 23.6 and 28.5 hours, respectively, to reach 11.97% (wb) moisture content (Figure 8). Hence, disregarding the drying air temperature, the circular unit displays an improved drying capability than the rectangular one, providing a higher efficiency deriving in a general upgrade of the drying facilities and infrastructure.

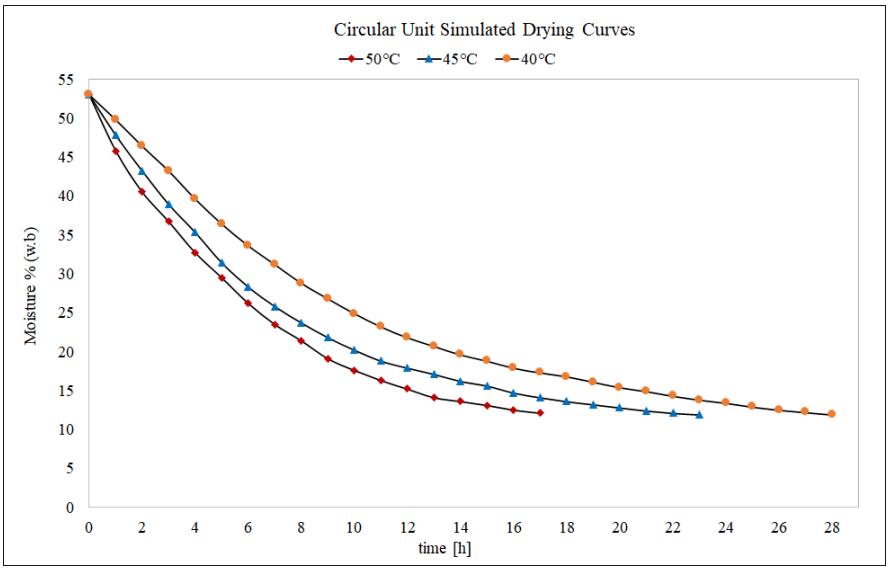

Figure 8. Circular unit comparative drying time plot at different drying air temperatures.

Even though both units displayed similar drying-curve behaviour, the improved performance exhibited by the circular dryer may be explained by the relationship between the stage temperature and the layer thickness stated in Equation 3, this also accords with the observations showed by [56], when setting a thinner layer of coffee, the temperature change between stages T1, T2, T3 and T4 (Figure 5 and Figure 9) will be lower, hence the moisture removal will occur faster. At the same time, the change of temperature with respect to the time (Equation 4) is expressed as a function of the grain-air convective heat transfer coefficient, which is stated as a function of the air mass flow per unit area (cross-section area), contemplating that the circular dryer holds a cross-sectional area larger in $0.105m^2$ it is expected a reduction in the drying time as a higher airflow is transiting through the geometry of the unit. This finding is supported by the evidence found by [35], where a direct relationship between the drying time and the cross-sectional airflow was proven. The drying time at 50°C, 45°C and 40°C was reduced theoretically by 18.3%, 14.5% and 12.3% respectively.

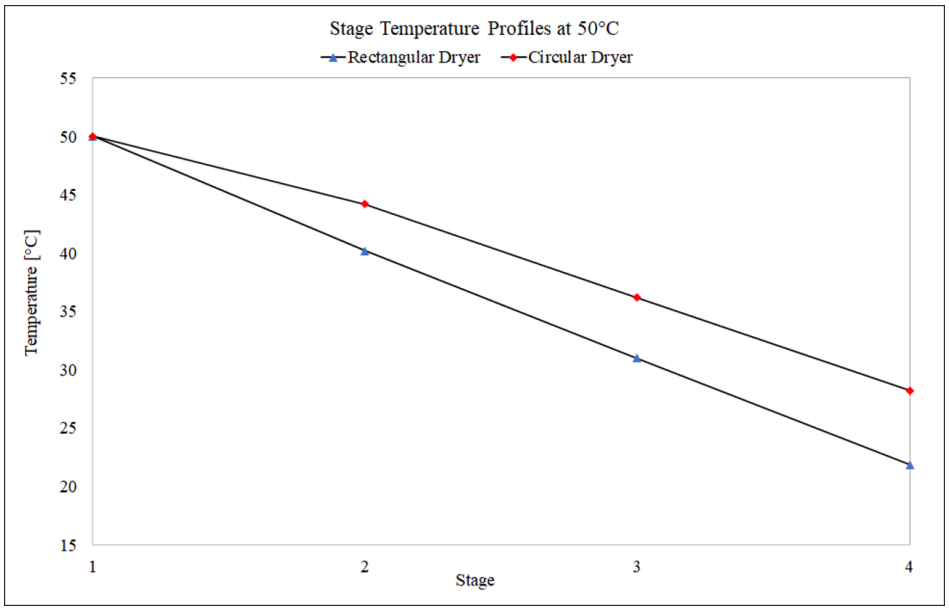

Figure 9. Comparative stage temperature profile plot at 50°C.

4.3.2. Diffusion coefficient

The coffee diffusion coefficient can be calculated at any time of the procedure according to Equation 12; after stabilizing the process, the diffusion coefficient of the incoming fresh batch of coffee was traced throughout the entire operation in both dryers, considering the stage change as well (Figure 10). During the first hour, the circular unit's diffusion coefficient was evidently higher than the described by the rectangular dryer since the air temperature is slightly higher in the circular unit, reflecting that the air undergoes fewer velocity losses, keeping a higher stage temperature; consequently, a high moisture removal occurs during this time frame. After one hour, the circular-shaped dryer's diffusion coefficient became slightly lower than its counterpart, thus describing a similar curve; this is because the moisture removal happened faster in the circular dryer, henceforward a rapid moisture decrease followed, consequently reducing the diffusion coefficient values considering the direct association between the moisture content and the diffusion coefficient.

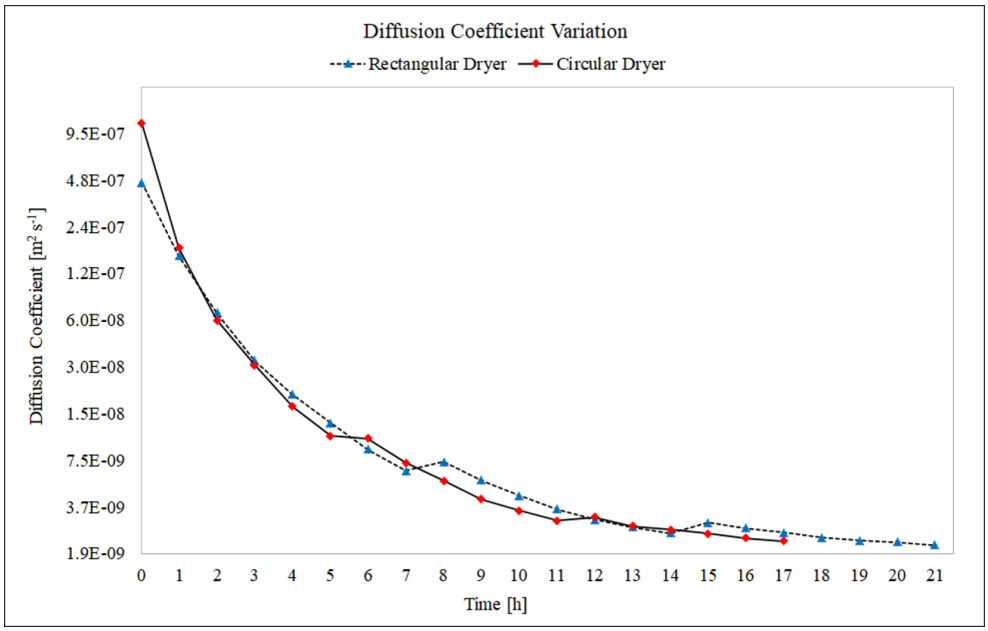

Figure 10. Comparative diffusion coefficient behaviour at 50°C.

It is also seen two steps in each curve, representing the coffee's chamber change into the new drying stage. When the chamber transfer occurred, a momentary rise in the diffusion coefficient can be seen, this is because the temperature is higher in the following stage (Figure 9). As reported by [57], the diffusion coefficient values are strongly influenced by the model used, it also depends on the material and inner structure assumptions as shown by [53], however the obtained results ranging from 1.101×10^{-6} to 2.104×10^{-9} m^2 s^{-1} share similarity with those found by [46]. The diffusion coefficient when the coffee reaches its required moisture is also within the range of diffusivities for different crops [58].

4.3.3. Specific heat capacity

Contemplating that the moisture removal happens faster in the circular shaped dryer, the specific heat change will also occur at a quicker rate in this unit seeing that the specific heat is expressed as a function of the moisture (Equation 8). The specific heat changed in both cases from c_p at 53% (wb) ≈ 7.8 kJ kg^{-1} K^{-1} to c_p at 12% (wb) ≈ 2.1 kJ kg^{-1} K^{-1}. However, the faster drop of the specific heat in the circular dryer also represents that less energy is required for increasing its temperature, meaning that less water is contained in the seed (Figure 11).

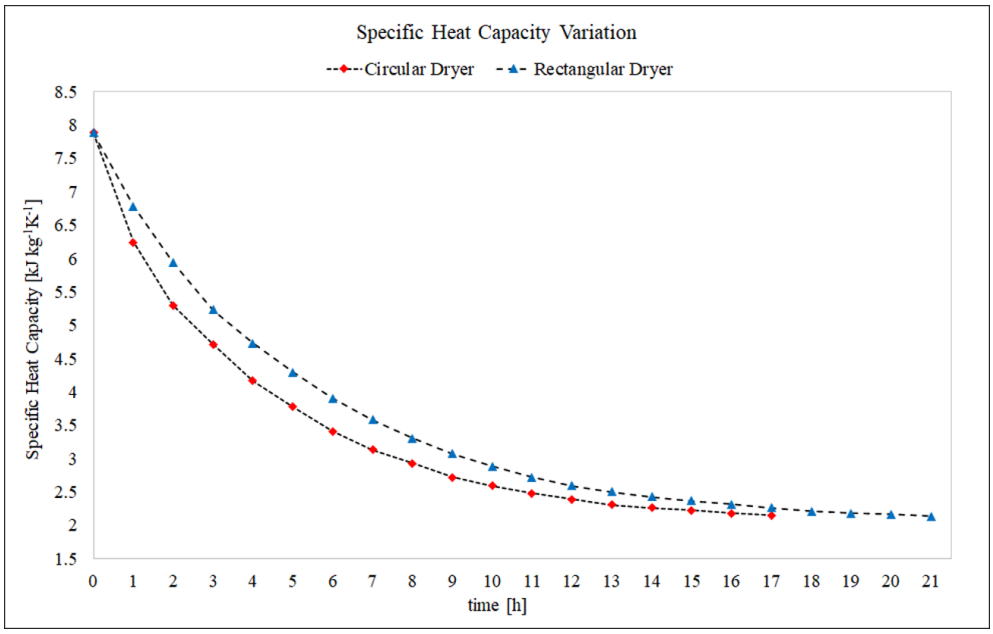

Figure 11. Comparative specific heat capacity change at 50°C.

The specific heat values seem to be in accordance with those found by [59,60], however, the results can also be affected by the calculation model since the regression terms can change [61].

4.3.4. Air Distribution and Velocity Profiles

Both simulations reached a steady scaled-residual convergence stabilization at an adequate number of iterations; the rectangular-shaped dryer converged slightly faster than the circular-shaped unit, keeping in mind that the simulation configuration had 2000 iterations, the latest convergence was obtained by the circular dryer's epsilon residual at 1670 iterations. The circular dryer scaled-residual convergence occurred at higher values, possibly explained by the fact that the circular dryer displays a less complicated geometry.

An XY midplane was inserted longitudinally across the rectangular dryer's geometry to display its velocity contours. As shown in Figure 12A, the sudden geometrical change after the inlet originates a local velocity increase, nevertheless, it is not afterwards maintained where a rapid loss in the velocity magnitude occurs. This singularity might be related to the air inlet geometry distribution, the chamber connecting the inlet with the drying unit generates a complex vortex system after the air collides against the dryer's body, illustrated in Figure 12B, causing not only a negative

impact to the air's velocity but also generating important air covering issues across the dryer's domain, directly affecting the air transit through the coffee beds, hence affecting the drying process uniformity.

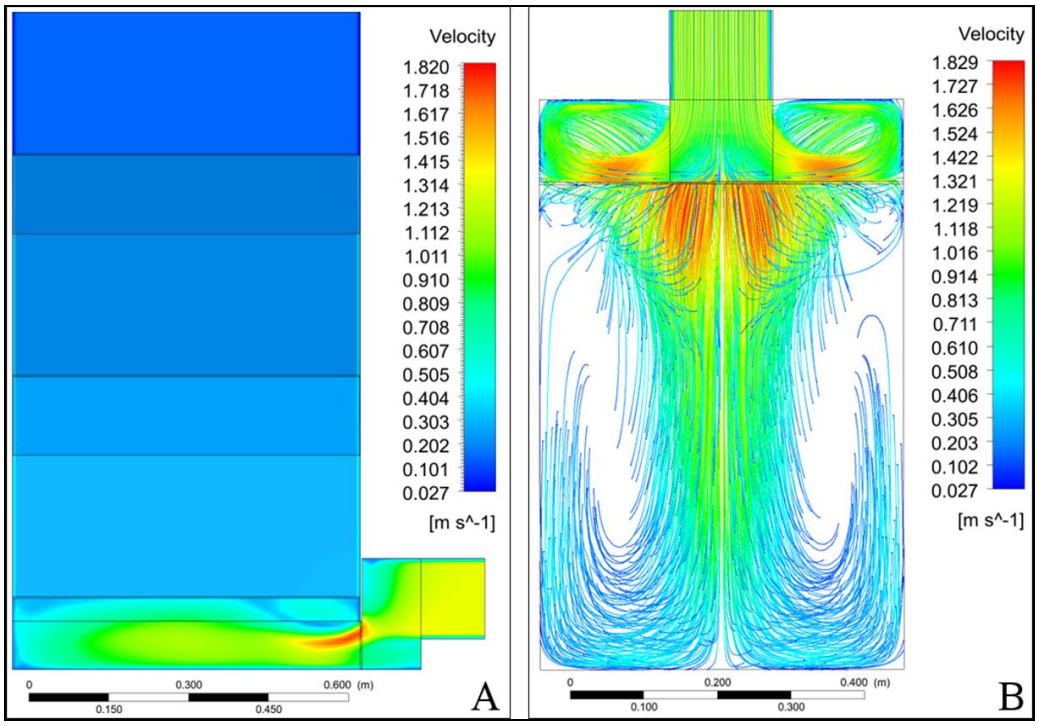

Figure 12. A. Rectangular-shaped unit velocity contours, **B.** Rectangular-shaped unit velocity streamlines top view.

Simultaneously, the contour plot displays an air velocity loss when passing through the coffee layers; nevertheless, this behaviour is expected and logical since a porous bed flow is considered and the air will undergo certain resistance as found by [51]. The air describes a low velocity in the grain beds, which could be improved if the initial velocity loss did not occur.

Figure 12B displays the top-streamline plot view, granting a visual illustration of the air circulation across the unit's geometry. After plotting 1000 points, an erratic and non-homogenous behaviour inside the dryer is seen; although the air distribution is symmetric, there are some sections without drying air presence. Hence, the drying in such zones will be incomplete or insufficient.

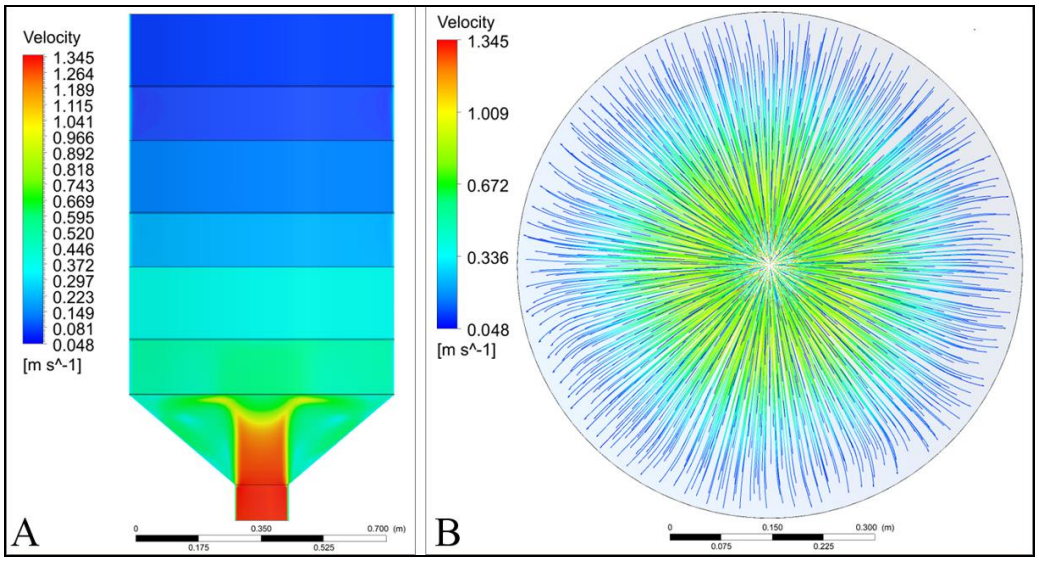

Figure 13. A. Circular-shaped unit velocity contours. **B.** Circular-shaped unit velocity streamlines top view.

Several findings were obtained after plotting the circular dryer simulation results, the velocity contour plot was also generated in the midplane of the unit. Figure 13A presents the velocity values across the dryer's geometry; it is seen that they are significantly higher than the obtained in the rectangular dryer analysis. At the entrance, the diffusor reduces the air velocity, however, the air inlet's vertical configuration, aligned with the equipment's vertical axis, ensures lower velocity losses than the reported by the rectangular unit; after generating a midplane in both geometries it was seen that the circular dryer provides an enhanced average air velocity higher in 29% than the rectangular one.

The air velocity in each stage of the circular dryer is higher than the described by the rectangular dryer, this means that the air is transiting faster through the circular dryer domains. [62] found that at larger drying air velocities the average air temperature flowing through the product will be also higher, hence, the drying time will be reduced. Consequently, Figure 13A outlines relevant information describing the stage velocity as another factor implied in the reduction of the drying time described by the circular shaped dryer. Although the diffusive tray generates extra resistance it helps to distribute the air evenly across the dryer’s volume, the velocity values are pretty acceptable and higher than expected, dynamizing the drying kinetics and improving the drying ratio between the air velocity and moisture removal.

It is seen in Figure 13B that the air streamlines are rather homogeneous, uniform, and symmetrical, covering most of all the dryer's transversal section. The improved distribution of the air will ensure an even drying coverage, throughout the grain bed, taking full advantage of the hot air's drying potential. Overall, these results indicate that the geometrical rearrangement of the drying unit offered several benefits and advantages, improving the drying process while enhancing the drying capacity and efficiency. Taken together, these results also provide important insights for further grain drying research, since they indicate a relevant relationship between the drying time as a function of the air velocity, temperature, bed height and airflow.

4.4. Conclusions

Two convective coffee dryers displaying two different drying chamber shapes have been investigated in this study. The drying capacity and drying air kinetics were of main interest to describe the drying process. The newly designed circular dryer exhibited a theoretical reduction in the drying time by 3.9 hours, representing an 18.3% drying time decrease as compared to the rectangular unit while reaching the required moisture content of 12% (wb). Hence the drying capacity is enhanced resulting in an increased capability to process wet coffee, accompanied by an expected lower energy and gas consumption while dynamizing the commercialization of the product potentially increasing the grower's profitability.

The computational fluid dynamics analysis confirmed that the drying air usage would be improved by changing the unit's geometry. When using a circular-shaped unit, the velocity was higher throughout the process, and the air distribution across the dryers' volumes displayed a more homogeneous behaviour, ensuring a uniform moisture removal in the product, improving its quality, innocuousness and potentially reducing its spoilage risk. Considering that the equipment is intended to improve the small farm coffee drying conditions, an easy re-design was arranged to maintain low manufacturing costs and simple operating processes. The extra elements such as the ventilator, motor and gas burner did not change in order to adapt the new dryer to the actual working conditions.

The results of this study clearly demonstrate that the newly designed cylindrical drying chamber shape can significantly improve the drying performance of coffee processed through the wet process. This might result in increased processing capacity and final coffee bean quality with a positive effect on the final income for the small-scale coffee producers not only in Colombia, but also in other regions where coffee is produced.

Conflict of Interest

We have no conflicts of interest to disclose.

Acknowledgments

The authors thank Prof. Jan Skočilas (Czech Technical University in Prague) for his assitance during the development of this study. This research was funded by the Internal Grant Agency of the Faculty of Tropical AgriSciences, Czech University of Life Sciences Prague, Grant number 20213101.

Contribution Statement

Eduardo Duque-Dussán: Conceptualization, Investigation, Methodology, Software, Writing – original draft. **Jan Banout:** Conceptualization, Supervision, Writing-review & editing, Funding acquisition.

Data Availability

The data that support the findings of this study are available from the corresponding author upon reasonable request.

Nomenclature

a: Arroba ≈ 12.5kg

a_s: Surface area of particles per unit volume [m^2 m^{-3}]

c_a: Specific heat capacity of air, [kJ kg^{-1} K^{-1}]

c_p: Specific heat capacity of the grain, [kJ kg^{-1} K^{-1}]

c_v: Specific steam heat capacity, [kJ kg^{-1} K^{-1}]

c_w: Specific heat capacity of water, [kJ kg^{-1} K^{-1}]

M_e: Balance moisture content, decimal.

r_0: Equivalent radius of the grain, [m]

ρ_b: Bulk density, [kg m^{-3}]

ρ_p: Dry weight density, [kg m^{-3}]

P_{vs}: Saturation vapor pressure, [kPa]

P_v: Partial vapor pressure, [kPa]

D: Humidity diffusion coefficient, [m^2 min^{-1}]

ε: Porosity [-]

G_a: Air mass flow per unit area, [kg m^{-2}]

h: Convective heat transfer coefficient, [kJ m^{-2} K^{-1}]

h_c: Convective grain heat transfer coefficient, [W m^{-2} K^{-1}]

H: Air humidity ratio, [kg_{steam} $kg_{dry\ air}^{-1}$]

H_0: Initial grain layer air humidity ratio, [kg_{steam} $kg_{dry\ air}^{-1}$]

H_f: Final grain layer air humidity ratio, [kg_{steam} $kg_{dry\ air}^{-1}$]

H_R: Air relative humidity, decimal notation.

ΔH: Removed moisture by drying air, [kg_{water} h^{-1}]

L: Water latent heat of vaporization, [kJ kg^{-1}]

M: Moisture content of the grain, decimal.

$\dot{Q}$: Volumetric rate, [m^3 min^{-1}]

S: Cross-section area perpendicular to airflow, [m^2]

T: Drying air temperature, [°C]

T_e: Drying air- grain equilibrium temperature [°C]

T_f: Air temperature after drying, [°C]

T_g: Grain temperature, [°C]

t: Time, [h]

Δt: Time interval, [h]

u: Velocity, [m s^{-1}]

V: Volume, [m^3]

CFD: Computational Fluid Dynamics

DPC: Dry Parchment Coffee

References

1. Pereira LL, Guarçoni RC, Pinheiro PF, Osório VM, Pinheiro CA, Moreira TR, et al. New propositions about coffee wet processing: Chemical and sensory perspectives. Food Chem. 2020;310: 125943. doi:10.1016/j.foodchem.2019.125943

2. Elhalis H, Cox J, Frank D, Zhao J. The role of wet fermentation in enhancing coffee flavor, aroma and sensory quality. Eur Food Res Technol. 2021;247: 485–498. doi:10.1007/s00217-020-03641-6

3. Kleinwächter M, Selmar D. Influence of drying on the content of sugars in wet processed green Arabica coffees. Food Chem. 2010;119: 500–504. doi:10.1016/j.foodchem.2009.06.048

4. Batista LR, Chalfoun SM, Silva CF, Cirillo M, Varga EA, Schwan RF. Ochratoxin A in coffee beans (Coffea arabica L.) processed by dry and wet methods. Food Control. 2009;20: 784–790. doi:10.1016/j.foodcont.2008.10.003

5. Manrique R, Vásquez D, Chejne F, Pinzón A. Energy analysis of a proposed hybrid solar–biomass coffee bean drying system. Energy. 2020;202: 1–8. doi:10.1016/j.energy.2020.117720

6. Tarzia A, dos Santos Scholz MB, de Oliveira Petkowicz CL. Influence of the postharvest processing method on polysaccharides and coffee beverages. Int J Food Sci Technol. 2010;45: 2167–2175. doi:10.1111/j.1365-2621.2010.02388.x

7. Culliao AGL, Barcelo JM. Fungal and mycotoxin contamination of coffee beans in Benguet province, Philippines. Food Addit Contam - Part A Chem Anal Control Expo Risk Assess. 2015;32: 250–260. doi:10.1080/19440049.2014.1001796

8. Suarez-Quiroz M, Gonzalez-Rios O, Barel M, Guyot B, Schorr-Galindo S, Guiraud J-P. Study of ochratoxin A-producing strains in coffee processing. Int J Food Sci Technol. 2004;39: 501–507. doi:10.1111/j.1365-2621.2004.00810.x

9. Bravo-Monroy L. A Network behind Coffee. J Rice Res Dev. 2019;2: 61–65. doi:10.36959/973/421

10. Barjolle D, Quiñones-Ruiz XF, Bagal M, Comoé H. The Role of the State for Geographical Indications of Coffee: Case Studies from Colombia and Kenya. World Dev. 2017;98: 105–119. doi:10.1016/j.worlddev.2016.12.006

11. García JC, Posada-Suárez H, Läderach P. Recommendations for the regionalizing of coffee cultivation in Colombia: A methodological proposal based on agro-climatic indices. PLoS One. 2014;9: 1–22. doi:10.1371/journal.pone.0113510

12. Peña-Quiñones AJ, Ramírez-Builes VH, Jaramillo-Robledo Á, Rendón-Sáenz JR, Arcila-Pulgarín J. Effects of Daylength and Soil Humidity on the Flowering of Coffee Coffea Arabica L. in Colombia. Rev Fac Nac Agron Medellín. 2011;64: 5745–5754.

13. Siagian P, Setyawan EY, Gultom T, Napitupulu FH, Ambarita H. A field survey on coffee beans drying methods of Indonesian small holder farmers. IOP Conf Ser Mater Sci Eng. 2017;237. doi:10.1088/1757-899X/237/1/012037

14. Duque-Orrego H, Saldarriaga-S F, López-Q JJ, Oliveros-Tascón CE. Economía del Secado del Café: Un Estudio de Caso. Avances Técnicos Cenicafé. Apr 2001: 1–8. Available: https://www.cenicafe.org/es/index.php/nuestras_publicaciones/avances_tecnicos/avance_tecnico_0286

15. Jurado-Chaná JM, Montoya-Restrepo EC, Oliveros-Tascón CE, García-Alzate J. Método para medir el contenido de humedad del café pergamino en el secado solar del café. Rev Cenicafé. 2009;60: 135–147. Available: https://www.cenicafe.org/es/publications/arc060%2802%29135-147.pdf

16. Montilla-Pérez J, Arcila-Pulgarín J, Aristizábal-Loaiza M, Montoya-Restrepo EC, Puerta-Quintero GI, Oliveros-Tascón CE, et al. Caracterización de Algunas Propiedades Físicas y Factores de Conversión del Café Durante el Proceso de Beneficio Húmedo Tradicional. Rev Cenicafé. 2008;59: 120–142. Available: http://www.cenicafe.org/es/publications/arc059(02)120-142.pdf

17. Mwithiga G, Kigo SN. Performance of a solar dryer with limited sun tracking capability. J Food Eng. 2006;74: 247–252. doi:10.1016/j.jfoodeng.2005.03.018

18. Gutiérrez-Flórez JM, Copete-López H. Hacia la Mejora del Secado Mecánico del Café en Colombia. TecnoLógicas. 2009; 109–132. doi:10.22430/22565337.241

19. de Brito RC, Tellabide M, Estiati I, Freire JT, Olazar M. Drying of particulate materials in draft tube conical spouted beds: Energy analysis. Powder Technol. 2021;388: 110–121. doi:10.1016/j.powtec.2021.04.074

20. Olazar M, San Jose MJ, Aguayo AT, Arandes JM, Bilbao J. Stable operation conditions for gas-solid contact regimes in conical spouted beds. Ind Eng Chem Res. 1992;31: 1784–1792. doi:10.1021/ie00007a025

21. Irudayaraj J, Haghighi K, Stroshine RL. Finite element analysis of drying with application to cereal grains. J Agric Eng Res. 1992;53: 209–229. doi:10.1016/0021-8634(92)80084-6

22. Chandrasekar V, Viswanathan R. Physical and Thermal Properties of Coffee. J Agric Eng Res. 1999;73: 227–234. doi:10.1006/jaer.1999.0411

23. Osorio Hernandez R, Ferreira Tinoco IDF, Correna Carlo J, Osorio Saraz JA, Aristizábal Torres ID. Bioclimatic analysis of three buildings for wet processing of coffee in Colombia. Rev Fac Nac Agron Medellín. 2018;71: 8609–8616. doi:10.15446/rfnam.v71n3.64566

24. Weigler F, Scaar H, Mellmann J. Investigation of Particle and Air Flows in a Mixed-Flow Dryer. Dry Technol. 2012;30: 1730–1741. doi:10.1080/07373937.2012.703742

25. Wang B, Wang J, Zhou G, Chen D. Drag Reduction by Microvortexes in Transverse Microgrooves. Adv Mech Eng. 2014;2014. doi:10.1155/2014/734012

26. Estiati I, Tellabide M, Saldarriaga JF, Altzibar H, Olazar M. Influence of the fountain confiner in a conical spouted bed dryer. Powder Technol. 2019;356: 193–199. doi:10.1016/j.powtec.2019.08.005

27. Sukunza X, Pablos A, Aguado R, Vicente J, Altzibar H, Olazar M. Continuous drying of fine and ultrafine sands in a fountain confined conical spouted bed. Powder Technol. 2021;388: 371–379. doi:10.1016/j.powtec.2021.04.081

28. Perazzini MTB, Freire FB, Ferreira MC, Freire JT. Stability and performance of a spouted bed in drying skimmed milk: Influence of the cone angle and air inlet device. Dry Technol. 2018;36: 341–354. doi:10.1080/07373937.2017.1331240

29. Cenkowski S, Jayas DS, Pabis S. Deep-Bed Grain Drying - A Review of Particular Theories. Dry Technol. 1993;11: 1553–1582. doi:10.1080/07373939308916919

30. Thompson TL, Peart RM, Foster GH. Mathematical Simulation of Corn Drying — A New Model. Trans ASAE. 1968;11: 0582–0586. doi:10.13031/2013.39473

31. Bakker-Arkema FW, Lerew LE, De Boer SF, Roth MG. Grain dryer simulation. Agricultural Experiment Station, Res. Rep 224, Michigan State University, East Lansing, USA; 1974.

32. Coradi PC, Borém FM, Reinato CH. Coffee Cherries Drying Process and the Influence of Environment Relative Humidity in the Mathematical Modeling, Moisture Content, and Enthalpy of Vaporization. Energ Na Agric. 2014;29: 148. doi:10.17224/energagric.2014v29n2p148-157

33. Hung N Van, Martinez R, Tuan T Van, Gummert M. Development and verification of a simulation model for paddy drying with different flatbed dryers. Plant Prod Sci. 2019;22: 119–130. doi:10.1080/1343943X.2018.1518723

34. Prakash B, Siebenmorgen TJ. MATHEMATICAL MODELING OF A CROSS-FLOW RICE DRYER WITH GRAIN INVERTERS. Trans ASAE. 2018;61: 1757–1765. doi:10.13031/trans.12927

35. Liu Q, Bakker-Arkema FW. A model-predictive controller for grain drying. J Food Eng. 2001;49: 321–326. doi:10.1016/S0260-8774(00)00229-6

36. Dalpasquale VA, Sperandio D, Kolling EEM. Performance of the Michigan drying simulation model with a new drying rate concept. Acta Sci - Agron. 2009;31: 553–557. doi:10.4025/actasciagron.v31i4.3872

37. Liu Z, Wu Z, Wang X, Song J, Wu W. Numerical simulation and experimental study of deep bed corn drying based on water potential. Math Probl Eng. 2015;2015: 13. doi:10.1155/2015/539846

38. Brooker DB, Bakker-Arkema FW, Hall CW. Drying and storage of grains and oilseeds. 2nd Revise. New York, NY, United States: Van Nostrand Reinhold, New York; 1992.

39. Ebrahimifakhar A, Yuill D. Inverse estimation of thermophysical properties and initial moisture content of cereal grains during deep-bed grain drying. Biosyst Eng. 2020;196: 97–111. doi:10.1016/j.biosystemseng.2020.05.021

40. Montoya-Restrepo EC, Oliveros-Tascón CE, Roa-Mejía G. Optimización Operacional del Secador Intermitente de Flujos Concurrentes para Café Pergamino. Rev Cenicafé. 1990;41: 19–33. Available: http://hdl.handle.net/10778/939

41. Rossi JR, Roa-Mejía G. Secagem e armazenamento de produtos agropecuários com uso de energia solar e ar natural. Secretaria da Indústria, Comércio, Ciência e Tecnologia, ACIESP (Academia de Ciências do Estado de São Paulo) n°22, 295p; 1980.

42. Trejos RA, Roa-Mejía G, Oliveros-Tascón CE. Humedad de equilibrio y calor latente de vaporización del café pergamino y del café verde. Rev Cenicafé. 1989;40: 5–15. Available: https://biblioteca.cenicafe.org/handle/10778/841

43. Dias CDA, Andrade ET De, Lemos IA, Borém FM, Barros EA. Sorption Isotherms and Isosteric Heat of Pericarp and Endosperm Tissues of Arabica Coffee Fruit. Eng Agrícola. 2020;40: 78–89. doi:10.1590/1809-4430-eng.agric.v40n1p78-89/2020

44. Corrêa PC, Goneli ALD, Júnior PCA, de Oliveira GHH, Valente DSM. Moisture sorption isotherms and isosteric heat of sorption of coffee in different processing levels. Int J Food Sci Technol. 2010;45: 2016–2022. doi:10.1111/j.1365-2621.2010.02373.x

45. Parra-Coronado A, Roa-Mejía G, Oliveros-Tascón CE. SECAFÉ Parte I: modelamiento y simulación matemática en el secado mecánico de café pergamino. Rev Bras Eng Agrícola e Ambient. 2008;12: 415–427. doi:10.1590/s1415-43662008000400013

46. Phitakwinai S, Thepa S, Nilnont W. Thin-layer drying of parchment Arabica coffee by controlling temperature and relative humidity. Food Sci Nutr. 2019;7: 2921–2931. doi:10.1002/fsn3.1144

47. Nilnont W, Thepa S, Janjai S, Kasayapanand N, Thamrongmas C, Bala BK. Finite element simulation for coffee (Coffea arabica) drying. Food Bioprod Process. 2012;90: 341–350. doi:10.1016/j.fbp.2011.06.007

48. Latham JP, Munjiza A, Lu Y. On the prediction of void porosity and packing of rock particulates. Powder Technol. 2002;125: 10–27. doi:10.1016/S0032-5910(01)00493-4

49. Azmir J, Hou Q, Yu A. CFD-DEM simulation of drying of food grains with particle shrinkage. Powder Technol. 2019;343: 792–802. doi:10.1016/j.powtec.2018.11.097

50. Severa L, Buchar J, Nedomová Š. Shape and size variability of roasted Arabica coffee beans. Int J Food Prop. 2012;15: 426–437. doi:10.1080/10942912.2010.487967

51. Zhong W, Xu K, Li X, Liao Y, Tao G, Kagawa T. Determination of pressure drop for air flow through sintered metal porous media using a modified Ergun equation. Adv Powder Technol. 2016;27: 1134–1140. doi:10.1016/j.apt.2016.03.024

52. Mizera, Herák D, Hrabě P, Kabutey A, Wasserbauer M, Pouzarová H. Describing of drying curves of green coffee beans using mathematical model. IOP Conf Ser Mater Sci Eng. 2018;420. doi:10.1088/1757-899X/420/1/012075

53. Ramirez-Martinez A, Benet J-C, Cherblanc F, García-Alvarado MA, Rodriguez-Jimenes G. Internal structure and water transport in the coffee bean. 17th Int Dry Symp (IDS 2010), Magdeburg, Ger. 2010; 1–8.

54. Kulapichitr F, Borompichaichartkul C, Suppavorasatit I, Cadwallader KR. Impact of drying process on chemical composition and key aroma components of Arabica coffee. Food Chem. 2019;291: 49–58. doi:10.1016/j.foodchem.2019.03.152

55. Dong W, Hu R, Chu Z, Zhao J, Tan L. Effect of different drying techniques on bioactive components, fatty acid composition, and volatile profile of robusta coffee beans. Food Chem. 2017;234: 121–130. doi:10.1016/j.foodchem.2017.04.156

56. Doymaz I, Pala M. The thin-layer drying characteristics of corn. J Food Eng. 2003;60: 125–130. doi:10.1016/S0260-8774(03)00025-6

57. Zhang S, Kong N, Zhu Y, Zhang Z, Xu C. 3D model-based simulation analysis of energy consumption in hot air drying of corn kernels. Math Probl Eng. 2013;2013. doi:10.1155/2013/579452

58. McMinn WAM, Magee TRA. Principles, methods and applications of the convective drying of foodstuffs. Food Bioprod Process Trans Inst Chem Eng Part C. 1999;77: 175–193. doi:10.1205/096030899532466

59. Cardoso DB, de Andrade ET, Calderón RAA, Rabelo MHS, de Almeida Dias C, Lemos IÁ. Determination of thermal properties of coffee beans at different degrees of roasting. Coffee Sci. 2018;13: 498–509. doi:10.25186/cs.v13i4.1491

60. Burmester K, Fehr H, Eggers R. A comprehensive study on thermophysical material properties for an innovative coffee drying process. Dry Technol. 2011;29: 1562–1570. doi:10.1080/07373937.2011.582595

61. Pérez-Alegría LR, Ciro VHJ, Abud LC. Physical and thermal properties of parchment coffee bean. Trans Am Soc Agric Eng. 2001;44: 1721–1726. doi:10.13031/2013.6983

62. Zhang R, Long J. Study on Drying Uniformity of Static Small-sized Drying Box for Fruits and Vegetables. Procedia Eng. 2017;205: 2615–2622. doi:10.1016/j.proeng.2017.10.201

5. Thermophysical Properties of Parchment Coffee: New Colombian Varieties.

Adapted from: Duque-Dussán E, Sanz-Uribe JR, Dussán-Lubert C, Banout J. Thermophysical properties of parchment coffee: New Colombian varieties. J Food Process Eng. 2023; 1–13. doi:10.1111/jfpe.14300

Abstract

The thermophysical properties of coffee have a special partaking during the drying process since a material-depending heat and mass transfer occurs between the bean and the drying air. Conditional to the thermophysical properties of the parchment coffee, the drying can be more or less efficient, affecting the final quality and seed safety. Several coffee varieties have been studied; however, the National Coffee Research Center of Colombia has developed new highly productive coffee varieties resistant to different diseases: Cenicafé 1 and Castillo®. Nevertheless, the thermophysical properties of these specific varieties were not yet investigated; moreover, the availability of information related to these properties of different coffee varieties in the literature is relatively scarce. Thus, this study targeted to determine the parchment coffee thermophysical properties of these new varieties at five different moisture contents % (wb): 53, 42, 32, 22 and 11%, using optimized techniques and methods to ensure high accuracy and exactness. It was found that the new varieties have larger, heavier, and denser beans; it was also seen that the bulk thermal conductivity and the bulk-specific heat are higher in these varieties than in the older ones. It was also revealed that the length, width, thickness, and surface area did not change as the moisture was removed, whereas the bulk density, kernel density, mass, bulk-specific heat, and bulk thermal conductivity decreased as the moisture was reduced. Displaying better thermophysical properties will improve the drying and roasting processes; hence, a better final product can be expected from these varieties.

Keywords: Coffee bean; Drying; Parchment coffee; Image analysis; Thermal and physical properties.

Practical applications

Knowing the thermal and physical properties of these new varieties will allow the growers and coffee processing facilities to predict, simulate and control different post-harvesting processes such as pulping, fermentation, drying, storing, and roasting. Also, the already developed mathematical models to estimate coffee drying times can be updated, improving the accuracy of the predictions, bed porosities, mass, and heat transfer in order to safeguard the innocuousness of the product.

5.1. Introduction

When coffee is processed using the wet method, it undergoes several steps until its final stage before being exported. It is picked, pulped, fermented, washed, and dried [1]. After washing and draining, the beans hold a moisture content of approximately 53% (wb), and they must be dried until reaching 10-12% (wb) [2]. Seeing that coffee has a very high moisture content, it becomes a suitable host for developing microorganisms, fungi, and molds [3]. That is why the drying process should occur as soon as possible, and it must be duly controlled until the final moisture content is reached. Leading to one issue that the coffee growers face when drying their product since the harvest peaks might overlap with the rainy seasons [4]; therefore, the drying process during this time is rather complicated, especially since they tend to sun-dry the coffee [5] and the temperature inside the drying facilities highly fluctuate.

One of the most important characteristics of grains and agricultural materials is the thermal and physical properties [6–8]; thanks to these attributes, the mass and heat transfer, resistance, storage information and quality standards can be predicted or calculated. These properties mainly affect the drying process [9], contemplating that the distribution in the drying bed depends on the material's size, mass, density (bulk and real), shape and other physical properties, while the drying time, efficiency, heat, and mass transfer, among others, depend on the thermal properties of the product.

The National Coffee Research Center of Colombia, seeking to provide Colombian coffee growers with coffee plants with high yield, good structure, and resistance to different diseases such as coffee rust or coffee berry disease (CBD), have developed new varieties that fulfil the previous requirements: Cenicafe 1 [10] and Castillo® [11]. Although these varieties have proved to provide high yields and disease resistance, the physical and thermal properties of the beans have not yet been calculated; on the other hand, the literature offers properties of older coffee varieties [12,13].

Considering the importance of the physical and thermal properties of coffee beans at different postharvest stages and seeing the lack of information from these high-value coffee varieties, the objective of this study was to determine the thermophysical properties (orthogonal dimensions, surface area, mass, bulk density, kernel density, bulk

thermal conductivity, and bulk-specific heat) of the new coffee varieties at five different moisture content values. It aims to gather accurate and relevant information about the changes in these properties as the grain dries. This will enable a deeper understanding of the transport processes that play an essential role in preserving grain quality.

5.2. Materials and Methods

This research was conducted at the National Coffee Research Center of Colombia (Cenicafé) in the postharvest discipline laboratories and facilities in the municipality of Manizales, Caldas (4°59'30.8"N 75°35'49.7"W; elevation of 1306 m.a.s.l). In this study, two varieties of *Coffea arabica L.* were studied: var. Cenicafé 1 (C1) and var. Castillo® (RC), both developed and bred by Cenicafé.

The physical and thermal characteristics of the parchment coffee were evaluated at five different moisture contents (% wb). A bifactorial experimental design in blocks was considered with three replications per variety; the first factor was the variety (C1 and RC), while the second factor was the moisture content (% wb): 53 %, 42%, 32%, 22% and 11% with a ±1% error margin. The block was defined as the experimental unit: the coffee load, 3 per variety, each composed of 50 kg of coffee berries at ripe stages 4, 5 and 6 [14].

The response variables were the grain's length (mm), width (mm), thickness (mm), surface area of the endocarp (mm^2), mass of the grain (g), kernel density (kg m^{-3}), bulk density (kg m^{-3}), bulk-specific heat (kJ kg^{-1} K^{-1}) and bulk thermal conductivity (W m^{-1} K^{-1}).

5.2.1. Sample preparation

After receiving and cleaning the berries, they were pulped, demucilaginated, washed, and dried; the washed and drained wet parchment coffee mass, weighing approximately 20 kg at 53% (wb), was first divided into five samples of 4 kg each before being placed in a forced convection mechanical dryer at 50°C to achieve the required moisture content.

To determine the initial moisture content of the parchment coffee mass, three 10 g samples of wet coffee were placed in a laboratory oven at 105°C for 16 hours to achieve complete grain dryness as specified in the international standard ISO6673:2003. The initial moisture content was determined by using the gravimetric ratio shown in Equation 1.

$$m_f = \frac{m_i(1 - M_i)}{(1 - M_f)} \quad (1)$$

The initial and final mass values (g) are given by m_i and m_f, while M_i and M_f correspond to the sample's initial and final moisture contents (% (wb)). After identifying the initial moisture content, knowing the initial mass value and the desired final moisture content, equation 1 was used to calculate the final mass of coffee in each tray that met the final moisture conditions, and then it was monitored until the target was reached.

As soon as the samples reached the desired moisture content, they were removed from the dryer, tagged, and sealed in airtight plastic bags to prevent moisture loss or gain, and were stored in a temperature and humidity-controlled storage room for further analysis.

5.2.2. Physical properties

At the established moistures, the orthogonal dimensions (mm) of the grain (length, width, and thickness), the surface area (mm^2) of the parchment (endocarp), mass (g), kernel density (kg m^{-3}), and bulk density (kg m^{-3}) were calculated. Per replication, 60 grains were randomly chosen based on moisture levels. Of these, 30 were used for mass calculations and kernel densities and the other 30 for endocarp area and geometric values measurement, in contrast, the additional properties were calculated in bulk.

5.2.2.1. Dimensions

The length (*l*), the width (*w*) and the thickness (*t*) of each grain in the sample were measured (mm) with a digital micrometer with a precision of 0.001 mm. Each of these three values was taken between the most distant points in the 3-dimensional space (Figure 1). All the beans were coded to ensure their traceability.

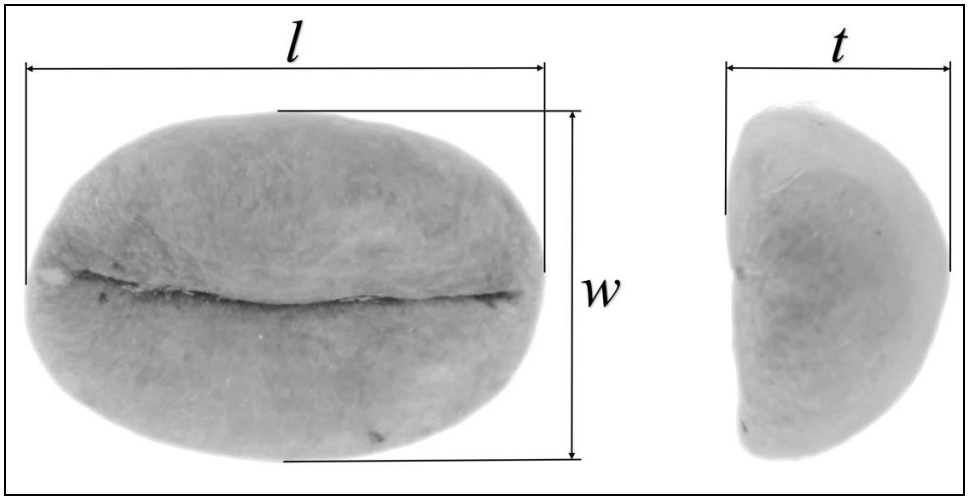

Figure 1. Length, width, and thickness of the grain.

5.2.2.2. Parchment (endocarp) surface area

In order to provide better contrast, the endocarp from each of the measured and traced beans was carefully removed, flattened, and placed on a blue RGB (53, 90, 255) surface, which depicted the highest contrast with the endocarp colors according to [15]. A picture of the endocarp parts was taken with a high-resolution camera at a constant height after capturing a 10 mm quartz pattern to analyze the image further. The samples were illuminated with two 12 W, 50-70 lm W^{-1} LED lights (bottom-top) with a color index of 70 to highlight the area of interest and reduce the brightness for a sharper capture. The complete setup is shown in Figure 2.

Images were imported into ImageJ (Fiji) software and scaled according to the 10 mm quartz pattern after being taken. A macro was developed so all the images could be

examined at once following the code protocol; after opening the picture, the program splits the RGB color matrix into three channels: Red, Green, and Blue. The Red channel was chosen since it provided the highest contrast between the blue background and the tan endocarp.

Afterwards, a threshold of 90/254 intensity was used to create a binary image out of the red intensity matrix (grayscale of the red channel). Where 1 indicated the target area and 0 the background. The resulting image was then analyzed considering areas larger than 0.2 mm2, an overlay was also added to identify both the borders and the included areas. The analysis outputwas the total surface area of the endocarp of each bean in mm2, attained by the software multiplying the number of pixels set times the resolution. Figure 3 displays the stages of the image during its study.

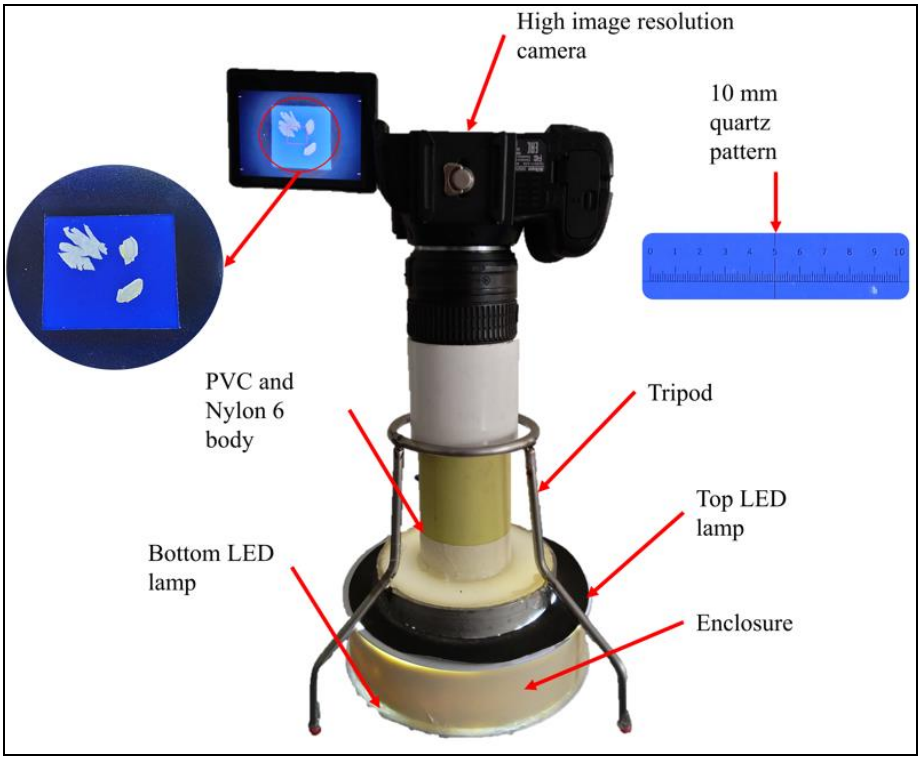

Figure 2. Coffee endocarp photographing setup.

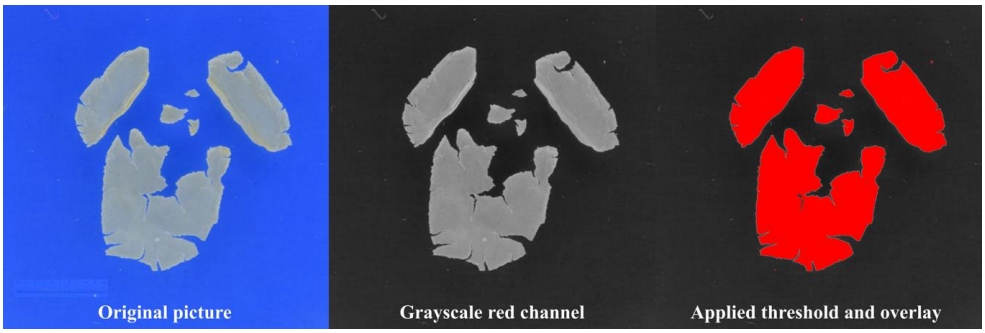

Figure 3. Image analysis process.

The resolution of the analysis when setting the scale with the pattern was 0.0002293 mm^2 $pixel^{-1}$; establishing a relationship between the orthogonal dimensions, and the surface area is one of the expected outputs.

5.2.2.3. Mass

The mass (g) of the 30 grains per moisture content was determined by using an analytical balance (Mettler Toledo ML204 NewClassic MF) with a capacity of 220 g and readability and resolution of 0.1mg. The grains were numbered to track them.

5.2.2.4. Kernel Density

The kernel density (kg m^{-3}) was calculated using the paraffin method [7,8], each of the grains numbered in section 1.2.3 was covered with paraffin, and the process was performed. The density of paraffin was calculated by pouring liquid paraffin into a known volume, weighing it after solidification, and calculating the mass/volume ratio.

5.2.2.5. Bulk density

The bulk density (kg m^{-3}) of the coffee was determined by filling a cylinder with a calibrated volume of 1 liter with free-falling coffee beans in accordance with the procedure outlined in ISO 6669:1995. Excess grains on top of the cylinder were removed by sliding a stainless-steel rectified ruler lengthwise along the cylinder's border. Once the grain mass in the cylinder was weighed, its mass divided by the

volume of the cylinder yielded the bulk density. Four replications were performed per moisture content per variety.

5.2.3. Thermal properties

In the moisture content range of interest, the bulk-specific heat capacity and the bulk thermal conductivity of parchment coffee were calculated.

5.2.3.1. Bulk-specific heat capacity Cp

To determine the bulk-specific heat capacity (kJ kg^{-1} K^{-1}) of the coffee ($C_{pcoffee}$), the method of mixtures [16,17] was used. A 100 g sample of coffee was heated indirectly in a water bath; a thermocouple temperature sensor controlled the grain temperature. To ensure a homogeneous temperature profile throughout all samples, the system was stabilized once the coffee mass reached 80°C ($T_{icoffee}$) for 10 minutes. It was then dropped into a calorimeter containing 500 g of water (m_{water}) at ambient temperature (T_{iwater}) previously measured by a DS18B20 digital temperature sensor mounted on top of the calorimeter, and the system was then gently stirred. As the temperature rose, the system reached equilibrium temperature (T_{eq}) and considering that the water gains (Q_{water}) the heat lost by the coffee (Q_{coffee}) and the specific heat capacity of the water is known (C_{pwater}), the following balance was obtained.

$$Q_{water} = -Q_{coffee}$$

Where:

$$Q_{water} = m_{water} C_{p_{water}} (T_{eq} - T_{i_{water}})$$

$$Q_{coffee} = m_{coffee} C_{p_{coffee}} (T_{eq} - T_{i_{coffee}})$$

Hence, the bulk-specific heat capacity can be calculated as shown in equation 2:

$$C_{p_{coffee}} = \frac{-m_{water} C_{p_{water}} \left(T_{eq} - T_{i_{water}}\right)}{m_{coffee} \left(T_{eq} - T_{i_{coffee}}\right)} \quad (2)$$

The bulk-specific heat capacity of the coffee measurement was replicated three times at each moisture content level per variety to decrease the error. The temperature change was measured by a DS18B20 digital temperature sensor and registered on an Arduino-based data logger.

5.2.3.2. Bulk thermal conductivity K

The conductometer shown in Figure 4 was designed and built to measure the bulk thermal conductivity (W m^{-1} K^{-1}) of parchment coffee. Its working principle relies on the line heat source method [18–20], where a constant heat source within a material rises the temperature of such medium. The linear temperature change in the material can be estimated and depending on the time it takes the temperature to travel through a certain length, the conductivity of the material can be determined.

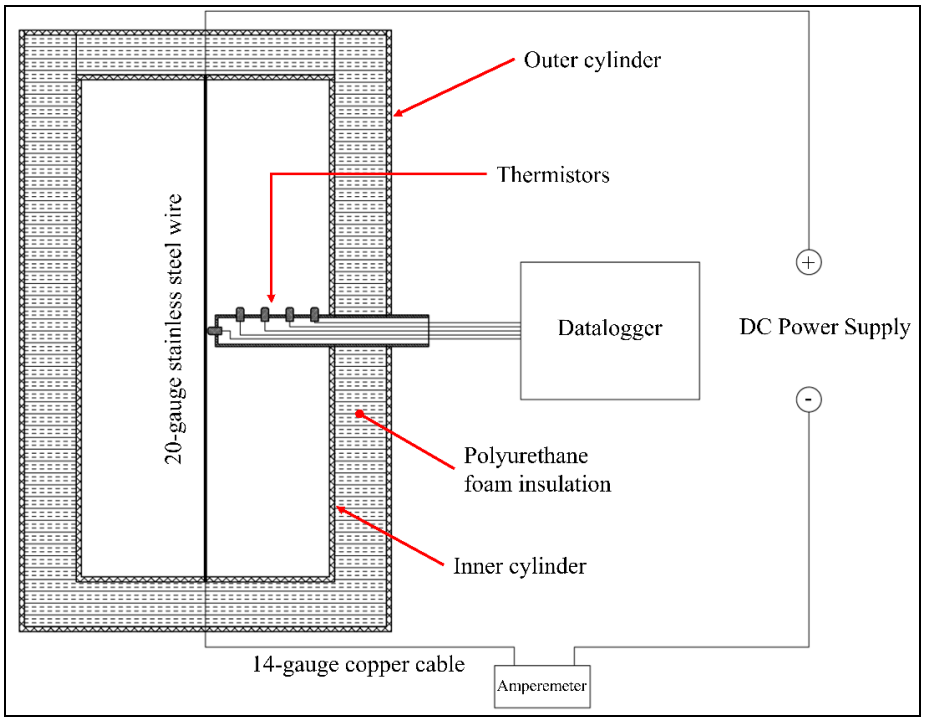

Figure 4. Conductometer setup.

In this case, a 20-gauge stainless steel wire, with a resistivity of 1.4 Ω m^{-1} was connected through a 14-gauge copper cable to a D.C. power supply. The power supply was set to deliver 1.2 V with a current of 4.33 A, raising the wire's temperature to 86°C. The inner cylinder of the apparatus was made out of a 110 mm PVC pipe with a length of 20 cm; the outer cylinder was constructed with a 160 mm PVC pipe, allowing a gap

between cylinders of 22.9 mm where polyurethane foam was applied as thermal insulation.

A set of five NTC100 thermistors were parallelly located to the wire 1 cm apart, starting from the central axis of the device towards the wall. Once the wire was heated, each thermistor registered the temperature change linearly for 45 min with intervals of 0.5s. The data was directly saved in an Arduino-based data logger with a mega ADK microcontroller board with a real-time clock, adjusted with a signal conditioning circuit and an SD storage module.

The process was repeated three times per moisture content; the obtained data was then used to calculate the bulk thermal conductivity using equation (3) [21]. Which involves the voltage (*V*), electrical current (*I*), distance from the central axis (*L*), time (*t**) and temperature (*T*).

$$K = \left[\frac{V\ I \ln\left(\frac{t_2^*}{t_1^*}\right)}{4\pi\ L\ (T_2 - T_1)} \right] \tag{3}$$

5.3. Results and Discussion

As shown in Table 1, both varieties exhibited similar physical and thermal properties; however, the RC variety had higher values in terms of length, width, and thickness. With the RC seed being longer, wider, and thicker, it makes sense that its surface area is also higher than the C1. However, it is also noted that the surface area and orthogonal dimensions do not change substantially when the moisture is removed, indicating that they may not be entirely dependent on the moisture content, as suggested by [12]. Both C1 and RC parchment coffees are larger than other varieties [12,22,23] or mutations such as Caturra [24].

Table 1. Mean, standard deviation and 95% confidence interval for the evaluated variables.

Variable	Variety	Moisture content % (wb)	Mean	Standard deviation	Confidence Interval	
					Lower bound	Upper bound
Length (mm)	C1	53	13.06	0.94	12.71	13.41
		42	12.80	0.62	12.57	13.03
		32	12.56	0.81	12.26	12.87
		22	12.39	0.82	12.08	12.69
		12	12.41	0.88	12.08	12.73
	RC	53	13.42	0.74	13.14	13.69
		42	13.27	0.76	12.99	13.56
		32	13.02	0.67	12.77	13.27
		22	13.26	0.73	12.99	13.53
		12	12.69	0.70	12.43	12.95
Width (mm)	C1	53	9.36	0.48	9.18	9.54
		42	8.93	0.55	8.3	9.4
		32	9.08	0.39	8.94	9.23
		22	9.09	0.42	8.93	9.24
		12	9.12	0.65	8.87	9.36
	RC	53	9.46	0.43	9.30	9.62
		42	9.38	0.75	9.10	9.66
		32	9.13	0.48	8.95	9.31
		22	9.32	0.49	9.14	9.50
		12	9.22	0.61	9.00	9.45
Thickness (mm)	C1	53	5.68	0.33	5.56	5.80
		42	5.45	0.29	5.34	5.56
		32	5.57	0.32	5.45	5.69
		22	5.47	0.39	5.32	5.61

		12	5.68	0.33	5.56	5.80
	RC	53	5.45	0.29	5.34	5.56
		42	5.57	0.32	5.45	5.69
		32	5.47	0.39	5.32	5.61
		22	5.68	0.33	5.56	5.80
		12	5.45	0.29	5.34	5.56
Surface area (mm^2)	C1	53	315.95	58.40	294.14	337.76
		42	275.71	24.60	266.53	284.90
		32	279.34	20.35	271.74	286.94
		22	277.65	27.69	267.31	287.99
		12	289.35	31.71	277.51	301.19
	RC	53	286.73	23.39	277.99	295.46
		42	303.05	25.71	293.45	312.65
		32	288.37	23.76	279.50	297.24
		22	295.35	27.05	285.25	305.46
		12	293.05	22.65	284.59	301.51
Bulk density ($kg\ m^{-3}$)	C1	53	702	0.002	700	710
		42	566	0.03	501	631
		32	486	0.01	451	520
		22	418	0.02	360	471
		12	388	0.002	381	390
	RC	53	696	0.003	695	701
		42	575	0.01	561	591
		32	491	0.01	472	512
		22	428	0.01	403	461
		12	393	0.01	373	421
	C1	53	959	0.00001	958	961
		42	897	0.00005	896	902

Kernel density (kg m^{-3})		32	839	0.00018	837	842
		22	781	0.00010	781	781
		12	722	0.00017	721	723
		53	954	0.00004	952	955
		42	891	0.00011	891	891
	RC	32	834	0.00010	832	835
		22	777	0.03341	775	801
		12	719	0.00007	718	720
Mass (g)		53	0.4975	0.01042	0.47	0.52
		42	0.4297	0.06302	0.27	0.59
	C1	32	0.3430	0.01434	0.31	0.38
		22	0.3036	0.00514	0.29	0.32
		12	0.3096	0.06393	0.15	0.47
		53	0.4696	0.01865	0.42	0.52
		42	0.3787	0.02644	0.31	0.44
	RC	32	0.3214	0.00433	0.31	0.33
		22	0.3083	0.01264	0.28	0.34
		12	0.2651	0.00652	0.25	0.28
C_p (kJ kg^{-1} K^{-1})		53	4.722	0.002	4.717	4.728
		42	4.127	0.007	4.110	4.145
	C1	32	3.572	0.004	3.563	3.581
		22	3.043	0.003	3.036	3.050
		12	2.502	0.002	2.496	2.508
		53	4.652	0.003	4.644	4.659
		42	4.065	0.000	4.064	4.065
	RC	32	3.507	0.009	3.485	3.529
		22	2.974	0.004	2.963	2.985
		12	2.443	0.013	2.411	2.475

K (W m^{-1} K^{-1})	C1	53	0.023	0.00011	0.023	0.023
		42	0.021	0.00018	0.020	0.021
		32	0.018	0.00003	0.018	0.018
		22	0.015	0.00016	0.015	0.016
		12	0.013	0.00023	0.013	0.014
	RC	53	0.022	0.00002	0.022	0.022
		42	0.019	0.00012	0.019	0.020
		32	0.017	0.00005	0.017	0.017
		22	0.014	0.00028	0.014	0.015
		12	0.012	0.00023	0.012	0.013

As Figure 5 shows, during drying, there was a significant shrinkage ratio of ~7% [25] for the endosperm (seed) than the one for the endocarp [26–28]. This generates an air chamber that restricts the moisture flow from the inner part to the surface, making the coffee drying process more energy-demanding than other grains [29]. However, the grain's outer orthogonal dimensions did not change significantly.

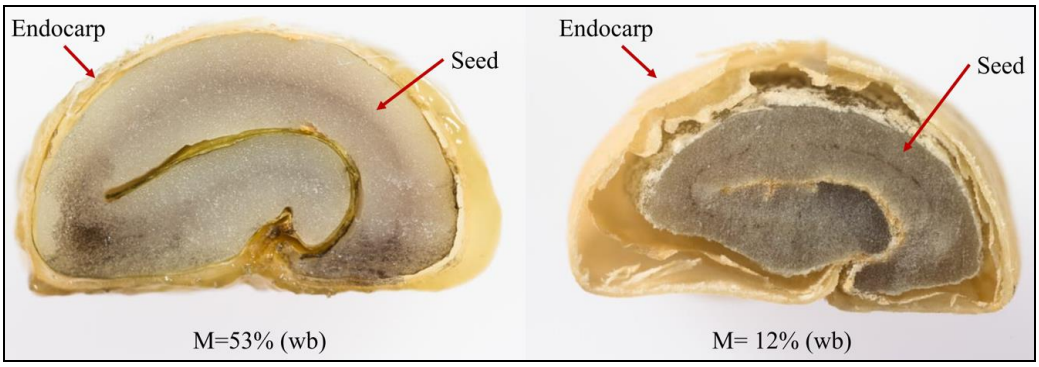

Figure 5. Parchment coffee cross-sections at different moisture contents *M*.

In contrast, there was a notable reduction in other properties with moisture removal. The bulk density of C1 and RC exhibited similar behavior, with RC's density slightly higher than C1's. Despite C1's higher kernel density at all moisture stages, C1 and RC had higher kernel density values than other varieties [12,24].

Some authors stated that the denser the seed, the better the quality of the coffee, arguing that the roasting process can be done evenly across the volume of the beans

[27,30,31], hence, the greater kernel density makes the two evaluated varieties more attractive to customers. According to table 1, the C1 bean mass was larger than its counterpart RC, which is indicative of a higher kernel density. This property showed that while RC grain is overall bigger than C1, it is also less dense and lighter; still, both RC and C1 produce heavier grains than other varieties (Figure7).

Likewise, the thermal properties of the bean change significantly according to the moisture content. The water held in the bean's inner structure strongly influences both the Cp and the K; C1 presented higher values than RC in both variables. Despite this, C1 and RC shared similar values, which were higher than those documented for Caturra by [24] and other varieties [12].

These results were positive as the evaluated properties affect the quality of the coffee and several postharvest processes, mainly the drying stage. When the new varieties are packed on the drying bed, the grains will have a larger surface area and a more extensive contact zone, intensifying the heat and mass transfer. Moreover, when presenting better bulk-thermal conductivity and bulk-specific heat, the drying process could be faster for such varieties, and their preservation, storage, and quality will be easier to attain.

Table 2 shows an averaged result for each variable per variety without considering the moisture content, with a 95% confidence interval.

Table 2. Mean, standard deviation and 95% confidence interval for the evaluated variables, averaged values.

Variable	Variety	Mean	Standard deviation	Confidence interval	
				Lower bound	Upper bound
Length (mm)	C1	12.64	0.85	12.51	12.78
	RC	13.13	0.76	13.01	13.25
Width (mm)	C1	9.12	0.52	9.03	9.20
	RC	9.30	0.57	9.21	9.39
Thickness (mm)	C1	5.53	0.35	5.48	5.59
	RC	5.56	0.28	5.52	5.61

Surface area (mm^2)	C1	287.60	37.84	281.50	293.71
	RC	293.31	24.92	289.29	297.33
Bulk density ($kg\ m^{-3}$)	C1	515	0.13	361	672
	RC	520	0.12	372	671
Kernel density ($kg\ m^{-3}$)	C1	840	0.093	724	955
	RC	839	0.090	727	950
Mass (g)	C1	0.377	0.084	0.272	0.481
	RC	0.349	0.079	0.251	0.447
C_p ($kJ\ kg^{-1}\ K^{-1}$)	C1	3.593	0.874	2.508	4.678
	RC	3.528	0.871	2.446	4.610
K ($W\ m^{-1}\ K^{-1}$)	C1	0.018	0.004	0.012	0.022
	RC	0.017	0.004	0.013	0.023

The averaged variable value per variety, disregarding the moisture, confirmed the information displayed in Table 1. RC held higher orthogonal dimensions, surface area, and bulk density, whereas C1 had higher kernel density, mass, bulk-specific heat, and bulk thermal conductivity values.

To find how the factors affected the response variables, an ANOVA table followed by a Tukey test is displayed in Table 3. The p-values and the test indicated no interaction between the moisture content and the variety for the length, but they did interact independently. The mean of the bean's width was higher in RC independently from the moisture content; there was no interaction between the variety and the moisture content, and they did not separately influence the thickness or the surface area.

Table 3. ANOVA analysis (p-values) and Tukey test (observation). V: Variety. M: Moisture content.

Variable	Variation source	p-value	Observation
Length	V	**<0.0001**	RC grain's length was in average larger independently from the moisture content.

(mm)	M	0.12	The moisture content did not affect the length.
	V*M	0.516	There was no interaction between the variety and the moisture content over the length.
Width (mm)	V	**0.023**	RC bean's width was in average larger independently from the moisture content.
	M	0.136	The moisture content did not affect the width.
	V*M	0.475	There was no interaction between the variety and the moisture content over the width.
Thickness (mm)	V	0.513	The variety did not influence the thickness.
	M	0.069	The moisture content did not influence the thickness of the grain
	V*M	0.652	There was no interaction between the variety and the moisture content over the thickness.
Surface area (mm^2)	V	0.478	The variety did not influence the surface area.
	M	0.682	Moisture content did not influence surface area
	V*M	0.247	There was no interaction between the variety and the moisture content over the surface area.
Bulk density ($kg\ m^{-3}$)	V	0.346	Variety did not influence bulk density
	M	**<0.0001**	The average bulk density was higher when the moisture content of the grain is 53% and decreases as the humidity decreases.
	V*M	0.808	There was no interaction between variety and moisture content over bulk density
Kernel density ($kg\ m^{-3}$)	V	0.804	The variety did not influence the kernel density.
	M	**<0.0001**	The average kernel density of the grain was different for each moisture, decreasing when the moisture content decreases.
	V*M	0.445	There was no interaction between variety and moisture content over kernel density.
Mass	V	**0.026**	Regardless of the moisture content, C1 had a higher average mass than the RC

(g)	M	**<0.0001**	The average mass of the grain was different for each moisture, decreasing when the moisture content decreases.
	V*M	0.590	There was no interaction between the variety and the moisture content on the mass.
C_p ($kJ\ kg^{-1}\ K^{-1}$)	V	**<0.0001**	The average C_p value was higher in C1, regardless the moisture content.
	M	**<0.0001**	The average C_p value was different for each moisture content, the highest being at 53% (wb), regardless of variety.
	V*M	0.462	There was no interaction between the variety and the moisture content on the C_p value.
K ($W\ m^{-1}\ K^{-1}$)	V	**<0.0001**	The average k value was higher in C1, regardless the moisture content.
	M	**<0.0001**	The average K value was different for each moisture content, the highest being at 53% (wb), regardless of variety.
	V*M	0.370	There was no interaction between the variety and the moisture content on the value of K

A statistically different bulk density was found for each moisture level, and the higher the grain moisture, the higher the bulk density. The average Cp value was higher in C1, regardless of the moisture content. The average Cp value differed for each moisture, the highest being at the value of 53%, irrespective of the variety. There was no interaction between the variety and the moisture content on the Cp value; the same phenomenon was seen in the bulk thermal conductivity K.

Because of the importance of the bulk density, kernel density, bulk-specific heat and thermal conductivity and their dependence on the moisture content, they were further compared (Figures 6, 7 8 and 9) with the values obtained for the same variables for the Caturra mutation published by [24].

As seen in Figure 6, both C1 and RC have higher bulk density ($kg\ m^{-3}$) values; the linear regressions for C1 and RC are:

$$\rho_{b,C1} = 266.053 + 763.742 M_{\%\,(wb)} \quad (r^2 = 0.94997) \tag{4}$$

$$\rho_{b,RC} = 278.088 + 740.38 M_{\%\,(wb)} \quad (r^2 = 0.95) \tag{5}$$

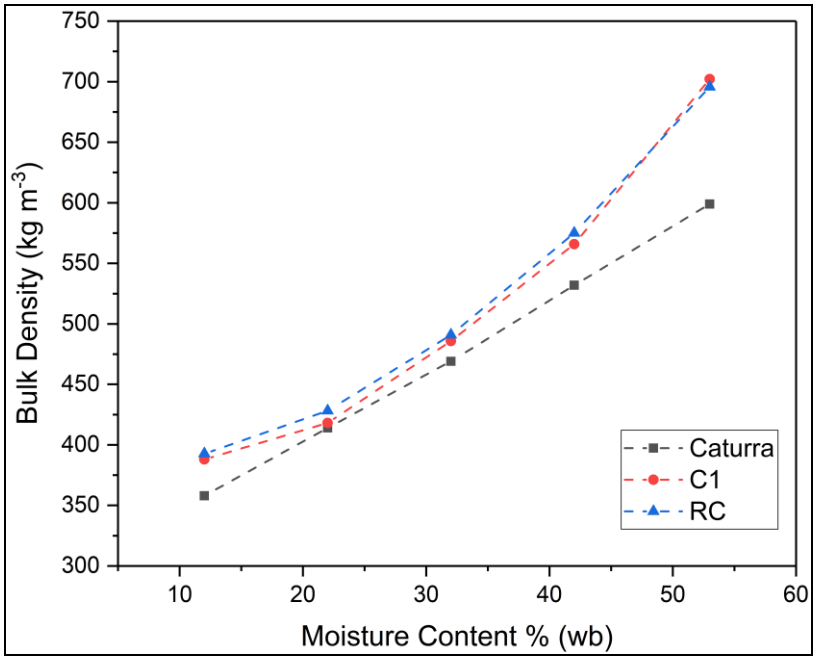

Figure 6. Comparative bulk densities as a function of the moisture content.

As seen in Figure 6, the bulk density values for Caturra were considerably lower than RC and C1. This property could impact storage and drying matters; since the bulk density is high, its porosity will be lower [32]. Hence, when drying, the air will be forced through the grain bed, performing a homogeneous moisture removal [33,34].

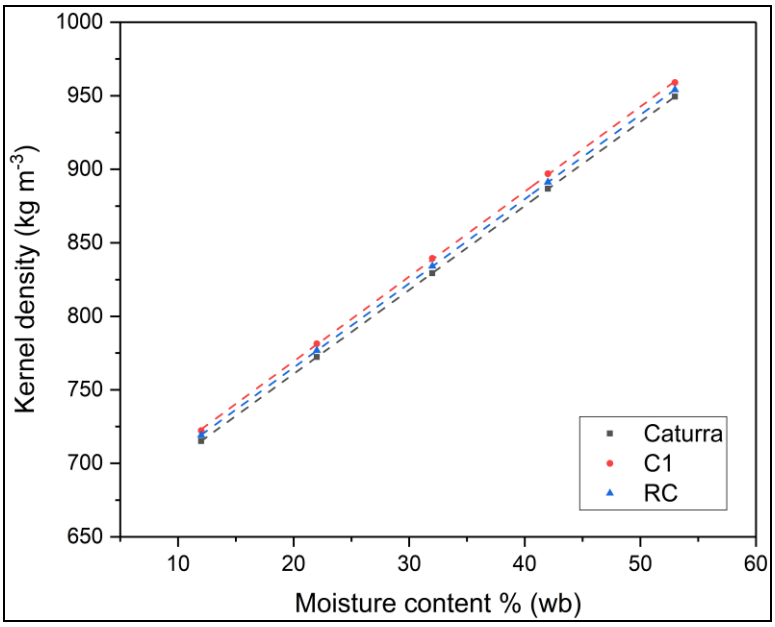

Figure 7. Comparative kernel densities as a function of the moisture content.

In Figure 7, the behavior of the kernel density (kg m^{-3}), as mentioned before, was highly affected by the moisture content. The three lines were closely related, yet, both C1 and RC were higher than Caturra. Their linear regression equations as a function of the moisture content were found to be:

$$\rho_{k,C1} = 577.54 M_{\%\,(wb)} + 653.82 \quad (r^2 = 0.9997) \tag{6}$$

$$\rho_{k,RC} = 572.95 M_{\%\,(wb)} + 650.56 \quad (r^2 = 0.9996) \tag{7}$$

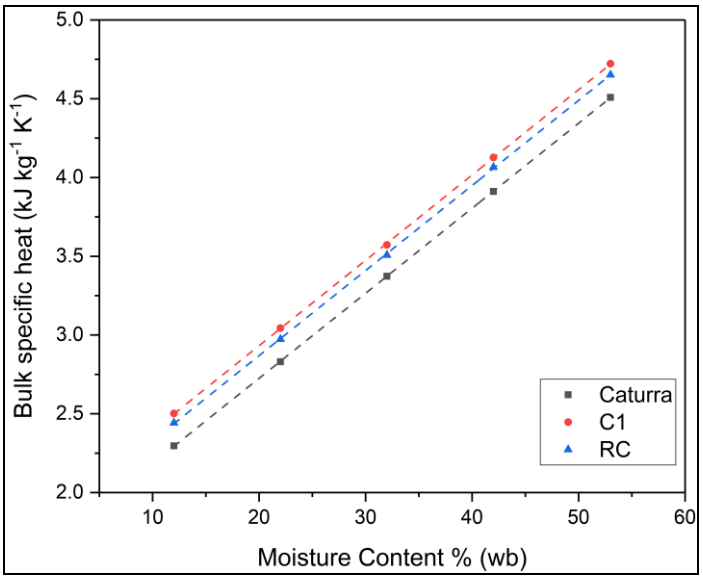

Figure 8. Comparative bulk-specific heats as a function of the moisture content.

C1 and RC had a higher bulk-specific heat than Caturra (Figure 8), meaning that the grains need more energy to raise their temperature. Nonetheless, it also means that they will hold the heat during a more extended period than their counterpart Caturra; this characteristic could have a positive impact on reducing drying times, allowing even moisture removal across the bean's volume [35,36]. Relevant outcomes when sun drying, for example, where the temperature fluctuations occur rapidly in time [37–39].

The bulk-specific heat (kJ kg^{-1} K^{-1}) linear regression equations for C1 and RC are shared as following:

$$C_{p,C1} = 5.42M_{\%\,(wb)} + 1.85 \quad (r^2 = 0.9998) \tag{8}$$

$$C_{p,RC} = 5.40M_{\%\,(wb)} + 1.78 \quad (r^2 = 0.9997) \tag{9}$$

Even though the bulk thermal conductivity values were low when compared to different agricultural products [40–42], both evaluated varieties presented higher bulk thermal conductivity values than the Caturra mutation and other varieties [12,23,24], implying that they are able to transfer heat faster than other ones (Figure 9). Suppose this property is combined with the fact that they also displayed higher Cp values, then, for such varieties, the heat will travel faster across the grain bed thanks to the bulk

thermal conductivity and will also remain for a more extended time due to the Cp. Processes such as drying and fermentation using the wet method [43,44] could be improved.

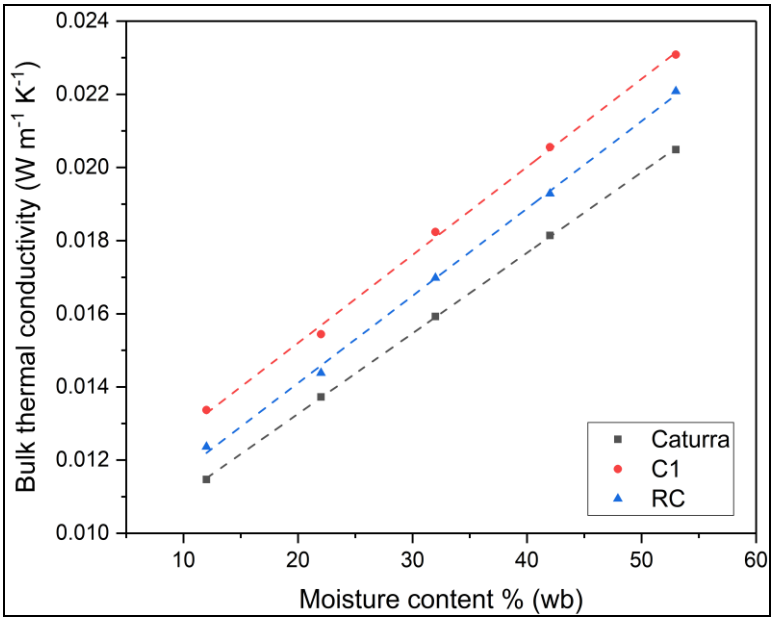

Figure 9. Comparative bulk thermal conductivities as a function of the moisture content.

The bulk thermal conductivity (W m^{-1} K^{-1}) linear regression equations for C1 and RC are presented as:

$$K_{C1} = 0.0241 M_{\%\,(wb)} + 0.0104 \quad (r^2 = 0.9984) \tag{10}$$

$$K_{RC} = 0.0239 M_{\%\,(wb)} + 0.0093 \quad (r^2 = 0.9986) \tag{11}$$

As seen in Figure 9, the bulk thermal conductivity values decreased as the moisture content decreased; nonetheless, a significant difference was noted between the evaluated varieties once the grain reached the desired moisture content.

5.4. Conclusions

The new parchment coffee beans of the new varieties developed by Cenicafé have different thermal and physical properties than the traditional varieties, so those processes that depend on them can be improved and optimized. The results of this study will help to understand the heat and mass transfer singularities during the drying process of the two studied varieties. They can also be used to design coffee dryers and update the drying simulation models to predict the coffee drying curves accurately. Furthermore, they allow for estimating the roast quality values and controlling possible storage damage.

There is no relationship between the moisture content of the parchment coffee and its geometric properties: length, width, thickness, and surface area. While the other physical properties studied: mass, bulk density, and kernel density, are dependent on moisture content, meaning that reducing moisture content will decrease their value and vice versa. Additionally, the study revealed that the bean's moisture content has a direct proportionality to the thermal properties such as bulk-specific heat and bulk thermal conductivity, both decreasing as moisture decreases and increasing as moisture rises.

Acknowledgments

The authors thank the members of the postharvest discipline of the National Coffee Research Center of Colombia (Cenicafé) for their assistance during the development of this study. This research was funded by the National Coffee Research Center of Colombia (Cenicafé) project number POS103010 and by the Internal Grant Agency of the Faculty of Tropical AgriSciences, Czech University of Life Sciences Prague, Grant number 20223109.

Contribution Statement

Eduardo Duque-Dussán: Conceptualization, Investigation, Methodology, Software, Writing – original draft. **Carmen Dussán-Lubert:** Data curation, Methodology, Software, Formal analysis. **Juan R. Sanz-Uribe:** Writing-Review, Conceptualization. **Jan Banout:** Conceptualization, Supervision, Writing-review & editing, Funding acquisition.

Conflict of Interest Statement

The authors declare no conflicts of interest.

Data Availability Statement

The data that support the findings of this study are available from the corresponding author upon reasonable request.

References

1. Tarzia A, dos Santos Scholz MB, de Oliveira Petkowicz CL. Influence of the postharvest processing method on polysaccharides and coffee beverages. Int J Food Sci Technol. 2010;45: 2167–2175. doi:10.1111/j.1365-2621.2010.02388.x

2. Manrique R, Vásquez D, Chejne F, Pinzón A. Energy analysis of a proposed hybrid solar–biomass coffee bean drying system. Energy. 2020;202: 1–8. doi:10.1016/j.energy.2020.117720

3. Batista LR, Chalfoun SM, Silva CF, Cirillo M, Varga EA, Schwan RF. Ochratoxin A in coffee beans (Coffea arabica L.) processed by dry and wet methods. Food Control. 2009;20: 784–790. doi:10.1016/j.foodcont.2008.10.003

4. García JC, Posada-Suárez H, Läderach P. Recommendations for the regionalizing of coffee cultivation in Colombia: A methodological proposal based on agro-climatic indices. PLoS One. 2014;9: 1–22. doi:10.1371/journal.pone.0113510

5. Firdissa E, Mohammed A, Berecha G, Garedew W. Coffee Drying and Processing Method Influence Quality of Arabica Coffee Varieties (Coffee arabica L.) at Gomma I and Limmu Kossa, Southwest Ethiopia. J Food Qual. 2022;2022: 1–8. doi:10.1155/2022/9184374

6. Phitakwinai S, Thepa S, Nilnont W. Thin-layer drying of parchment Arabica coffee by controlling temperature and relative humidity. Food Sci Nutr. 2019;7: 2921–2931. doi:10.1002/fsn3.1144

7. Mohsenin NN. Physical Properties of Plant and Animal Materials. 1st Editio. New York, NY, United States: Routledge; 1970. doi:10.4324/9781003062325

8. Mohsenin NN. Thermal Properties of Food and Agricultural Materials. 1st Editio. London: CRC Press; 1980. doi:10.1201/9781003062332

9. Brooker DB, Bakker-Arkema FW, Hall CW. Drying and storage of grains and oilseeds. 2nd Revise. New York, NY, United States: Van Nostrand Reinhold, New York; 1992.

10. Flórez C, Maldonado C, Cortina H, Moncada M, Montoya-Restrepo EC, Ruales L, et al. Cenicafé 1: Nueva variedad de porte bajo, altamente productiva, resistente a la roya y al CBD, con mayor calidad física del grano. Av técnicos Cenicafé No 469. 2016; 1–8. Available: https://www.cenicafe.org/es/publications/AVT0469.pdf

11. Flórez C, Arias J, Maldonado C. Variedades Castillo Zonales Resistencia a la roya con mayor productividad. Cenicafé. 2018;489: 3–3. doi:http://dx.doi.org/10.13140/RG.2.2.22423.62889

12. Chandrasekar V, Viswanathan R. Physical and Thermal Properties of Coffee. J Agric Eng Res. 1999;73: 227–234. doi:10.1006/jaer.1999.0411

13. Severa L, Buchar J, Nedomová Š. Shape and size variability of roasted Arabica coffee beans. Int J Food Prop. 2012;15: 426–437. doi:10.1080/10942912.2010.487967

14. Pineda MF, Tinoco HA, Lopez-Guzman J, Perdomo-Hurtado L, Cardona CI, Rincon-Jimenez A, et al. Ripening stage classification of Coffea arabica L. var. Castillo using a Machine learning approach with the electromechanical impedance measurements of a contact device. Mater Today Proc. 2022;1675: 1–26. doi:10.1016/j.matpr.2022.04.669

15. Castrillón J, Sanz J, Ramos P. Algoritmo Para La Identificación De Café Lavado Afectado Por La Broca Del Café. Cenicafé. 2017;68: 7–19.

16. Monirul Islam Chowdhury M, Sarker RI, Bala BK, Hossain MA. Physical properties of gram as a function of moisture content. Int J Food Prop. 2001;4: 297–310. doi:10.1081/JFP-100105195

17. Siriprom W, Chantarasunthon K, Teanchai K. Physical and thermal properties of chitosan. Adv Mater Res. 2014;979: 315–318. doi:10.4028/www.scientific.net/AMR.979.315

18. Zhu W, Su XS, Li X, Sun QF. The deviation of thermal conductivity under different operating power is analyzed by linear heat source superposition method. Arab J Geosci. 2021;14. doi:10.1007/s12517-021-06718-y

19. Vacquier V. The measurement of thermal conductivity of solids with a transient linear heat source on the plane surface of a poorly conducting body. Earth Planet Sci Lett. 1985;74: 275–279. doi:10.1016/0012-821X(85)90027-5

20. Banaszkiewicz M, Seiferlin K, Spohn T, Kargl G, Kömle N. A new method for the determination of thermal conductivity and thermal diffusivity from linear heat source measurements. Rev Sci Instrum. 1997;68: 4184–4190. doi:10.1063/1.1148365

21. T. Morita, R. Paul Singh. Physical and Thermal Properties of Short-Grain Rough Rice. Trans ASAE. 1979;22: 0630–0636. doi:10.13031/2013.35074

22. Montilla-Pérez J, Arcila-Pulgarín J, Aristizábal-Loaiza M, Montoya-Restrepo EC, Puerta-Quintero GI, Oliveros-Tascón CE, et al. Caracterización de Algunas Propiedades Físicas y Factores de Conversión del Café Durante el Proceso de Beneficio Húmedo Tradicional. Rev Cenicafé. 2008;59: 120–142. Available: http://www.cenicafe.org/es/publications/arc059(02)120-142.pdf

23. Ghosh BN, Gacanja W. A study of the shape and size of wet parchment coffee beans. J Agric Eng Res. 1970;15: 91–99. doi:10.1016/0021-8634(70)90080-6

24. Pérez-Alegría LR, Ciro VHJ, Abud LC. Physical and thermal properties of parchment coffee bean. Trans Am Soc Agric Eng. 2001;44: 1721–1726. doi:10.13031/2013.6983

25. Duque-Dussán E, Banout J. Improving the drying performance of parchment coffee due to the newly redesigned drying chamber. J Food Process Eng. 2022;45. doi:10.1111/jfpe.14161

26. Nilnont W, Thepa S, Janjai S, Kasayapanand N, Thamrongmas C, Bala BK. Finite element simulation for coffee (Coffea arabica) drying. Food Bioprod Process. 2012;90: 341–350. doi:10.1016/j.fbp.2011.06.007

27. Burmester K, Eggers R. Heat and mass transfer during the coffee drying process. J Food Eng. 2010;99: 430–436. doi:10.1016/j.jfoodeng.2009.12.021

28. Sfredo MA, Finzer JRD, Limaverde JR. Heat and mass transfer in coffee fruits drying. J Food Eng. 2005;70: 15–25. doi:10.1016/j.jfoodeng.2004.09.008

29. Duque-Dussán E, Villada-Dussán A, Roubík H, Banout J. Modeling of Forced and Natural Convection Drying Process of a Coffee Seed. J ASABE. 2022;65: 1061–1070. doi:10.13031/ja.15156

30. Cardoso DB, de Andrade ET, Calderón RAA, Rabelo MHS, de Almeida Dias C, Lemos IÁ. Determination of thermal properties of coffee beans at different degrees of roasting. Coffee Sci. 2018;13: 498–509. doi:10.25186/cs.v13i4.1491

31. Fadai NT, Melrose J, Please CP, Schulman A, Van Gorder RA. A heat and mass transfer study of coffee bean roasting. Int J Heat Mass Transf. 2017;104: 787–799. doi:10.1016/j.ijheatmasstransfer.2016.08.083

32. López-Córdoba A, Goyanes S. Food Powder Properties. Ref Modul Food Sci. 2017; 1–7. doi:10.1016/b978-0-08-100596-5.21198-0

33. Cenkowski S, Jayas DS, Pabis S. Deep-Bed Grain Drying - A Review of Particular Theories. Dry Technol. 1993;11: 1553–1582. doi:10.1080/07373939308916919

34. Liu Z, Wu Z, Wang X, Song J, Wu W. Numerical simulation and experimental study of deep bed corn drying based on water potential. Math Probl Eng. 2015;2015: 13. doi:10.1155/2015/539846

35. Ramírez-Martínez A, Salgado-Cervantes MA, Rodríguez-Jimenes GC, García-Alvarado MA, Cherblanc F, Bénet JC. Water transport in parchment and endosperm of coffee bean. J Food Eng. 2013;114: 375–383. doi:10.1016/j.jfoodeng.2012.08.028

36. Ramirez-Martinez A, Benet J-C, Cherblanc F, García-Alvarado MA, Rodriguez-Jimenes G. Internal structure and water transport in the coffee bean. 17th Int Dry Symp (IDS 2010), Magdeburg, Ger. 2010; 1–8.

37. Briceño-Martínez B, Castillo-Calderón J, Carrión-Jaura R, Díaz-Sinche D. Proposal for implantation of coffeedrying greenhouse with paraboliccover and adapted modular structure. Revista de Ciencia y Tecnología. 2020: 36–46.

38. Elavarasan K, Verma V, Shamasundar BA. Development of prototype solar-biomass hybrid dryer and its performance evaluation using salted fish (Cynoglossus spp.). Indian J Fish. 2017;64: 123–129. doi:10.21077/ijf.2017.64.special-issue.76242-17

39. Udomkun P, Romuli S, Schock S, Mahayothee B, Sartas M, Wossen T, et al. Review of solar dryers for agricultural products in Asia and Africa: An innovation landscape approach. J Environ Manage. 2020;268: 110730. doi:10.1016/j.jenvman.2020.110730

40. Sreenarayanan V V., Chattopadhyay PK. Thermal conductivity and diffusivity of rice bran. J Agric Eng Res. 1986;34: 115–121. doi:10.1016/S0021-8634(86)80004-X

41. Siriprom W, Chantarasunthon K, Teanchai K. Physical and thermal properties of chitosan. Adv Mater Res. 2014;979: 315–318. doi:10.4028/www.scientific.net/AMR.979.315

42. Doymaz I, Pala M. The thin-layer drying characteristics of corn. J Food Eng. 2003;60: 125–130. doi:10.1016/S0260-8774(03)00025-6

43. Pereira LL, Guarçoni RC, Pinheiro PF, Osório VM, Pinheiro CA, Moreira TR, et al. New propositions about coffee wet processing: Chemical and sensory perspectives. Food Chem. 2020;310: 125943. doi:10.1016/j.foodchem.2019.125943

44. Elhalis H, Cox J, Frank D, Zhao J. The role of wet fermentation in enhancing coffee flavor, aroma and sensory quality. Eur Food Res Technol. 2021;247: 485–498. doi:10.1007/s00217-020-03641-6

6. Design and Evaluation of a Hybrid Solar Dryer for Postharvesting Processing of Parchment Coffee.

Adapted from: Duque-Dussán E, Sanz-Uribe JR, Banout J. Design and evaluation of a hybrid solar dryer for postharvesting processing of parchment coffee. Renewable Energy. 2023;215: 118961. doi:10.1016/j.renene.2023.118961

Abstract

Due to the extended drying time open-sun and solar drying of coffee procedures undergo, the development of microorganisms, mycotoxins and molds threaten the product. Alternatives such as mechanical dryers are available, nevertheless, their running costs and setups are usually expensive and unaffordable for small-scale coffee growers. Therefore, this research aimed to design, build and evaluate a hybrid solar dryer which mixes solar and mechanical drying principles. It uses a traditional solar tunnel-type dryer as a base featuring a biomass burner which uses coffee trunks left from the yearly crop renovation as biofuel. A heat exchanger heats the drying air, afterwards blown into a plenum chamber that homogenizes the air's static pressure before crossing the coffee bed, ensuring an even moisture removal. Also, the hybrid unit includes a photovoltaic system to obtain a fully self-sufficient drying unit. The newly developed dryer was tested under three different configurations: Solar and mechanical day and night (C1), solar during the day and mechanical during the night (C2) and fully solar with non-mechanical aid (C3). The results displayed a notable drying time reduction in the three evaluated configurations: C1 reduced the drying time by 70.47%, C2 by 45.75% and C3 by 21.5%. Also, the predictive model for different plenum chamber heights was obtained through computational fluid dynamics simulations, where the ideal height was 0.25 m. A biomass consumption of 1.9 kg h^{-1} was registered. Also improved temperature and relative humidity profiles were achieved. Its design easily adapts to the existing tunnel and parabolic-type solar dryers.

Keywords: Biomass; Coffee; Coffee Drying; Hybrid Dryer; Tunnel Dryer, Mechanical Drying.

6.1. Introduction

It is widely recognized that wet coffee processing preserves the grain's natural flavours and organoleptic properties while providing a better-quality coffee [1]. Farmer to farmer, the process differs; still, the stages are generally as follows: ripe berry detachment (selective harvest), pulping the berry to remove the fruit flesh (Mesocarp) and outer skin (Exocarp), removing the seed-covering mucilage by natural or enzyme accelerated degradation (fermentation) or mechanical principles, washing and drying [2]. As the wet parchment coffee usually holds an average moisture content of 53-55% (wb) after washing [3], drying is usually the most challenging step since it must be lowered to 10-12% (wb) in order to meet storage and commercialization requirements while avoiding growth of microorganisms, fungi or mycotoxins, preserving the grain's quality and safety [4,5].

The most common ways to dry coffee are sun-drying and mechanical drying [6–8]. Sun energy can be used in two main ways. To begin with, there is open sun-drying, when the coffee producer spreads the beans out on an open surface and lets the sun and natural air convection remove the excess moisture. This configuration is also seen in fruit, meat, and vegetable drying [9].

This setup, however, is not recommended due to the high number of factors that could threaten the product: animals, pests, rain, and a low level of process control. Thus, solar dryers emerged as the second form of solar energy use. Solar-drying methods include direct, indirect, mixed [10], and hybrid drying [11,12]; parabolic and tunnel dryers are the most common [13,14]. By using these dryers, the product can be dried more efficiently while mitigating the threats mentioned above. Nonetheless, these dryers are still weather-dependent and can pose an issue. As an example, in many Latin-American countries, the peak coffee harvest coincides with the rainy season [15], making coffee drying more difficult.

Employing solar energy to dry coffee brings along several benefits, for instance, the final grain quality is higher seeing that the drying process temperatures rarely surpass the 50°C, this temperature, if exceeded could kill the embryo of the bean, leading to a rapid seed structure deterioration affecting the quality [16]. It is also

considered as an environmentally friendly practice with low implementation and operation costs [17]. However, these drying alternatives also hold various issues, sun and solar drying of coffee are usually passive processes which require large areas, therefore low drying rates are expected limiting the drying capacity in the farm, not only representing a bottleneck in the process where drying a single batch can take up to 10-14 days with a thin layer thickness of 0.02-0.03 m [18–20] but also it endangers the innocuousness of the seed as stated above; these issues affect mainly the smallholders seeing that using solar energy to dry their goods is a common practice due to their social and economic conditions. Simultaneously the share of coffee smallholders is quite large, as an example, approximately the 95% of the 563000 coffee growing families in Colombia are considered as smallholders, having less than 5 ha [21] sown in coffee being 1.5 ha the average plot size [22,23].

By contrast, mechanical dryers allow moisture to be removed faster, which significantly reduces drying times [8,24–26]. Additionally, these dryers have a greater grain capacity, resulting in faster drying and more dry coffee per batch than solar dryers. In comparison, 10 m^2 of a solar dryer will process 125 kg of dry parchment coffee when maintaining a 0.03 m layer thickness in the above time frame, while a mechanical dryer can process the same amount of time in 20-25 h [3,8]. There are, however, some disadvantages to mechanical drying; equipment, operation, and running costs can reduce acquisition interest. Despite the availability of some small grower-designed mechanical dryers, their elevated fuel consumption, mainly fossil fuels such as liquefied petroleum gas (LPG) or natural gas, and the high energy requirement of the fan discourage their purchase, especially by growers who live in isolated regions.

Furthermore, if strict control is not carried out, the temperature of the drying air can easily exceed the recommended maximum drying temperature of 50°C, leading to the rapid decomposition of the seed due to the embryo's demise [27,28]. Besides affecting the taste and quality of the grain, this will also affect its storage and microbiological activity [5,27].

In order to keep the coffee plantations young and productive, the literature suggests the coffee growers to renew 1/5 of their plantation per year [29,30], this process generates an average yield of 32 tons of dry coffee trunks per hectare [31],

meaning that a smallholder with 1.2 ha plot has a biomass availability of 7.68 tons per year. This biomass holds a calorific value of 19.75 MJ kg^{-1} [32], and despite this, most of the trunks are left on the field with occasional use as firewood for household applications.

Consequently, the aim of this study sought to design and evaluate a hybrid solar dryer for parchment coffee for small-scale and family-farm coffee growers. The newly designed hybrid dryer combines the benefits of both solar and mechanical drying while minimizing the drawbacks of both techniques. In addition, the new hybrid solar dryer was designed emphasizing the maximum use of residual biomass from coffee growing and pruning as a secondary source of energy for drying.

6.2. Materials and Methods

The hybrid solar dryer comprised a solar segment defined as a standard solar tunnel dryer, so existing technologies could be adapted to the newly designed modifications; and a mechanical part consisting of a biomass burner where coffee trunks were used as biofuel. The mechanical segment contained a heat exchanger that warmed the drying air, which was then blown into an airtight plenum chamber placed under the solar segment to ensure static air pressure homogenization prior to crossing the coffee bed. In addition, the apparatus also included a photovoltaic (PV) system and a charge controller so energy could be stored in a battery, allowing the fan to perform 24 hours a day with energetic independence.

6.2.1. Design of the Hybrid Solar Dryer

The dryer design was done under the design for economic manufacture (DEM) principles [33]. Three main design specification were defined as:

- To reduce the drying time of the coffee by at least 40% compared with the traditional tunnel dryer.
- To provide a simple and robust design that could be easily adapted to existing tunnel dryers.
- Minimum maintenance routine needed.

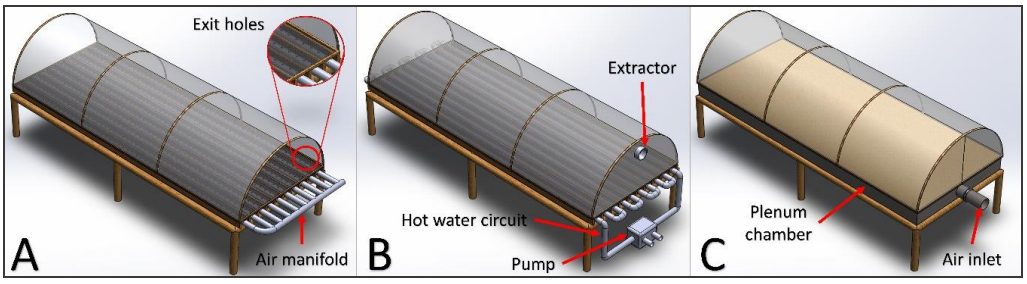

Figure 1. Concepts generated. **A**. Air manifold concept. **B**. Heat exchanger and negative pressure chamber concept. **C**. Positive pressure plenum chamber concept with an initial 0.25 m height.

Once these requirements were established 3 different concepts that could solve the issues were proposed (Figure 1), each one of them was then evaluated by computational fluid dynamics (CFD) simulations in order to verify the air distribution inside the dryer to ensure uniform moisture removal, as well as their compliance with the design conditions.

Since the newly developed technology had to be adaptable to existing technologies, the drying area and general setup complied with the most common solar tunnel used in Colombia by smallholders [34,35] with a drying area of 10 m^2 (L = 5 m, W = 2 m). The fluid geometries for the CFD simulations were specified as air volumes and a porous bed to represent the coffee layer. Porosity varies as a function of bulk and kernel density; in addition, inertial and viscous flow resistances change as the bean dries [36].

Considering that the suggested airflow when mechanically drying coffee is 0.1 kg min^{-1} per kg of dry parchment coffee (DPC) and 10 m^2 of drying area provides 90 kg of DPC when using a 0.02 m thick coffee layer [37,38], leads to the ideal airflow $\dot{Q}_{ideal}$ = 9 m^3 min^{-1}. The CFD simulations evaluated each concept in three different scenarios: using its ideal air velocity V_{ideal} and using its V_{ideal} ± 0.5 m s^{-1} to provide a wider range of results. The V_{ideal} was calculated from the $\dot{Q}_{ideal}$ and the cross-sectional area of each concept air inlet/outlet. After performing the CFD simulations and verifying the concept's accuracy with the design specifications, concept C was selected. The CFD simulations were defined using a K-ε turbulence model, as initial conditions the air velocity and the atmospheric pressure were used. In all the simulations the coffee was defined as a porous medium, with a variating porosity as a function of the moisture

content as defined by [39]. The contact regions were thoroughly controlled by mesh match. Fine mesh was considered with a controlled orthogonal quality and skewness for high precision (min=0.9889 and max=0.089 respectively). Also, to reduce wall friction factors, an inflation of 3 layers was used in the edges.

Figure 1 illustrates how the concept was initially evaluated at a height of 0.25 m for the plenum chamber. After selecting the model C, CFD was used to study four different chamber heights (0.15, 0.25, 0.35, and 0.45 m), to find the minimum chamber height that homogenizes air pressure. Each height was examined at three different velocities, at its V_{ideal} and at its $V_{ideal} \pm 0.5$ m s^{-1}. The simulations provided not only the air pressure and velocity profiles but also the pressure histograms, which were further analysed looking to generate a model to select the appropriate chamber height evaluating the pressure's coefficient of variation (C_v), being C_v<10% the ideal value.

6.2.1.1. Drying Chamber

In the newly developed hybrid solar dryer, the solar segment has been defined as a traditional solar tunnel dryer, in accordance with the recommended materials and construction methods for this type of dryer [35]. With a length of 5 m and width of 2 m, the unit had a total drying area of 10 m^2, where the coffee was laid on 85% thick (15% opening) black mesh. Double laminate PROSOLAR plastic fabric was used to cover the drying area in a parabolic shaped 0.025 m tubes to concentrate the sun's rays on the product. The dryer stood 1.8 m high, and the height from ground level to the drying area was 0.9 m, also a 0.05 m angle profile steel structure was added underneath the drying area to hold the plenum chamber and avoid unwanted deformities.

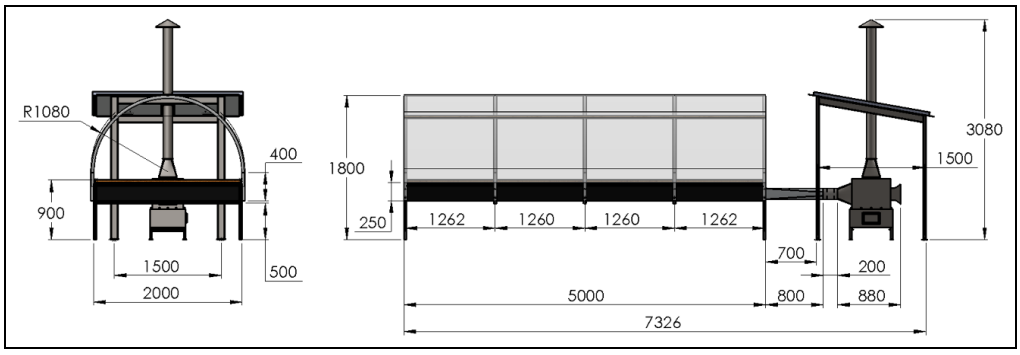

Figure 2. General dimensions (mm) of the hybrid solar dryer.

The plenum chamber material was chosen to be a 0.02 m thick high-density polyethylene (HDPE) geomembrane. Hot ambient air, previously heated by a heat exchanger, is then blown into the plenum chamber, where the static pressure of drying air is homogenized before exiting through the coffee layer. A control dryer was also built using the same dimensions (5×2 m), mesh, plastic cover, and capacity as a normal solar tunnel dryer; this was done to compare the behaviour of the newly designed unit with that of the conventional drying process when carrying out the tests under the same climate conditions as seen in Figure 3. Both units were lengthwise north-south oriented, in order to take higher advantage of the solar radiation. The curtains were open during the day (if dry) and closed during the nights to avoid remoisturizing.

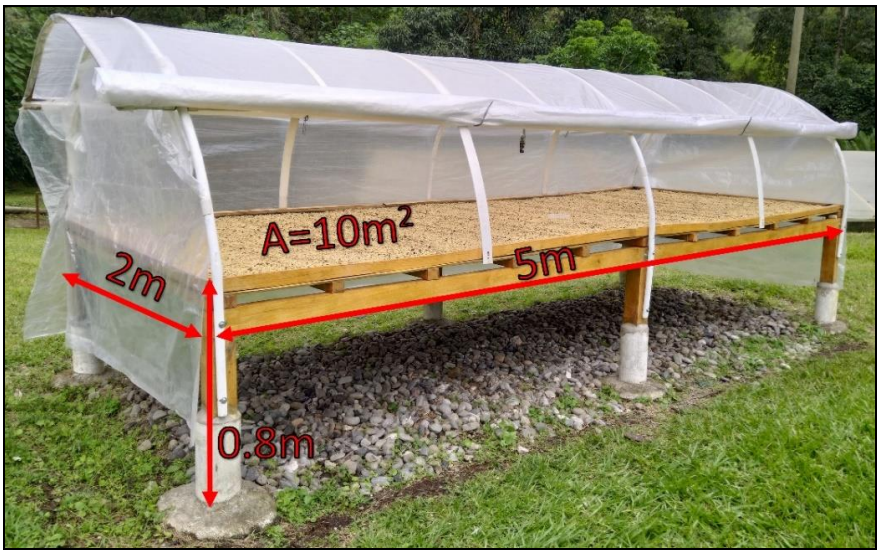

Figure 3. 10 m^2 Control dryer.

6.2.1.2. Biomass Burner

The biomass burner was designed to maintain easy trunk manipulation by considering the size of the solid biofuel. The ideal biomass size was determined as 0.2-0.3 m long dry coffee trunks; hence the combustion chamber of the burner had the dimensions of L=0.53, W=0.43, and H=0.25 m to provide the required air heat elevation keeping a reduced combustion zone where the biomass fits properly with low pretreatment required. Additionally, the burner was insulated with a 0.035 m refractory concrete wall to prevent heat loss. From the burner, combustion and exhaust gases exit

vertically through the chimney. However, between the chimney and the burner was the heat transfer area, which allowed atmospheric air to be heated before being blown into the plenum chamber as shown in Figure 4.

All the segment was entirely constructed from gauge 14 A36 steel sheet metal, ER70S-6 wire was used for high penetration MIG welding in areas with high thermal stresses, and E6013 and E7018 welding rods in areas with low thermal stresses. The entire section was then coated with CORROTEC ECP100 anti-corrosive and then with a CORROTEC 905 high temperature resistant aluminum finish paint, resistant to 232-590°C.

The heat exchanger was designed based on the Tubular Exchanger Manufacturers Association (TEMA) standards for double-pipe heat exchangers, where based on the temperature elevation the energy requirement was established, then, the logarithmic mean temperature difference was calculated and finally, the Number of Transfer Units (NTU method) could be applied for a cross flow to calculate the heat transfer area required. In addition to the biomass calorific value and combustion properties, the steel properties, the ambient air temperature values, the chimney flue, the fan flow, were analysed to obtain a desired drying air temperature ranging between 40 to 48°C. Ideally, the heat transfer area should have been 0.5 m^2, however, the fins added 0.05 m^2, resulting in a total heat transfer area of 0.55 m^2.

The theoretical biomass consumption was calculated from Equation 2, obtained from Equation 1 provided by [40] which yields the theoretical efficiency of the heat exchanger as:

$$\eta_{HX} = \frac{\dot{m}_a \, C_{Pa} \, \Delta T_a}{\dot{m}_f \, (h_B)} \tag{1}$$

$$\dot{m}_f = \frac{Q_a \, \rho_a \, C_{Pa} \, \Delta T_a}{\eta_{HX} \, (h_B)} \tag{2}$$

Where η_{HX} is the heat exchanger theoretical efficiency, assumed as 35%; $\dot{m}_a$ represents the air flow rate, afterwards expressed as the fan's flow Q_a (550 $m^3 \, h^{-1}$) times

the air density ρ_a (1.09 kg m^{-3}); C_{Pa} is the specific heat capacity of the air; ΔT is the difference between the outlet air and the ambient air temperatures; $\dot{m}_f$ is the fuel consumption, and h_B is the heat combustion of the biomass. The theoretical biomass consumption was $\dot{m}_f$ =2.25 kg h^{-1}. However, a flue controller was installed in the chimney to regulate biomass combustion as well as to control drying air temperature by limiting airflow.

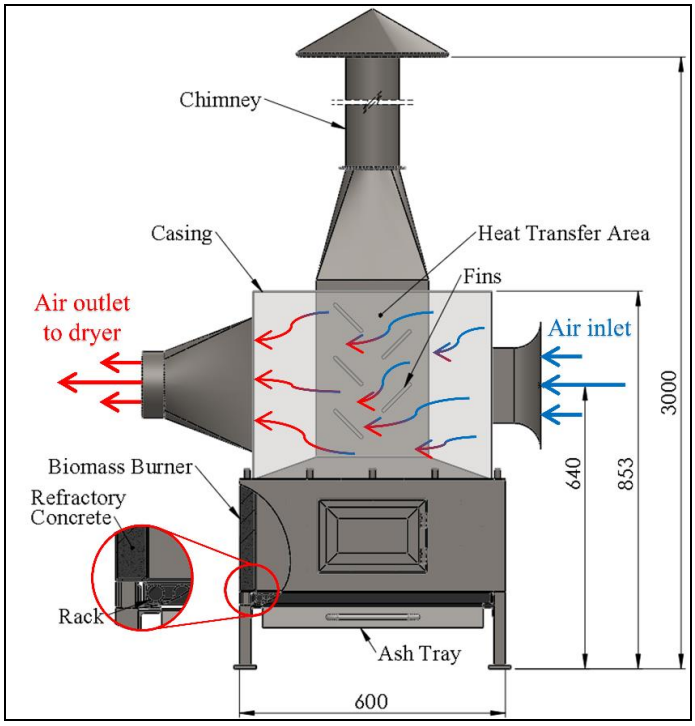

Figure 4. Biomass burner setup.

6.2.1.3. Forced Convection and PV Module Systems

An 88 W 110 V/60 Hz 4-blade axial Sinowell 0.177 m in-duct steel fan with a diameter of 0.15 m was installed right after the drying air outlet from the heat exchanger. Its airflow of 550 m^3 h^{-1} ensured the ideal flow for the amount of coffee to be processed. An ASHRAE-standard 15° round to rectangular transition was placed after the fan to reduce the air velocity and stretch the air evenly into the plenum chamber. Under the transition, a hinged gate was added to allow ambient air to enter the dryer through the plenum chamber when solar drying was fully operational.

The hybrid solar dryer was designed to take advantage of the 12 night-time hours when solar drying does not occur. As air heating is accomplished by using the

thermal energy contained in biomass through the heat exchanger, the only energy-demanding element in the design was the fan. Because of this, a photovoltaic system was designed to generate and store electric energy in a battery so the apparatus could function when the sun was not shining or with very low radiation, such as during the rainy season. This allowed the dryer to be totally energy independent, ideal for rural and isolated locations.

Because the fan had an electric power demand of 88 W, 2 solar panels of 265 Wh each were chosen to drive the PV system [41]. Calculations were performed using 4.8 peak solar hours, the average of the coffee-producing region in Colombia as registered by the National Coffee Research Center.

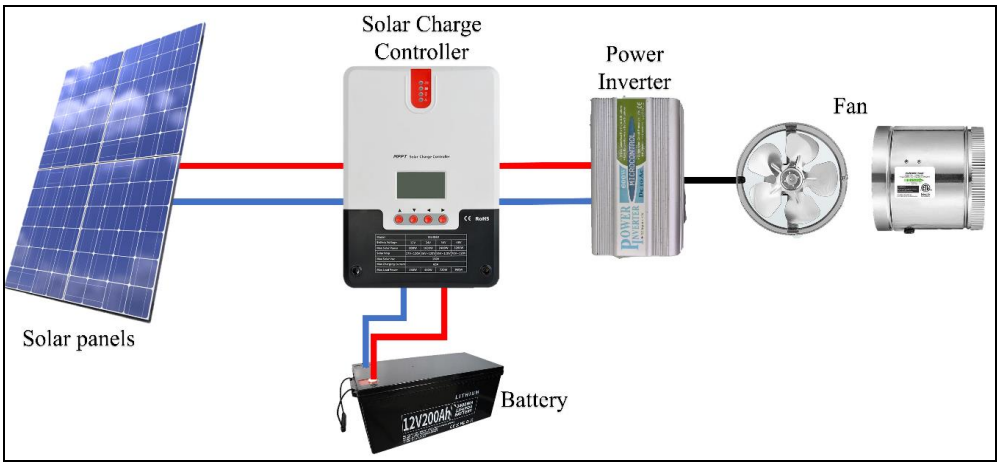

Figure 5. PV System setup.

As seen in Figure 5, an MPT Powersave SR-ML4860 Solar charge controller was located following the solar panels, in order to regulate and divide the electric flow so that the battery could be charged while the fan was running. With the aim of storing enough electricity for night-time blowing, a 12 V 200 A battery with a capacity of 2400 Wh was used. The DC coming from the battery was converted to AC needed by the fan using an HP-600 modified sine wave DC-AC power inverter integrated with a microcontroller.

6.2.2. Hybrid Coffee Solar Dryer Performance

6.2.2.1. Experimental Procedure

The dryer was tested under three different configurations at the National Coffee Research Center of Colombia (Cenicafé) in the postharvest discipline facilities in the municipality of Manizales, Caldas (4.991889, -75.597139; elevation of 1306 m.a.s.l). The experiments were performed between September and November 2022 to test the dryer under the worst-case weather scenario; for the location, during this time of the year, the second-semester rain season is at its maximum, and it also coincides with the second-semester harvest peak. *Coffea arabica L*. var. Cenicafé 1 was used during all the experiments.

During the first configuration (C1), traditional solar drying was combined with mechanical drying (24/7), in which the biomass burner and fan worked throughout the drying process until the bean reached a final moisture content M_f of 11% (wb). For the second configuration (C2), solar drying was used during the day, but the biomass burner and fan were used at night to aid the drying.

In the last configuration (C3), solar drying was performed without the assistance of the biomass burner. This configuration was intended to demonstrate that the plenum chamber located under the coffee bed restricts ambient air from coming into contact with the coffee bed (with the hinged door closed). As a result of the high relative humidity (RH) of the air at night, it was expected that this would positively affect the coffee mass in that it tends to gain moisture, especially when it is reaching its equilibrium moisture content [3].

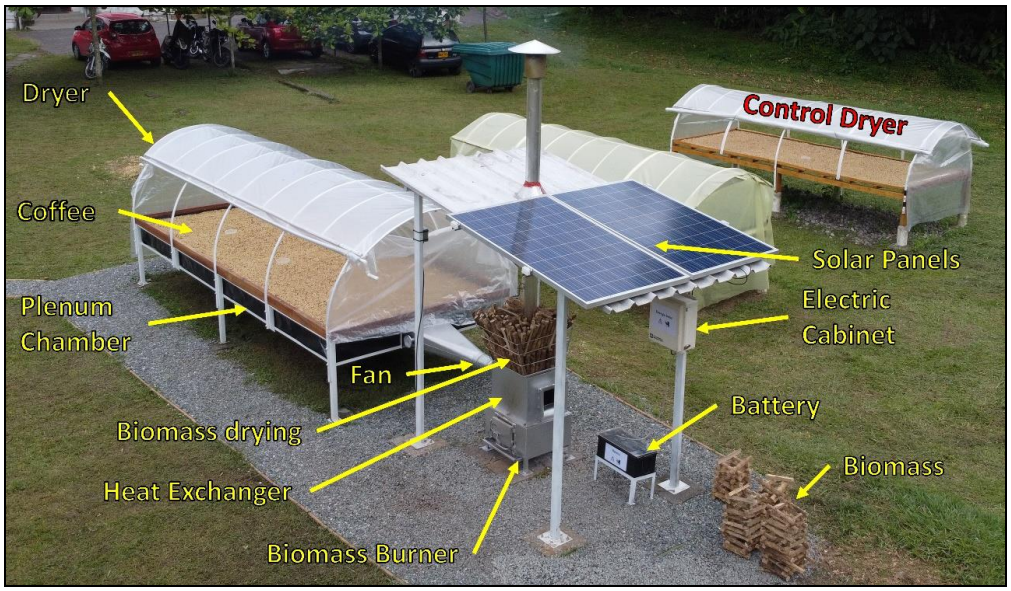

Figure 6. Hybrid solar tunnel dryer setup.

The configurations were replicated three times each. All replications were conducted with the same amount of coffee loaded into the control dryer, so the hybrid solar dryer's behavior could be compared to the conventional solar tunnel dryer's. In each replication, 328 kg of wet parchment coffee was used at an initial moisture content M_o of 53% (wb). One-half of the load was to be dried in the hybrid dryer and the other half in the control dryer; the coffee berries were picked at ripe stages 4, 5 and 6 [42] at Naranjal Central Station (4.972279, -75.652530), one of Cenicafe's experimental fields. The berries were then pulped, fermented, and washed at the research centre's post-harvest seed processing facility.

6.2.2.2. Instrumentation

Once the hybrid and the control dryer were loaded, three baskets were placed per dryer longitudinally across the drying area to control the moisture content through gravimetric principles [43]. Each basket was loaded with 200 g of wet parchment coffee; once the coffee mass reached 104-105 g, the equilibrium moisture content of 10-12% (wb) was reached. However, once the coffee exhibited a moisture content below 18% (wb), a Kett PM450 moisture meter for grains was used for better control and accuracy. The mass/moisture content of coffee was registered every hour until attaining the desired moisture level.

Both the hybrid and the control dryer featured UT330C/IP67 UNI-T humidity/temperature/pressure dataloggers registering data every 10 minutes located at 0.8 m from the coffee bed, so the temperature and relative humidity in the drying chamber could be traced during the entire drying process. In contrast, a TBM50040B9 Stainless Steel Winters Bi-metal Thermometer controlled the drying air temperature [44]. The coffee bed was mixed with a coffee mixing rake four times a day to ensure even moisture removal.

During C1 and C2, each coffee trunk fed to the biomass burner was weighed using a XPE505C Comparator with a readability of 0.01 mg, and its mass was recorded to calculate the real biomass consumption. Before being burned, the trunks were placed in a basket on top of the heat exchanger's casing to use the emitted heat from the apparatus to dry some still-wet trunks lowering their moisture content until ~13% (wb).

6.2.2.3. Performance and Data Analyses

In order to obtain relevant information about the efficiency and the drying phenomenon as such, the diffusion coefficient D (m^2 s^{-1}) of the coffee in each configuration was calculated from Equation (3), provided by [22] and [45].

$$D = 4.1582 \times 10^{-8} e^{\left[(0.1346\, T_g + 2.2055) M - \frac{1184}{T_g + 273.15}\right]} \quad (3)$$

Where T_g is the grain's temperature and M is the moisture content of the grain expressed in decimal notation and in dry basis (db). The temperature control was done by a set of parallelly arranged HH912T Omega thermocouples which registered T_g in a datalogger.

The recorded moisture content of the parchment coffee permitted to also calculate the bulk specific heat capacity C_p (kJ kg^{-1} K^{-1}) (Equation 4) and the bulk thermal conductivity K (W m^{-1} K^{-1}) (Equation 5) of the coffee using the models provided by [39].

$$c_p = 1.3556 + 5.7859M \quad (4)$$

$$K = 0.00241 M_{(wb)} + 0.0104$$

(5)

In terms of system efficiency, the methodology shared by [46] was followed, where the natural convection scenario (η_c) can be depicted by the Equation (6) and the forced convection case (η_f) by Equation (7).

$$\eta_c = \frac{W\ \Delta H}{I\ A\ t}$$

(6)

$$\eta_f = \frac{W\ \Delta H}{I\ A\ t + E_f}$$

(7)

Where W is the mass of evaporated water from the product (kg) per unit of time, ΔH represents the latent heat of vaporization of the water (kJ kg^{-1}), I stands for the solar radiation (W m^{-2}) on the surface measured with a KIMO SL-200 Solarimeter, A is the area of the dryer (m^2), t denotes the drying time (s) and E_f signifies the energy consumption of the fan (kW h).

The drying rates (DR) and pickup efficiency (η_p) of each configuration was assessed following the procedure shared by [47], where:

$$DR = \frac{(M_o - M_f)}{t}$$

(8)

$$\eta_p = \frac{h_o - h_i}{h_{as} - h_i}$$

(9)

Where M_o and M_f are the initial and final moisture content of the sample respectively, then h_o and h_i stand for the absolute humidity of the air leaving and

entering the drying chamber (%), whereas h_{as} stand for the absolute humidity of the air entering the drier at the point of adiabatic saturation (%).

6.2.2.4. Cost Analysis

The dryer cost is estimated as the total sum of construction materials and labor expenses. The cost of drying *Dc* can be estimated as explained by [47] as the ratio of annual cost (*Ac*) and amount of dried product per year (*Dq*), *Dq* was calculated taking into consideration that the average farm size in Colombia is 1.5 ha [23], and the average production of DPC per hectare per year is reported to be 1500 kg [48], therefore a farmer with an average sized plot could produce 2250 kg of DPC per year.

$$Dc = \frac{Ac}{Dq} \tag{10}$$

Also, as shared by [10], the annual costs of the dryer were calculated using Equation 11.

$$Ac = \left(Tc + \sum_{i=1}^{L} m_i \omega^i\right) \frac{(\omega - 1)}{\omega(\omega^L - 1)} \tag{11}$$

Where *Tc* stands for the dryer cost in USD, *L* its life (15 years), m_i depicts the maintenance costs in USD (assumed to be the 2% of the total dryer cost), and ω represents the ratio 100+inflation rate/100+interest rate.

It was of interest to calculate the payback period, for this, Equation 12 [49] was used.

$$Pb = \frac{ln\left(1 - \frac{Tc}{S}(d - f)\right)}{\ln\left(\frac{1+f}{1+d}\right)} \tag{12}$$

Where *Pb* represents the payback period, *S* dryer annual savings (USD), *d* describes the rate of interest and *f* the rate of inflation.

6.3. Results and Discussion

6.3.1. Theoretical Design and CFD simulations

There were several issues with the air distribution within the pipes in Model A, as seen in Figure 7 both the air pressure and flow were heterogeneous, the airflow transited mainly through the central pipe. As a result, moisture may be removed unevenly, or the heated air may escape to the atmosphere which is counterproductive. Additionally, the construction of this concept seemed complicated, conflicting with the design specifications. On the other hand, concept B exhibited homogeneous air circulation within the dryer premises, even pressure was also attained through the coffee layer, nonetheless, concept B also revealed a complicated water circulation system that required a pump and regular maintenance, in addition, seeing that this concept intended to heat air when crossing the pipe system, the climatic conditions could be an issue [50]. Further, the drying chamber would need to ensure complete hermeticity to force the atmospheric air through the coffee layer, a challenging condition to fulfil since the coffee mass should be mixed regularly during drying [51,52].

When evaluating Concept C, the pressure was even across the plenum chamber's volume, and even though there are pressure variations, the difference is not representative (Table 1). In addition to being simple and robust, this setup requires minimal maintenance so that the dryer can provide appropriate performance on the farm meeting the design specifications. Furthermore, its plenum chamber can be easily adapted to existing tunnel dryers, and the geomembrane is widely available for the farmers in agricultural supplies shops, hence it was selected.

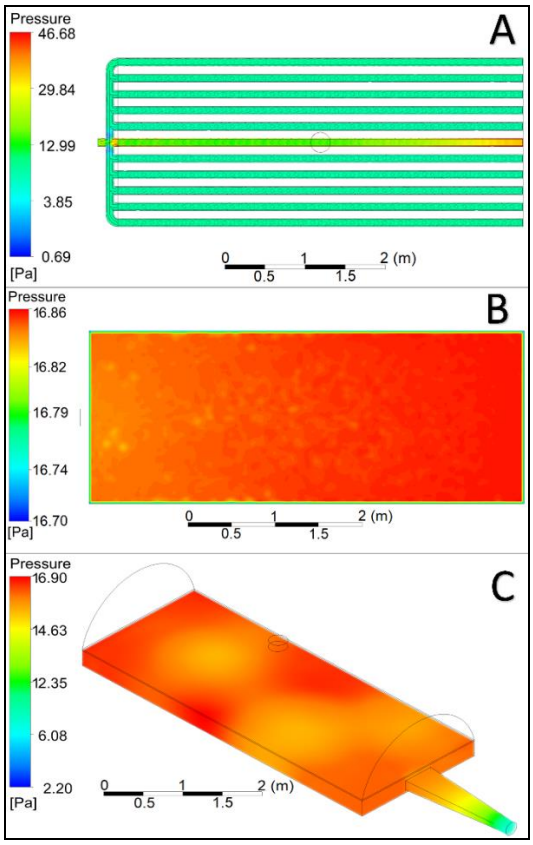

Figure 7. Results of the CFD simulations, pressure volume rendering at the V_{ideal}. **A.** Concept A top view. **B.** Concept B top view. **C.** Concept C isometric view.

The CFD simulations of the plenum chamber concept evaluated at four different heights at their respective V_{ideal} ± 0.5 m s-1 results are shared in Table 1.

Table 1. CFD plenum chambers analysis results.

Plenum Chamber Height (m)	Velocity (m s^{-1})	P_{max} (Pa)	P_{min} (Pa)	ΔP (Pa)	Mode (Pa)	C_v (%)	Mean (Pa)	Variance
0.15	14.5	18.11	3.0787	15.031	7.25	39.36	6.84	2.69
	15	18.9	3.36	15.54	7.25	34.85	8.19	2.85
	15.5	16.56	2.34	14.22	5	40.89	7.9	3.23
0.25	3	13.7	10.38	3.32	11.9	5.71	11.48	0.65
	3.5	16.90	13.78	3.12	15.7	5.31	15.26	0.81
	4	23.4	17.9	5.5	20.4	5.33	19.79	1.05
0.35	1	2.9	2.6	0.3	2.76	2.62	2.75	0.07

	1.5	7	4.78	2.22	6.35	7.62	6.1	0.46
	2	10.9	9.2	1.7	10.1	3.16	9.98	0.32
	0.5	2.345	2.258	0.087	2.28	0.82	2.28	0.02
0.45	1	8.500	8.038	0.462	8.2	0.99	8.16	0.080
	1.5	18.627	17.505	1.122	17.9	1.09	17.89	0.19

The velocity values variation is due to the inlet's cross-section change depending on the height; a circular inlet was used in all the simulations with a diameter of 0.1, 0.2, 0.3 and 0.4 m, respectively [53]. Although the selection criteria relied on the coefficient of variation (C_v<10%) and the design specifications, it was also essential to consider the air pressure in the chamber's domain. Table 1 shows that the 0.25 m height not only complies with the coefficient of variation condition but also displays high-pressure values, and its material requirements are less than larger plenum chambers. Also, higher pressures will allow the air to break through the coffee's viscous and inertial resistances and exit easier the porous bed as shared by [36] and [54].

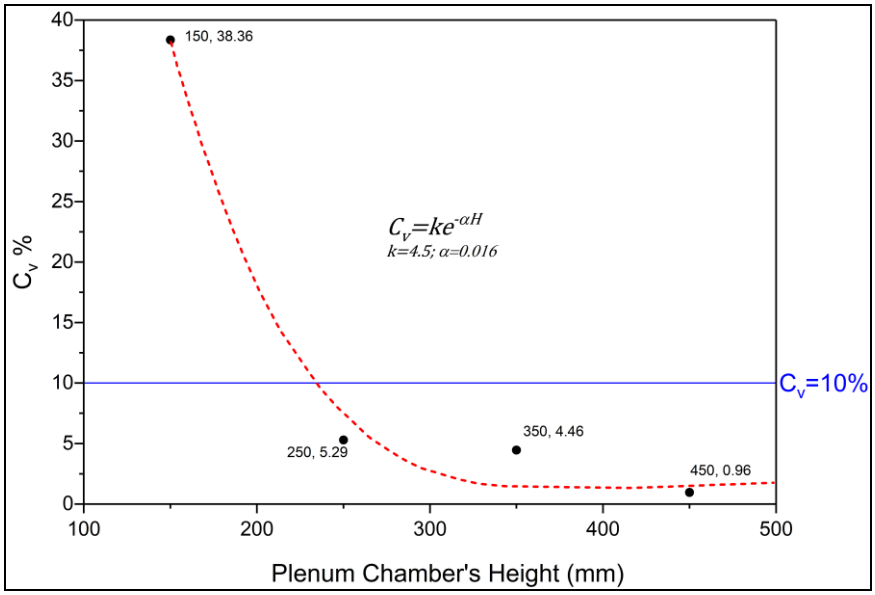

Figure 8. Coefficient of variation model.

The predictive model for the coefficient of variation generated from the CFD simulations is shown in Figure 8, even though the 0.25 m plenum chamber height was chosen in this study. If another plenum chamber for a similar hybrid solar dryer was to

be built or the chamber needed to be changed, the model would provide a predictive coefficient of variation for the pressure [38,55].

Even though it is seen that the plenum chamber homogenizes the static air pressure across its volume [56] it was also relevant to calculate the temperature change in the air domain. After, an integrated CFD-heat loss simulation and a linear heat analysis, it was seen that the temperature difference between the air inlet and the back of the plenum chamber was ΔT_p=-1.3°C. The value, however, was insignificant since the temperature is well preserved mainly because of the chamber's material and the heat losses to the atmosphere were negligible.

6.3.2. Thermal Properties and Efficiencies

The diffusion coefficient variation *D* changed from 2.97E^{-6} to 1.18E^{-9} m^2 s^{-1}, these values agree with those shared in the literature for parchment coffee [3,18,22], also the obtained data fit in the range of the diffusion coefficients of different agricultural products and foodstuffs as shared by [57]. Nevertheless, the behaviour of the diffusion coefficient was different for each configuration evaluated.

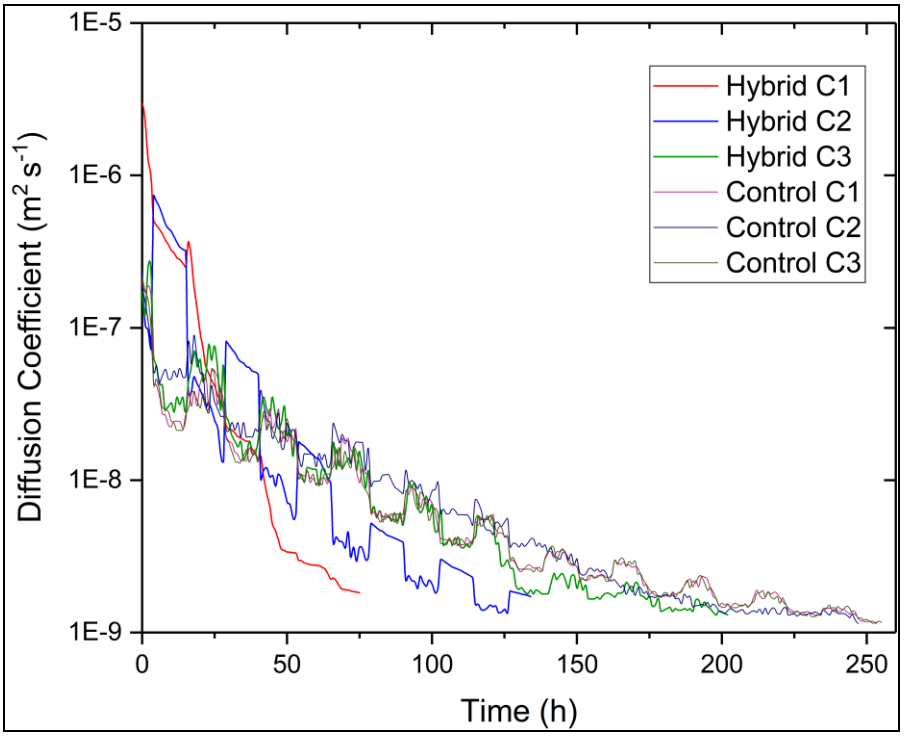

Figure 9. Diffusion coefficient variation in time.

As displayed in Figure 9, the Hybrid C1's diffusion coefficient dropped rapidly when compared with the others, seeing that the diffusion coefficient is defined as a function of the moisture content and the grain temperature, is logical that the Hybrid C1 depicted such curve. The grain temperature was higher, hence the first *D* value, then, due to its 24/7 setup, a rapid moisture removal occurred, promptly lowering the diffusion coefficient values because of its moisture content dependance. By the end of this curve, it is also seen that a steadier diffusion coefficient change occurred since the equilibrium moisture content was being achieved and the water removal in such stage happens at a slower rate [58].

The Hybrid C2's *D* follows a valley-peak performance due to the temperature fluctuation inside the dryer considering that during the night, the biomass burner supplied hot air, significantly increasing the grain temperature and moisture removal as also recorded by [3]. The Hybrid C3 and the Control C1 and C3 showed a similar behavior between them considering that the drying was set as full natural convection, nevertheless, the Hybrid C3 lowered the diffusion coefficient after 120 hours of drying significantly due to the non-moisture gain when attaining the equilibrium moisture content (see section 3.3.3), whereas the Control C2 had a steady change in the diffusion coefficient, during the experiments, it is possible that that specific configuration presented less variation in grain temperature and moisture removal.

The values of the bulk specific heat capacity C_p varied from 4.42 kJ kg^{-1} K^{-1} when the samples were loaded into the dryer with an average moisture content of 53% (wb) to 1.99±0.04 kJ kg^{-1} K^{-1} when the sample reached its desired moisture content of 11% (wb). The bulk thermal conductivity values ranged from 0.023 W m^{-1} K^{-1} when the coffee was wet, to 0.013 W m^{-1} K^{-1} once it was dry. Both the C_p and the *K* values concurred with those published in the literature for the Cenicafé 1 variety [39]. Moreover, as shared by [39] this specific variety holds higher thermal properties, meaning that higher values of *K* will allow the heat to travel through the grain's domain and a higher C_p holds the heat for a longer period, therefore, the drying process can happen faster when using Cenicafé 1 variety. The drying rate *DR* and efficiency values are shared in Table 2.

Table 2. Drying rate and efficiencies per configuration.

Configuration	DR ($\%_M$ h^{-1})	System Efficiency η (%)	Pick up Efficiency η_P (%)
Hybrid C1	0.56	36.7	40.1
Hybrid C2	0.31	28.9	31.7
Hybrid C3	0.21	23.4	25.3
Control C1	0.16	18.6	21.5
Control C2	0.17	19.1	22.6
Control C3	0.16	18.4	21.1

As shared in Table 2, it is seen that the hybrid configurations portrayed higher drying rates and efficiencies. The Hybrid C1 efficiencies double those attained by its control unit, and in terms of drying rate, the 24/7 configuration displayed an elevated moisture removal in time due to the combination of both mechanical and solar drying processes [20,59]. The Hybrid C2 arrangement had the ability to work mechanically during the nights, permitting to remove moisture for twelve more hours, deriving in an improved drying rate and higher efficiencies [9,60]. Even the Hybrid C3, which operation was fully through natural convection displayed higher values than the three control units, this situation derived from the fact that the plenum chamber forbids the humid air to cross the coffee layer during the nighttime, avoiding moisture gain as described by [61].

The pick-up efficiency of the Hybrid C1 and C2 were slightly higher than the others since the mechanical condition rises the air's temperature while reducing its relative humidity, therefore the capacity of the air to remove moisture is increased [46,62].

6.3.3. Evaluation of the Drying Configurations

The replication results were averaged so that a general drying behaviour could be achieved. Nevertheless, the hybrid dryer's behaviour was relatively constant during the three configurations. The climate conditions were also even during the tests, with

low solar radiation, high cloudiness, and light rain during the day and heavy rain at night.

6.3.3.1. Configuration 1

The results of C1 displayed a high moisture removal during the daytime and a slower one during the night-time but still higher than its counterpart, as seen in Figure 10. On average, the hybrid solar dryer finished the process after 75 hours, whereas the control dryer took 254 hours to dry the same amount of coffee. The drying times for the control dryer are in accordance with those already shared in the literature for such drying types and conditions [3,8,22,24]. It is relevant, however, to state that in 254 h, the hybrid solar dryer would process 3.39 of the identical coffee batches; therefore, a significant time reduction was seen when comparing both dryers, especially because drying time was reduced by 70.47%.

It is essential to mention that the control dryer displays no moisture removal during the night due to its solar-dependent condition. Also, as explained by [63], the coffee in the control dryer experienced high moisture regain after crossing the 25% (wb). This phenomenon is not present in the hybrid-type dryer because of its availability to perform during the night. Even though the hybrid unit displayed a notable slope change during the night, moisture removal is still happening. This allows not only the process to occur faster but also to keep the product safe, seeing that moisture regain can pose a threat to the grain’s quality and innocuousness as described by [64].

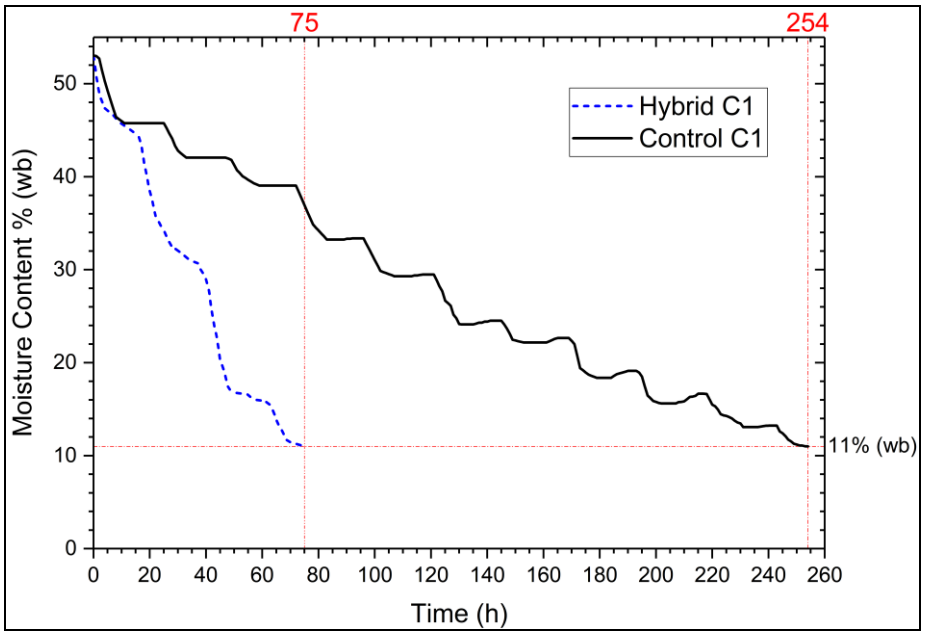

Figure 10. Configuration 1 comparative drying times.

The hybrid's slope during the daytime is rather marked; this means that the solar component is a high partaker during the hybrid drying. A similar situation is shared in the literature when drying other food materials [59,60,62]. Also, the daytime ambient temperature and relative humidity account for it, seeing that at night, the relative humidity of the air reached up to 99.9% between 2-4 am.

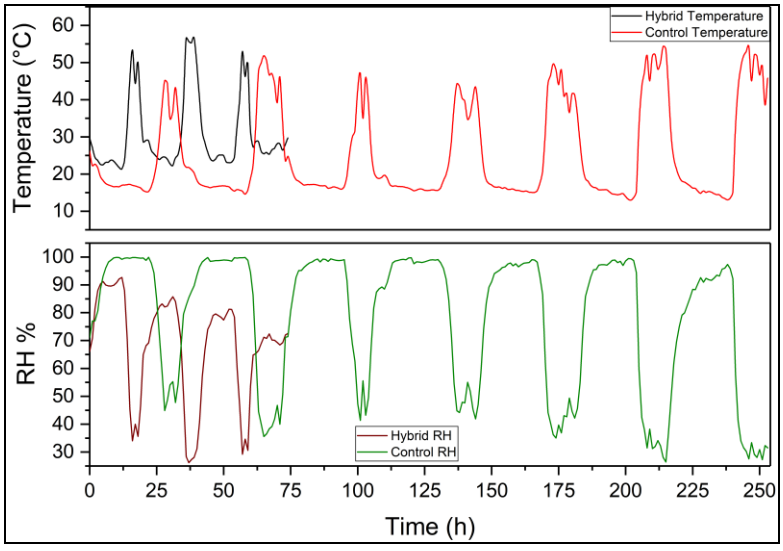

Figure 11. Drying chamber's temperature and relative humidity: Configuration 1.

Figure 11 displays the hybrid and control dryer's temperature and relative humidity behaviour. When observing the temperature profiles, it is seen that the hybrid

unit's temperature was higher than its counterpart, not only in the high-temperature phases but also in the low-temperature phase, the hybrid unit was up to 5°C higher. It is also seen that the control dryer takes more time to raise its temperature, allowing the hybrid dryer to overpass the high-low temperature cycle. The low temperatures in the hybrid unit are less uniform than those portrayed by the control, this along with the higher temperature values happened thanks to the heated air coming through the plenum chamber, which, during the whole process, had an average temperature of 42°C, a night an average temperature of 38°C was recorded. In contrast, an average drying temperature of 46°C was logged during the day. The average real biomass consumption was 1.931 kg h^{-1}, evidently lower than the theoretical one, meaning that the heat exchanger was more efficient than assumed. The biomass consumption values were also lower than the consumption of coffee husk [59,65] or chipped coffee trunks [32,59,66], also used as biofuel when mechanically drying coffee due to the denser structure of the solid trunks.

The relative humidity also displayed higher values in the control dryer, reaching up to 99.9%, common values as attained by [60] and [67]. At the same time, the hybrid unit held values significantly lower than the control dryer in the high RH region and low RH region, where up to 20% differences were seen; this is a normal phenomenon when evaluating mechanical drying against solar/sun drying [8,67,68]. This, combined with the temperature profiles and the mixed forced convection drying scenario, explains why the hybrid unit dried the batches faster [69].

6.3.3.2. Configuration 2

When using the mechanical segment (burner and fan) just during the night-time, the drying time was reduced by 113 h, meaning that the hybrid dryer processed the coffee batch 45.75% faster than the control dryer. The control drying curves are similar to those illustrated in Figure 12, indicating that there was no moisture removal during the night, furthermore, the moisture increase phenomena was recorded again. Also, the total drying time (247 h) was analogous with the one obtained by the control unit in C1.

While the control drying curves expressed no novelty, the hybrid-type dryer displayed an almost constant slope behaviour, as seen in Figure 12. This is a very relevant fact since an almost constant moisture removal was achieved by matching the

natural convection one with the forced convection one, meaning that the drying process when using the hybrid solar dryer in configuration two could be predicted. Moving from a stochastic scenario, usually portrayed by fully solar drying [70,71], towards a deterministic one, characteristic of mechanical drying [72]. This effect could be beneficial for coffee growers to foresee and control their drying process and schedule the harvest, fermentation, washing and selling steps to dynamize the entire postharvest stage.

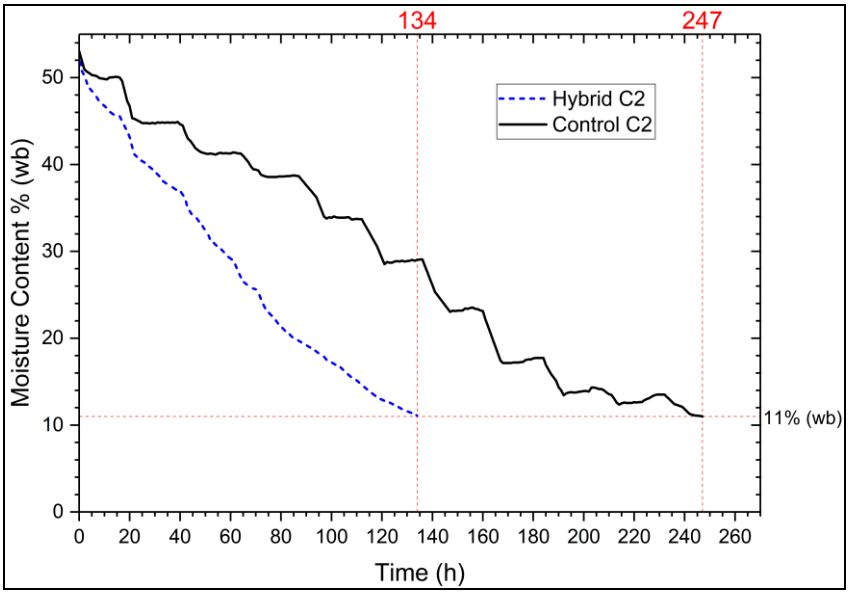

Figure 12. Configuration 2 comparative drying times.

This finding could change during the dry season; nevertheless, as stated in the literature, the harvest peaks coincide with the rainy season across all of Colombia [15,73,74]. Therefore, the available coffee during the dry period will dry faster, avoiding bottleneck generation, evading microorganism development and other types of threats [75].

The recorded temperature profile in the drying chamber in C2 shared similar results with the one attained in C1. However, C2's control dryer had significantly lower temperatures when compared to the hybrid ones. For instance, after 62 hours of drying, the high region control's temperature matches the low region's hybrid temperature; during the entire process, the hybrid dryer displayed higher temperatures as Figure 13 displays. It also takes C2 more time to raise the temperatures, and the low temperatures

are held during a more extended period. The hybrid dryer varied easier, suggesting that its behaviour is more dynamic and uses the available energy more efficiently.

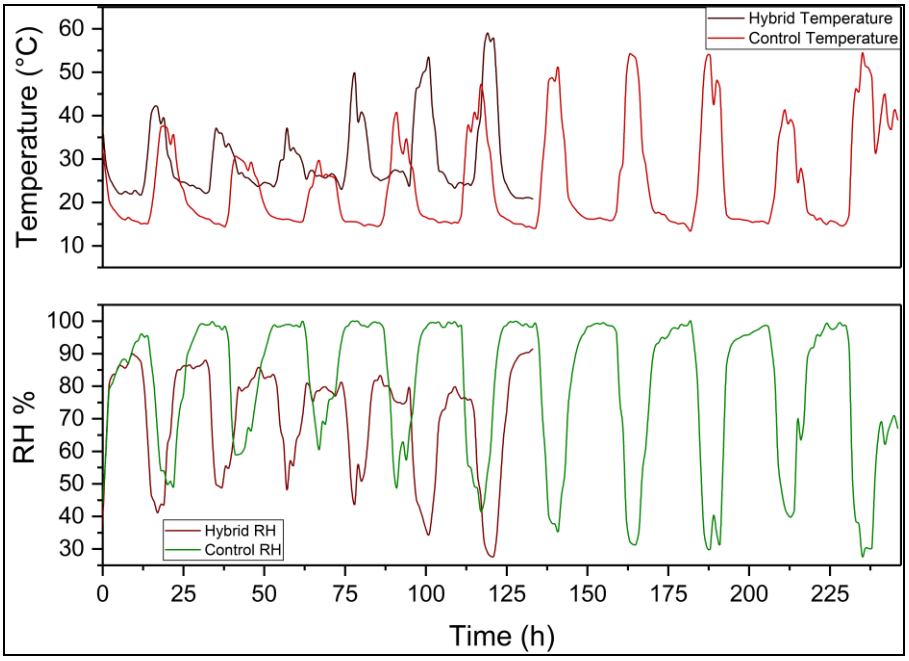

Figure 13. Drying chamber's temperature and relative humidity: Configuration 2.

In terms of relative humidity, the air in the control unit was more humid than the hybrid unit throughout the process. When looking at the hybrid's RH crests, it was seen that their values fluctuated more than those depicted by the control dryer. This represents that the air is not yet saturated, and its moisture removal capacity is still present [76,77], differing from its counterpart where an even 95-99% was recorded.

The average biomass consumption during C2 was 1.984 kg h^{-1}, slightly higher than the one recorded during the first configuration; however, it is still lower than the theoretical one. Also, seeing that the biomass burner worked just during the nights, from 134 h, roughly 67 h were night-time, similar to the 75 h recorded in C1. Also, the night's ambient temperature is lower; therefore, more heat is necessary to warm up the transfer area and to maintain it throughout all night. The average drying air temperature was 38°C, the same as C1's.

6.3.3.3. Configuration 3

The role of the plenum chamber under the coffee-holding mesh when performing C3 was positively relevant, seeing that the plenum chamber kept the coffee

mass isolated from the cold and moist night air. Even when using the hybrid unit without any mechanical help, it managed to dry the coffee mass in 200 hours, 55 hours less than the control dryer under the same operating conditions.

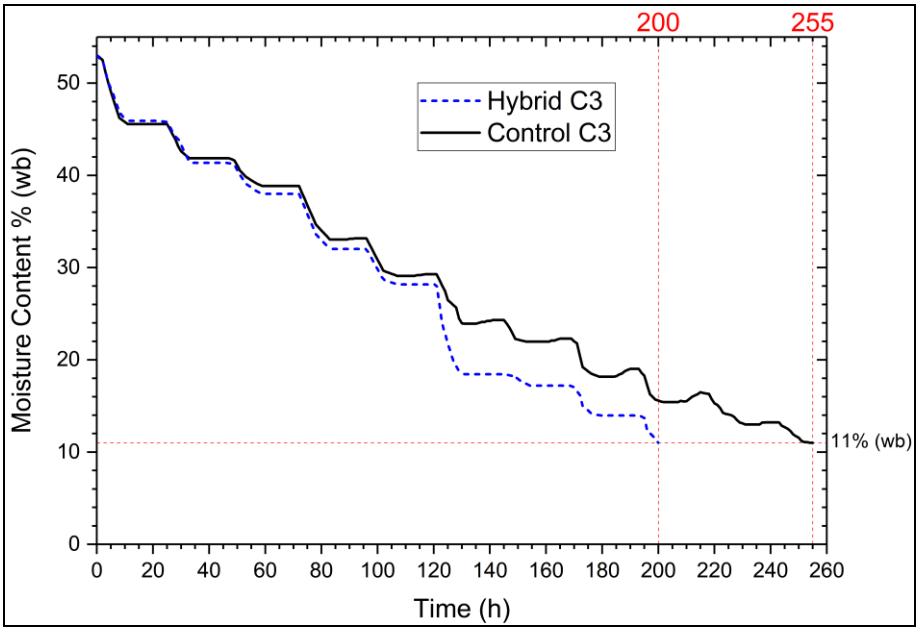

Figure 14. Configuration 3 comparative drying times.

It was seen that between 120 and 130 hours, a large amount of moisture is removed by the hybrid dryer, whereas this effect was partially seen in the control unit at the same time range as Figure 14 portrays. Also, the horizontal segments in the drying curves represent the night-time when moisture was not removed. It was noticed then that the control dryer displayed high moisture gain when surpassing the 25% (wb) moisture content, especially at 190 and 215 hours; this remoisturizing effect [3] is not visible in the hybrid unit. Therefore, avoiding contact between the product and the night air derives in moisture content homogenization as the diffusion process inside the seed occurs from its inner towards its outer domain [27,68,78]. Hence, when the daytime arrived, the drying process resumed and finished faster because the moisture content was naturally displaced and evened in the seed throughout the night. Due to this factor, and the natural coffee seed's anatomy, the seed hardening could eventually occur quicker, lowering undesired moisture gain from the atmospheric air as shared by [61].

6.3.4. Economic Evaluation

Considering that the evaluated area of 10 m^2 processes 90 kg of DPC in 75, 134 and 200 hours (C1, C2 and C3, respectively), it was calculated then how long it would take to dry the 2250 kg produced by the small coffee grower in each configuration. It is also important to mention that when carrying on this research, the price of 125 kg oscillated around 450 USD, and if 200 USD are destined for paying for the equipment, the direct payback period would be 24.1 months seeing that the apparatus' total cost was 2470 USD. However, it is shared in Table 3 the results of the analysis shared in section 2.2.4 compared to the standard tunnel-type dryer, which has a construction cost of 300 USD [34].

Table 3. Economic evaluation of the hybrid dryer and its comparison to a traditional solar tunnel dryer.

Parameter	Hybrid Solar Dryer	Tunnel Solar Dryer
Total dryer cost (USD)	2470	300
Annual cost (USD)	70	25
Total drying time (h) (Dq = 2250 kg)	C_1:2057; C_2:3676; C_3:5487	6914
Drying capacity (kg year $^{-1}$)	C_1:9577; C_2:5360; C_3:3588	2850
Payback period (years)	C_1:2.3; C_2:4.2; C_3:5.8	1.8

As shared in Table 3, the annual cost and the total dryer cost are more elevated for the hybrid solar dryer, mainly because of the steelwork; it is essential to mention that the constructed prototype was done with high thicknesses and detailed finishes; therefore, a commercial version would be expected to be cheaper. Also, it should be noted that the construction material price varies widely depending on availability and the region. Despite its price, due to the amount of coffee that can be processed, the hybrid unit displays an acceptable payback period, similar to the solar tunnel dryer's (C1). Considering the lifetime of the dryer (15 years), the hybrid solar dryer would be drying free of cost during the 85 (C1), 72 (C1) and 61% (C3) of its life period.

It should be recorded that the drying capacity of the solar tunnel dryer is 2850 kg per year (assuming coffee production all year long), just 600 kg above the average

output of a smallholder (2250 kg) owning to an average size plot, therefore, a 10 m^2 tunnel solar dryer would not be enough for a farmer with a slightly larger farm. In contrast, the drying capacity of the hybrid solar dryer could be up to three times higher than the tunnel.

Due to these factors, it is expected acceptance from part of the coffee growers, considering that a mechanical dryer of a similar capacity could cost up to 2000 USD [59] and the maintenance, fuel and energy costs would considerably extend its payback period. Also, traditionally in Latin America, parabolic or tunnel dryers are common to find in farms [14,79,80]. Hence, their adaptation into a hybrid system would be more accessible. From another perspective, the apparatus could be attractive because of its energy independence and carbon-neutral print and greenhouse gas emission reduction, seeing that a regular mechanical dryer could consume 1 liter of propane per hour, liberating in just one day 54 kg of CO_2 [81] and still would need grid energy to power the fan. Even though the burner holds a carbon-neutral fuel, the particulate matter (PM) from the combustion could eventually seem like an issue; however, this could be controlled by thoroughly using dry biomass and oxygen control, ensuring that complete combustion happens; finally, filters could also be used to reduce the PM discharge [82,83].

6.4. Conclusions

During the three evaluated working configurations, the hybrid tunnel solar dryer processed the coffee faster than the control dryer. This fact not only helps to improve the postharvest process delays due to the drying stage, but it also allows to lower the microorganism, mycotoxins, and mold development threats to the product. Although the hybrid's drying time is longer when compared to fully mechanical drying, its flexibility allows the coffee grower to improve the post-harvesting planning without the need to sell the coffee wet. Furthermore, the product holds better seed quality and structure since moisture gain is avoided.

Not only the already existing solar tunnel dryers can be easily upgraded to the newly developed hybrid tunnel dryer, but also, the short payback period and the coffee drying capacity of the hybrid unit could be an essential factor for the smallholders to

adopt and transfer this technology. Apart from its benefits to the drying process, it works with sustainable and renewable energy sources, which is ideal for isolated places. Similarly, it helps to solve the issues generated due to the large number of coffee trunks generated in the farms.

Although the construction and experiments were carried out in Colombia, this unit could be implemented in any of the coffee-producing countries, expanding the impact of the dryer towards a sustainable-processed coffee while improving the grower's conditions. If the coffee is dried faster, it could also be sold faster for better prices, improving the economic dimension of the grower, which will improve its social conditions. In addition, using renewable energy sources meets the environmental sustainability requirements, finding a balance between the three most essential pillars of sustainable development.

Acknowledgements

The authors would like to thank the members of the postharvest discipline of the National Coffee Research Center of Colombia (Cenicafé) for their assistance during the development of this investigation. This research was funded by the National Coffee Research Center of Colombia, project number POS103010 and by the Internal Grant Agency of the Faculty of Tropical AgriSciences, Czech University of Life Sciences Prague, grant number 20223109.

Contribution Statement

Eduardo Duque-Dussán: Conceptualization, Investigation, Methodology, Software, Writing – original draft. **Juan R. Sanz-Uribe:** Data curation, Methodology, Formal analysis. **Jan Banout:** Conceptualization, Supervision, Writing-review & editing, Funding acquisition.

Data Availability

Research data are available on request from the corresponding author.

Declaration of Competing Interest

We have no conflicts of interest to disclose.

References

1. Elhalis H, Cox J, Frank D, Zhao J. The role of wet fermentation in enhancing coffee flavor, aroma and sensory quality. European Food Research and Technology. 2021;247: 485–498. doi:10.1007/s00217-020-03641-6

2. Kleinwächter M, Selmar D. Influence of drying on the content of sugars in wet processed green Arabica coffees. Food Chem. 2010;119: 500–504. doi:10.1016/j.foodchem.2009.06.048

3. Duque-Dussán E, Villada-Dussán A, Roubík H, Banout J. Modeling of Forced and Natural Convection Drying Process of a Coffee Seed. Journal of the ASABE. 2022;65: 1061–1070. doi:10.13031/ja.15156

4. Batista LR, Chalfoun SM, Silva CF, Cirillo M, Varga EA, Schwan RF. Ochratoxin A in coffee beans (Coffea arabica L.) processed by dry and wet methods. Food Control. 2009;20: 784–790. doi:10.1016/j.foodcont.2008.10.003

5. Culliao AGL, Barcelo JM. Fungal and mycotoxin contamination of coffee beans in Benguet province, Philippines. Food Addit Contam Part A Chem Anal Control Expo Risk Assess. 2015;32: 250–260. doi:10.1080/19440049.2014.1001796

6. Phitakwinai S, Thepa S, Nilnont W. Thin-layer drying of parchment Arabica coffee by controlling temperature and relative humidity. Food Sci Nutr. 2019;7: 2921–2931. doi:10.1002/fsn3.1144

7. Trejos RA, Roa-Mejía G, Oliveros-Tascón CE. Humedad de equilibrio y calor latente de vaporización del café pergamino y del café verde. Revista Cenicafé. 1989;40: 5–15. Available: https://biblioteca.cenicafe.org/handle/10778/841

8. Parra-Coronado A, Roa-Mejía G, Oliveros-Tascón CE. SECAFÉ Parte I: modelamiento y simulación matemática en el secado mecánico de café pergamino. Revista Brasileira de Engenharia Agrícola e Ambiental. 2008;12: 415–427. doi:10.1590/s1415-43662008000400013

9. Elavarasan K, Verma V, Shamasundar BA. Development of prototype solar-biomass hybrid dryer and its performance evaluation using salted fish

(Cynoglossus spp.). Indian Journal of Fisheries. 2017;64: 123–129. doi:10.21077/ijf.2017.64.special-issue.76242-17

10. Simate IN. Optimization of mixed-mode and indirect-mode natural convection solar dryers. Renew Energy. 2003;28: 435–453. doi:10.1016/S0960-1481(02)00041-1

11. Atalay H, Aslan V. Advanced exergoeconomic and exergy performance assessments of a wind and solar energy powered hybrid dryer. Renew Energy. 2023;209: 218–230. doi:10.1016/j.renene.2023.03.137

12. Kong D, Wang Y, Li M, Liang J. Experimental investigation of a novel hybrid drying system powered by a solar photovoltaic/thermal air collector and wind turbine. Renew Energy. 2022;194: 705–718. doi:10.1016/j.renene.2022.05.102

13. Firdissa E, Mohammed A, Berecha G, Garedew W. Coffee Drying and Processing Method Influence Quality of Arabica Coffee Varieties (Coffee arabica L.) at Gomma I and Limmu Kossa, Southwest Ethiopia. J Food Qual. 2022;2022: 1–8. doi:10.1155/2022/9184374

14. Briceño-Martínez B, Castillo-Calderón J, Carrión-Jaura R, Díaz-Sinche D. Proposal for implantation of coffeedrying greenhouse with paraboliccover and adapted modular structure. Revista de Ciencia y Tecnología. 2020: 36–46.

15. García JC, Posada-Suárez H, Läderach P. Recommendations for the regionalizing of coffee cultivation in Colombia: A methodological proposal based on agro-climatic indices. PLoS One. 2014;9: 1–22. doi:10.1371/journal.pone.0113510

16. Osorio Hernandez R, Ferreira Tinoco IDF, Correna Carlo J, Osorio Saraz JA, Aristizábal Torres ID. Bioclimatic analysis of three buildings for wet processing of coffee in Colombia. Rev Fac Nac Agron Medellin. 2018;71: 8609–8616. doi:10.15446/rfnam.v71n3.64566

17. Tun MM, Raclavská H, Juchelková D, Růžičková J, Šafář M, Štrbová K, et al. Spent coffee ground as renewable energy source: Evaluation of the drying processes. J Environ Manage. 2020;275. doi:10.1016/j.jenvman.2020.111204

18. Phitakwinai S, Thepa S, Nilnont W. Thin-layer drying of parchment Arabica coffee by controlling temperature and relative humidity. Food Sci Nutr. 2019;7: 2921–2931. doi:10.1002/fsn3.1144

19. Varadharaju N, Karunanidhi C, Kailappan R. Coffee cherry drying: A two-layer model. Drying Technology. 2001;19: 709–715. doi:10.1081/DRT-100103947

20. Deeto S, Thepa S, Monyakul V, Songprakorp R. The experimental new hybrid solar dryer and hot water storage system of thin layer coffee bean dehumidification. Renew Energy. 2018;115: 954–968. doi:10.1016/j.renene.2017.09.009

21. Bravo-Monroy L. A Network behind Coffee. Journal of Rice Research and Developments. 2019;2: 61–65. doi:10.36959/973/421

22. Duque-Dussán E, Banout J. Improving the drying performance of parchment coffee due to the newly redesigned drying chamber. J Food Process Eng. 2022;45. doi:10.1111/jfpe.14161

23. Barjolle D, Quiñones-Ruiz XF, Bagal M, Comoé H. The Role of the State for Geographical Indications of Coffee: Case Studies from Colombia and Kenya. World Dev. 2017;98: 105–119. doi:10.1016/j.worlddev.2016.12.006

24. Sandeep TN, Channabasamma BB, Gopinandhan TN, Nagaraja JS. The effect of drying temperature on cup quality of coffee subjected to mechanical drying. Journal of Plantation Crops. 2021;49: 35–41. doi:10.25081/jpc.2021.v49.i1.7059

25. Silva GM da, Ferreira AG, Coutinho RM, Maia CB. Energy and exergy analysis of the drying of corn grains. Renew Energy. 2021;163: 1942–1950. doi:10.1016/j.renene.2020.10.116

26. Gu X, Dai J, Li H, Dai Y. Experimental and theoretical assessment of a solar assisted heat pump system for in-bin grain drying: A comprehensive case study. Renew Energy. 2022;181: 426–444. doi:10.1016/j.renene.2021.09.049

27. Ramírez-Martínez A, Salgado-Cervantes MA, Rodríguez-Jimenes GC, García-Alvarado MA, Cherblanc F, Bénet JC. Water transport in parchment and

endosperm of coffee bean. J Food Eng. 2013;114: 375–383. doi:10.1016/j.jfoodeng.2012.08.028

28. Borém FM, Marques ER, Alves E. Ultrastructural analysis of drying damage in parchment Arabica coffee endosperm cells. Biosyst Eng. 2008;99: 62–66. doi:10.1016/j.biosystemseng.2007.09.027

29. Rendón JR. Producción de café variedad Castillo® en altas densidades de siembra con uno y dos tallos por sitio. Revista Cenicafé. 2021;72: e72106. doi:10.38141/10778/72106

30. Aguirre Cuellar B, Lobo JC, Elcure FM. Shading in family coffee farms as an environmental incentive promoter for ecosystem services in Tolima, Colombia. Int J Agric Sustain. 2022;0: 1–13. doi:10.1080/14735903.2022.2041234

31. Aristizábal-Marulanda V, Cardona A. CA, Martín M. Supply chain of biorefineries based on Coffee Cut-Stems: Colombian case. Chemical Engineering Research and Design. 2022;187: 174–183. doi:10.1016/j.cherd.2022.08.060

32. Rodríguez Valencia N, Antonio D, Franco Z. Los subproductos del cafe: Fuente de energia renovable. Avances Técnicos Cenicafé. 2010;393. doi:10.38141/10779/0393

33. O'Grady P, Ramers D, Bowen J. Artificial intelligence constraint nets applied to design for economic manufacture and assembly. Computer Integrated Manufacturing Systems. 1988;1: 204–210. doi:10.1016/0951-5240(88)90052-3

34. Oliveros-Tascón CE, Ramírez-Gómez CA, Sanz-Uribe JR, Peñuela-Martínez A. Secador Solar de Túnel para Café Pergamino. Cenicafé - Centro Nacional de Investigaciones de Café, Avances Técnicos. 2006;353: 8. Available: https://www.cenicafe.org/es/publications/avt0353.pdf

35. Oliveros-Tascón CE, Ramírez-Gómez CA, Tibaduiza-Vianchá CA, Sanz-Uribe JR. Construcción de secadores solares tipo túnel con nuevos materiales. Cenicafé - Centro Nacional de Investigaciones de Café, Avances Técnicos. 2017;482: 8.

36. Zhong W, Xu K, Li X, Liao Y, Tao G, Kagawa T. Determination of pressure drop for air flow through sintered metal porous media using a modified Ergun equation. Advanced Powder Technology. 2016;27: 1134–1140. doi:10.1016/j.apt.2016.03.024

37. Ghosh P, Venkatachalapathy N. Processing and Drying of Coffee - A review. International Journal of Engineering Research & Technology. 2014;3: 784–794. Available: https://www.ijert.org/research/processing-and-drying-of-coffee-a-review-IJERTV3IS120482.pdf

38. Mwithiga G, Kigo SN. Performance of a solar dryer with limited sun tracking capability. J Food Eng. 2006;74: 247–252. doi:10.1016/j.jfoodeng.2005.03.018

39. Duque-Dussán E, Sanz-Uribe JR, Dussán-Lubert C, Banout J. Thermophysical properties of parchment coffee: New Colombian varieties. J Food Process Eng. 2023; 1–13. doi:10.1111/jfpe.14300

40. Parra-Coronado A, Roa-Mejía G, Oliveros-Tascón CE, Sanz-Uribe JR. Optimización operacional de secadores mecánicos para café pergamino. CENICAFE; 2017.

41. Khanlari A, Sözen A, Afshari F, Tuncer AD. Energy-exergy and sustainability analysis of a PV-driven quadruple-flow solar drying system. Renew Energy. 2021;175: 1151–1166. doi:10.1016/j.renene.2021.05.062

42. Pineda MF, Tinoco HA, Lopez-Guzman J, Perdomo-Hurtado L, Cardona CI, Rincon-Jimenez A, et al. Ripening stage classification of Coffea arabica L. var. Castillo using a Machine learning approach with the electromechanical impedance measurements of a contact device. Mater Today Proc. 2022;1675: 1–26. doi:10.1016/j.matpr.2022.04.669

43. Jurado-Chaná JM, Montoya-Restrepo EC, Oliveros-Tascón CE, García-Alzate J. Método para medir el contenido de humedad del café pergamino en el secado solar del café. Revista Cenicafé. 2009;60: 135–147. Available: https://www.cenicafe.org/es/publications/arc060%2802%29135-147.pdf

44. Benlioğlu MM, Karaağaç MO, Ergün A, Ceylan İ, Ali İHG. A detailed analysis of a novel auto-controlled solar drying system combined with thermal energy

storage concentrated solar air heater (CSAC) and concentrated photovoltaic/thermal (CPV/T). Renew Energy. 2023;211: 420–433. doi:10.1016/j.renene.2023.04.108

45. Montoya-Restrepo EC, Oliveros-Tascón CE, Roa-Mejía G. Optimización Operacional del Secador Intermitente de Flujos Concurrentes para Café Pergamino. Revista Cenicafé. 1990;41: 19–33. Available: http://hdl.handle.net/10778/939

46. Leon MA, Kumar S, Bhattacharya SC. A comprehensive procedure for performance evaluation of solar food dryers. Renewable and Sustainable Energy Reviews. 2002;6: 367–393. doi:10.1016/S1364-0321(02)00005-9

47. Banout J, Ehl P, Havlik J, Lojka B, Polesny Z, Verner V. Design and performance evaluation of a Double-pass solar drier for drying of red chilli (Capsicum annum L.). Solar Energy. 2011;85: 506–515. doi:10.1016/j.solener.2010.12.017

48. Duque-Orrego H, Saldarriaga-S F, López-Q JJ, Oliveros-Tascón CE. Economía del Secado del Café: Un Estudio de Caso. Avances Técnicos Cenicafé. Apr 2001: 1–8. Available: https://www.cenicafe.org/es/index.php/nuestras_publicaciones/avances_tecnicos/avance_tecnico_0286

49. Singh PP, Singh S, Dhaliwal SS. Multi-shelf domestic solar dryer. Energy Convers Manag. 2006;47: 1799–1815. doi:10.1016/j.enconman.2005.10.002

50. Lee JH, Shin JH, Chang SM, Min T. Numerical analysis on natural convection heat transfer in a single circular fin-tube heat exchanger (part 1): Numerical method. Entropy. 2020;22: 1–10. doi:10.3390/E22030363

51. Sanghi A, Ambrose RPK, Maier D. CFD simulation of corn drying in a natural convection solar dryer. Drying Technology. 2018;36: 859–870. doi:10.1080/07373937.2017.1359622

52. Kjær LS, Poulsen M, Sørensen K, Condra T. Modelling of hot air chamber designs of a continuous flow grain dryer. Engineering Science and Technology, an International Journal. 2018;21: 1047–1055. doi:10.1016/j.jestch.2018.02.002

53. Sonthikun S, Chairat P, Fardsin K, Kirirat P, Kumar A, Tekasakul P. Computational fluid dynamic analysis of innovative design of solar-biomass hybrid dryer: An experimental validation. Renew Energy. 2016;92: 185–191. doi:10.1016/j.renene.2016.01.095

54. Estiati I, Tellabide M, Saldarriaga JF, Altzibar H, Olazar M. Influence of the fountain confiner in a conical spouted bed dryer. Powder Technol. 2019;356: 193–199. doi:10.1016/j.powtec.2019.08.005

55. Southwell DB, Langrish TAG, Fletcher DF. Use of computational fluid dynamics techniques to assess design alternatives for the plenum chamber of a small spray dryer. Drying Technology. 2001;19: 257–268. doi:10.1081/DRT-100102902

56. Renaudo CA, Bertin DE, Bucalá V. Design Impact on Airflow Patterns in Fluidization Units. Chem Eng Technol. 2019;42: 2365–2375. doi:10.1002/ceat.201800580

57. McMinn WAM, Magee TRA. Principles, methods and applications of the convective drying of foodstuffs. Food and Bioproducts Processing: Transactions of the Institution of of Chemical Engineers, Part C. 1999;77: 175–193. doi:10.1205/096030899532466

58. Corrêa PC, Goneli ALD, Júnior PCA, de Oliveira GHH, Valente DSM. Moisture sorption isotherms and isosteric heat of sorption of coffee in different processing levels. Int J Food Sci Technol. 2010;45: 2016–2022. doi:10.1111/j.1365-2621.2010.02373.x

59. Manrique R, Vásquez D, Chejne F, Pinzón A. Energy analysis of a proposed hybrid solar–biomass coffee bean drying system. Energy. 2020;202: 1–8. doi:10.1016/j.energy.2020.117720

60. Hamdani, Rizal TA, Muhammad Z. Fabrication and testing of hybrid solar-biomass dryer for drying fish. Case Studies in Thermal Engineering. 2018;12: 489–496. doi:10.1016/j.csite.2018.06.008

61. Lee SS, Kim JH, Hong SB, Yun SH. Effect of humidification and hardening treatment on seed germination of rice. Korean Journal of Crop Science. 1998;43: 157–160.

62. Udomkun P, Romuli S, Schock S, Mahayothee B, Sartas M, Wossen T, et al. Review of solar dryers for agricultural products in Asia and Africa: An innovation landscape approach. J Environ Manage. 2020;268: 110730. doi:10.1016/j.jenvman.2020.110730

63. Kath J, Mittahalli Byrareddy V, Mushtaq S, Craparo A, Porcel M. Temperature and rainfall impacts on robusta coffee bean characteristics. Clim Risk Manag. 2021;32: 100281. doi:10.1016/j.crm.2021.100281

64. Burmester K, Eggers R. Heat and mass transfer during the coffee drying process. J Food Eng. 2010;99: 430–436. doi:10.1016/j.jfoodeng.2009.12.021

65. Oliveira LS, Franca AS. An Overview of the Potential Uses for Coffee Husks. Coffee in Health and Disease Prevention. Elsevier Inc.; 2015. doi:10.1016/B978-0-12-409517-5.00031-0

66. Tesfaye A, Workie F, Kumar VS. Production and Characterization of Coffee Husk Fuel Briquettes as an Alternative Energy Source. Advances in Materials Science and Engineering. 2022;2022. doi:10.1155/2022/9139766

67. Hung N Van, Martinez R, Tuan T Van, Gummert M. Development and verification of a simulation model for paddy drying with different flatbed dryers. Plant Prod Sci. 2019;22: 119–130. doi:10.1080/1343943X.2018.1518723

68. Zhang S, Kong N, Zhu Y, Zhang Z, Xu C. 3D model-based simulation analysis of energy consumption in hot air drying of corn kernels. Math Probl Eng. 2013;2013. doi:10.1155/2013/579452

69. Heydari A. Experimental analysis of hybrid dryer combined with spiral solar air heater and auxiliary heating system: Energy, exergy and economic analysis. Renew Energy. 2022;198: 1162–1175. doi:10.1016/j.renene.2022.08.110

70. Midilli A, Kucuk H, Yapar Z. A new model for single-layer drying. Drying Technology. 2002;20: 1503–1513. doi:10.1081/DRT-120005864

71. Richardson CW. Stochastic simulation of daily precipitation, temperature, and solar radiation. Water Resour Res. 1981;17: 182–190. doi:10.1029/WR017i001p00182

72. Lugon J, Silva Neto AJ. Solution of porous media inverse drying problems using a combination of stochastic and deterministic methods. Journal of the Brazilian Society of Mechanical Sciences and Engineering. 2011;33: 400–407. doi:10.1590/S1678-58782011000400003

73. Peña-Quiñones AJ, Ramírez-Builes VH, Jaramillo-Robledo Á, Rendón-Sáenz JR, Arcila-Pulgarín J. Effects of Daylength and Soil Humidity on the Flowering of Coffee Coffea Arabica L. in Colombia. Rev Fac Nac Agron Medellin. 2011;64: 5745–5754.

74. Avelino J, Cristancho M, Georgiou S, Imbach P, Aguilar L, Bornemann G, et al. The coffee rust crises in Colombia and Central America (2008–2013): impacts, plausible causes and proposed solutions. Food Secur. 2015;7: 303–321. doi:10.1007/s12571-015-0446-9

75. Schemminger J, Mbuge D, Hofacker W. Ambient air cereal grain drying – Simulation of the thermodynamic and microbial behavior. Thermal Science and Engineering Progress. 2019;13: 100382. doi:10.1016/j.tsep.2019.100382

76. Dias CDA, Andrade ET De, Lemos IA, Borém FM, Barros EA. Sorption Isotherms and Isosteric Heat of Pericarp and Endosperm Tissues of Arabica Coffee Fruit. Engenharia Agrícola. 2020;40: 78–89. doi:10.1590/1809-4430-eng.agric.v40n1p78-89/2020

77. Rodríguez-Robles F, Monroig-Saltar F. Parametric Thermodynamic Models of Parchment Coffee Beans during HARC2S Dehydration. J Food Process Technol. 2014;05: 1–7. doi:10.4172/2157-7110.1000322

78. Dutta SK, Nema VK, Bhardwaj RK. Drying behaviour of spherical grains. Int J Heat Mass Transf. 1988;31: 855–861. doi:10.1016/0017-9310(88)90142-1

79. Oliveros-Tascón CE, Ramirez-Gómez CA, Sanz-Uribe JR, Peñuela-Martínez A. Secador parabólico mejorado. Cenicafé - Centro Nacional de Investigaciones de

Café, Avances Técnicos. 2008;376: 8. Available: https://www.cenicafe.org/es/publications/avt0376.pdf

80. Ramirez-Gómez CA, Oliveros-Tascón CE, Roa-Mejía G. Construya El Secador Solar Parabólico. Cenicafé - Centro Nacional de Investigaciones de Café, Avances Técnicos. 2002; 1–8.

81. Aurell J, Hubble D, Gullett BK, Holder A, Washburn E, Tabor D. Characterization of Emissions from Liquid Fuel and Propane Open Burns. Fire Technol. 2017;53: 2023–2038. doi:10.1007/s10694-017-0670-2

82. Philip N, Duraipandi S, Sreekumar A. Techno-economic analysis of greenhouse solar dryer for drying agricultural produce. Renew Energy. 2022;199: 613–627. doi:10.1016/j.renene.2022.08.148

83. Atalay H, Yavaş N, Turhan Çoban M. Sustainability and performance analysis of a solar and wind energy assisted hybrid dryer. Renew Energy. 2022;187: 1173–1183. doi:10.1016/j.renene.2022.02.020

Conclusions

This thesis provides a comprehensive and in-depth analysis of coffee drying and the different challenges to address to keep the product safe and improve the bottleneck generated due to the drying process aiming to improve the smallholders' living standards sustainably while providing a deeper understanding of the coffee drying process under different conditions.

The Finite Element Method that depicted the process prediction can be used not only to simulate the drying process of the coffee in different scenarios but also to provide relevant information on the transport phenomenon, moisture profile distribution and its change in time, allowing future research to focus on these places and control microorganism and fungi development. Reducing the gap of the stochastic nature of natural convection drying towards a more deterministic one permits decision-making regarding the ideal drying method at a specific moment of the year, depending on the climate conditions.

Furthermore, understanding the air distribution and dynamics inside mechanical dryers widens the design considerations, focusing on attaining better moisture removal and air distribution for effective water removal, increasing the dryer's efficiency and reducing energy and fuel consumption, considering not only the forced air inlet but also thinking on the optimal shape of the dryer. Likewise, finetuning the mathematical models that describe the drying process and moisture diffusion will enhance the accuracy of the mechanical drying predictions. Therefore, the drying programs can be reliable and improve the cash flow on site.

Parchment coffee's improved thermal and physical properties play a relevant role in updating the mathematical models for precise simulations. Also, depicting better thermal and physical properties improves the drying process in general. If the surface area is larger, the contact region between grains will also be more significant, and the porosity will change, allowing air to flow better through the layer. Correspondingly, seeing that the thermal conductivity is higher in the new varieties, the heat transfer happens faster between grain and grain, and this heat will remain for more time inside the grain due to the higher specific heat values.

Finally, the novel hybrid solar dryer allows the coffee grower to dry more flexibly, faster, and with components that can easily adapt to the existing solar drying technologies. Also, its energetical independence could be an ideal solution for isolated household farms, allowing not only to solve the coffee drying issues but also to help to sort out the residual biomass by-product of the coffee renewal process and other agricultural waste. Its cutting-edge design and fabrication ensure a quality coffee output and optimal working and drying performance, likewise, the hybrid solar dryer's use can be applied in all the coffee producing countries, disregarding if they produce coffee through the wet, natural or honey process, moreover, the dryer could be also used to dry different grains and foodstuffs, widening its applications.

References

Aguirre Cuellar B, Lobo JC, Elcure FM. 2022. Shading in family coffee farms as an environmental incentive promoter for ecosystem services in Tolima, Colombia. International Journal of Agricultural Sustainability **0**:1–13. Available from https://doi.org/10.1080/14735903.2022.2041234.

Al-Kayiem HH. 2016. Hybrid techniques to enhance solar thermal: The way forward. International Journal of Energy Production and Management **1**:50–60.

Aristizábal-Marulanda V, Cardona A. CA, Martín M. 2022. Supply chain of biorefineries based on Coffee Cut-Stems: Colombian case. Chemical Engineering Research and Design **187**:174–183. Elsevier. Available from https://doi.org/10.1016/j.cherd.2022.08.060.

Atalay H, Yavaş N, Turhan Çoban M. 2022. Sustainability and performance analysis of a solar and wind energy assisted hybrid dryer. Renewable Energy **187**:1173–1183. Elsevier Ltd.

Avelino J, Cristancho M, Georgiou S, Imbach P, Aguilar L, Bornemann G, Läderach P, Anzueto F, Hruska AJ, Morales C. 2015. The coffee rust crises in Colombia and Central America (2008–2013): impacts, plausible causes and proposed solutions. Food Security **7**:303–321.

Bakker-Arkema FW, Lerew LE, De Boer SF, Roth MG. 1974. Grain dryer simulation. Agricultural Experiment Station, Res. Rep 224, Michigan State University, East Lansing, USA.

Banaszkiewicz M, Seiferlin K, Spohn T, Kargl G, Kömle N. 1997. A new method for the determination of thermal conductivity and thermal diffusivity from linear heat source measurements. Review of Scientific Instruments **68**:4184–4190.

Banout J, Ehl P, Havlik J, Lojka B, Polesny Z, Verner V. 2011. Design and performance evaluation of a Double-pass solar drier for drying of red chilli (Capsicum annum L.). Solar Energy **85**:506–515.

Barjolle D, Quiñones-Ruiz XF, Bagal M, Comoé H. 2017. The Role of the State for Geographical Indications of Coffee: Case Studies from Colombia and Kenya. World Development **98**:105–119.

Barrios-Rodríguez YF, Rojas Reyes CA, Triana Campos JS, Girón-Hernández J, Rodríguez-Gamir J. 2021. Infrared spectroscopy coupled with chemometrics in coffee post-harvest processes as complement to the sensory analysis. LWT **145**:111304. Available from https://linkinghub.elsevier.com/retrieve/pii/S0023643821004576.

Benlioğlu MM, Karaağaç MO, Ergün A, Ceylan İ, Ali İHG. 2023. A detailed analysis of a novel auto-controlled solar drying system combined with thermal energy storage concentrated solar air heater (CSAC) and concentrated photovoltaic/thermal (CPV/T). Renewable Energy **211**:420–433. Elsevier Ltd.

Berhanu T, Ali M, Essubalew G. 2014. Impact of Sun Drying Methods and Layer Thickness on the Quality of Highland Arabica Coffee Varieties at Limmu, Southwestern Ethiopia. Journal of Horticulture **01**:1–7.

Borém FM, Marques ER, Alves E. 2008. Ultrastructural analysis of drying damage in parchment Arabica coffee endosperm cells. Biosystems Engineering **99**:62–66.

Bravo-Monroy L. 2019. A Network behind Coffee. Journal of Rice Research and Developments **2**:61–65.

Briceño-Martínez B, Castillo-Calderón J, Carrión-Jaura R, Díaz-Sinche D. 2020. Proposal for implantation of coffeedrying greenhouse with paraboliccover and adapted modular structure. Revista de Ciencia y Tecnología:36–46. UNIV POLITECNICA SALESIANA ECUADOR-SALESIAN POLYTECNIC UNIV, CALLE TURUHUAYO 3-69 & CALLE VIEJA, CUENCA, 00000, ECUADOR, Loja, Ecuador.

Brooker DB, Bakker-Arkema FW, Hall CW. 1992. Drying and storage of grains and oilseeds2nd Revise. Van Nostrand Reinhold, New York, New York, NY, United States.

Budiyanto B, Uker D, Izahar T. 2021. Arakteristik Fisik Kualitas Biji Kopi Dan Kualitas Kopi Bubuk Sintaro 2 Dan Sintaro 3 Dengan Berbagai Tingkat Sangrai. Jurnal Agroindustri **11**:54–71. Available from https://ejournal.unib.ac.id/index.php/agroindustri/article/view/16009.

Cardona CI, Tinoco HA, Perdomo-Hurtado L, Duque-Dussan E, Banout J. 2022. Computational Fluid Dynamics Modeling of a Pneumatic Air Jet Nozzle for an application in Coffee Fruit Harvesting. Pages 1–7 2022 International Conference on Electrical, Computer and Energy Technologies (ICECET). IEEE. Available from https://ieeexplore.ieee.org/document/9872877/.

Coradi PC, Borém FM, Reinato CH. 2014. Coffee Cherries Drying Process and the Influence of Environment Relative Humidity in the Mathematical Modeling, Moisture Content, and Enthalpy of Vaporization. Energia Na Agricultura **29**:148.

Culliao AGL, Barcelo JM. 2015. Fungal and mycotoxin contamination of coffee beans in Benguet province, Philippines. Food Additives and Contaminants - Part A Chemistry, Analysis, Control, Exposure and Risk Assessment **32**:250–260. Taylor & Francis. Available from http://dx.doi.org/10.1080/19440049.2014.1001796.

Deeto S, Thepa S, Monyakul V, Songprakorp R. 2018. The experimental new hybrid solar dryer and hot water storage system of thin layer coffee bean dehumidification. Renewable Energy **115**:954–968. Elsevier Ltd. Available from https://doi.org/10.1016/j.renene.2017.09.009.

Diamante LM, Munro PA. 1993. Mathematical modelling of the thin layer solar drying of sweet potato slices. Solar Energy **51**:271–276.

Doymaz I, Pala M. 2003. The thin-layer drying characteristics of corn. Journal of Food Engineering **60**:125–130.

Duque-Dussán E, Sanz-Uribe JR, Banout J. 2023. Design and evaluation of a hybrid solar dryer for postharvesting processing of parchment coffee. Renewable Energy **215**:118961. Available from https://linkinghub.elsevier.com/retrieve/pii/S0960148123008674.

Duque-Dussán E, Villada-Dussán A, Roubík H, Banout J. 2022. Modeling of Forced and Natural Convection Drying Process of a Coffee Seed. Journal of the ASABE **65**:1061–1070. Available from https://elibrary.asabe.org/abstract.asp?AID=53603&t=3&dabs=Y&redir=&redirType=.

Duque-Orrego H, Saldarriaga-S F, López-Q JJ, Oliveros-Tascón CE. 2001, April. Economía del Secado del Café: Un Estudio de Caso. Avances Técnicos Cenicafé:1–8. Chinchiná, Caldas, Colombia. Available from https://www.cenicafe.org/es/index.php/nuestras_publicaciones/avances_tecnicos/avance_tecnico_0286.

Duque-Dussán E, Banout J. 2022. Improving the drying performance of parchment coffee due to the newly redesigned drying chamber. Journal of Food Process Engineering **45**. Available from https://onlinelibrary.wiley.com/doi/10.1111/jfpe.14161.

Duque-Dussán E, Sanz-Uribe JR, Dussán-Lubert C, Banout J. 2023. Thermophysical properties of parchment coffee: New Colombian varieties. Journal of Food Process Engineering:1–13. Available from https://onlinelibrary.wiley.com/doi/10.1111/jfpe.14300.

Elavarasan K, Verma V, Shamasundar BA. 2017. Development of prototype solar-biomass hybrid dryer and its performance evaluation using salted fish (Cynoglossus spp.). Indian Journal of Fisheries **64**:123–129.

Fadai NT, Melrose J, Please CP, Schulman A, Van Gorder RA. 2017. A heat and mass transfer study of coffee bean roasting. International Journal of Heat and Mass Transfer **104**:787–799. Elsevier Ltd. Available from http://dx.doi.org/10.1016/j.ijheatmasstransfer.2016.08.083.

Fagundes B, Damasceno FA, Andrade RR, Saraz JAO, Barbari M, Vega FAO, Nascimento JAC. 2020. Comparison of airflow homogeneity in compost dairy barns with different ventilation systems using the CFD model. Agronomy Research **18**:788–796.

Firdissa E, Mohammed A, Berecha G, Garedew W. 2022. Coffee Drying and Processing Method Influence Quality of Arabica Coffee Varieties (Coffee arabica L.) at Gomma I and Limmu Kossa, Southwest Ethiopia. Journal of Food Quality **2022**:1–8.

García JC, Posada-Suárez H, Läderach P. 2014. Recommendations for the regionalizing of coffee cultivation in Colombia: A methodological proposal based on agro-climatic indices. PLoS ONE **9**:1–22.

Ghosh P, Venkatachalapathy N. 2014. Processing and Drying of Coffee - A review. International Journal of Engineering Research & Technology **3**:784–794. Available from https://www.ijert.org/research/processing-and-drying-of-coffee-a-review-IJERTV3IS120482.pdf.

Gu X, Dai J, Li H, Dai Y. 2022. Experimental and theoretical assessment of a solar assisted heat pump system for in-bin grain drying: A comprehensive case study. Renewable Energy **181**:426–444. Elsevier Ltd.

Guiné RPF. 2018. The Drying of Foods and Its Effect on the Physical-Chemical, Sensorial and Nutritional Properties. ETP International Journal of Food Engineering **4**:93–100.

Gutiérrez-Flórez JM, Copete-López H. 2009. Hacia la Mejora del Secado Mecánico del Café en Colombia. TecnoLógicas:109–132. Available from https://revistas.itm.edu.co/index.php/tecnologicas/article/view/241.

Hamdani, Rizal TA, Muhammad Z. 2018. Fabrication and testing of hybrid solar-biomass dryer for drying fish. Case Studies in Thermal Engineering **12**:489–496. Elsevier Ltd. Available from https://doi.org/10.1016/j.csite.2018.06.008.

Hicks A. 2002. Post-harvest Processing and Quality Assurance for Speciality/Organic Coffee Products. FAO Regional Office for Asia and the Pacific:6. Available from http://www.journal.au.edu/au_techno/2002/jan2002/article2.pdf.

Hii CL, Law CL, Cloke M. 2009. Modeling using a new thin layer drying model and product quality of cocoa. Journal of Food Engineering **90**:191–198.

Hung N Van, Martinez R, Tuan T Van, Gummert M. 2019. Development and verification of a simulation model for paddy drying with different flatbed dryers. Plant Production Science **22**:119–130. Taylor & Francis. Available from https://doi.org/10.1080/1343943X.2018.1518723.

Kamal IM, Sobolik V, Kristiawan M, Mounir SM, Allaf K. 2008. Structure expansion of green coffee beans using instantaneous controlled pressure drop process. Innovative Food Science & Emerging Technologies **9**:534–541. Available from https://linkinghub.elsevier.com/retrieve/pii/S1466856408000258.

Kath J, Mittahalli Byrareddy V, Mushtaq S, Craparo A, Porcel M. 2021. Temperature and rainfall impacts on robusta coffee bean characteristics. Climate Risk Management **32**:100281. Elsevier B.V. Available from https://doi.org/10.1016/j.crm.2021.100281.

Kong D, Wang Y, Li M, Liang J. 2022. Experimental investigation of a novel hybrid drying system powered by a solar photovoltaic/thermal air collector and wind turbine. Renewable Energy **194**:705–718. Elsevier Ltd.

Kulapichitr F, Borompichaichartkul C, Suppavorasatit I, Cadwallader KR. 2019. Impact of drying process on chemical composition and key aroma components of Arabica coffee. Food Chemistry **291**:49–58. Elsevier. Available from https://doi.org/10.1016/j.foodchem.2019.03.152.

Liu Q, Bakker-Arkema FW. 2001. A model-predictive controller for grain drying. Journal of Food Engineering **49**:321–326.

Luna González A, Macías Lopez A, Taboada Gaytán OR, Morales Ramos V. 2019. Cup quality attributes of Catimors as affected by size and shape of coffee bean (Coffea arabica L.). International Journal of Food Properties **22**:758–767.

Manrique R, Vásquez D, Chejne F, Pinzón A. 2020. Energy analysis of a proposed hybrid solar–biomass coffee bean drying system. Energy **202**:1–8.

Midilli A, Kucuk H, Yapar Z. 2002. A new model for single-layer drying. Drying Technology **20**:1503–1513.

Muñoz-Neira MJ, Roa-Ardila MF, Correa-Celi CR. 2020. Comparative analysis of drying coffee beans using microwave and conventional oven. Revista Facultad de Ingenieria:100–108.

Mwithiga G, Kigo SN. 2006. Performance of a solar dryer with limited sun tracking capability. Journal of Food Engineering **74**:247–252.

Natesan VT, Mani P, Prasad TJS, Krishna JM, Sekar S. 2020. Applications of thin layer modelling techniques and advances in drying of agricultural products. AIP Conference Proceedings **2311**.

Oliveira LS, Franca AS. 2015. An Overview of the Potential Uses for Coffee Husks. Page Coffee in Health and Disease Prevention. Elsevier Inc. Available from http://dx.doi.org/10.1016/B978-0-12-409517-5.00031-0.

Oliveros-Tascón CE, Liliana López-Valencia ;, Claudia ;, Buitrago M, Edilson ;, Moreno-Cárdenas L. 2010. Determinación Del Contenido De Humedad Del Café Durante El Secado En Silos. Cenicafé **61**:108–118.

Oliveros-Tascón CE, Ramirez-Gómez CA, Sanz-Uribe JR, Peñuela-Martínez A. 2008. Secador parabólico mejorado. Cenicafé - Centro Nacional de Investigaciones de Café, Avances Técnicos **376**:8. Available from https://www.cenicafe.org/es/publications/avt0376.pdf.

Oliveros-Tascón CE, Ramírez-Gómez CA, Sanz-Uribe JR, Peñuela-Martínez A. 2006. Secador Solar de Túnel para Café Pergamino. Cenicafé - Centro Nacional de Investigaciones de Café, Avances Técnicos **353**:8. Available from https://www.cenicafe.org/es/publications/avt0353.pdf.

Oliveros-Tascón CE, Ramírez-Gómez CA, Tibaduiza-Vianchá CA, Sanz-Uribe JR. 2017. Construcción de secadores solares tipo túnel con nuevos materiales. Cenicafé - Centro Nacional de Investigaciones de Café, Avances Técnicos **482**:8.

Osorio-Arias J, Delgado-Arias S, Cano L, Zapata S, Quintero M, Nuñez H, Ramírez C, Simpson R, Vega-Castro O. 2020. Sustainable Management and Valorization of Spent Coffee Grounds Through the Optimization of Thin Layer Hot Air-Drying Process. Waste and Biomass Valorization **11**:5015–5026. Springer Netherlands. Available from https://doi.org/10.1007/s12649-019-00793-9.

Osorio Hernandez R, Ferreira Tinoco IDF, Correna Carlo J, Osorio Saraz JA, Aristizábal Torres ID. 2018. Bioclimatic analysis of three buildings for wet processing of coffee in Colombia. Revista Facultad Nacional de Agronomía Medellín **71**:8609–8616. Available from https://revistas.unal.edu.co/index.php/refame/article/view/64566.

Parra-Coronado A, Roa-Mejía G, Oliveros-Tascón CE. 2008a. SECAFÉ Parte II: recomendaciones para el manejo eficiente de los secadores mecánicos de café pergamino. Revista Brasileira de Engenharia Agrícola e Ambiental **12**:428–434. Available from http://www.agriambi.com.br.

Parra-Coronado A, Roa-Mejía G, Oliveros-Tascón CE. 2008b. SECAFÉ Parte I: modelamiento y simulación matemática en el secado mecánico de café pergamino. Revista Brasileira de Engenharia Agrícola e Ambiental **12**:415–427.

Perazzini H, Leonel A, Perazzini MTB. 2021. Energy of activation, instantaneous energy consumption, and coupled heat and mass transfer modeling in drying of sorghum grains. Biosystems Engineering **210**:181–192. Elsevier Ltd. Available from https://doi.org/10.1016/j.biosystemseng.2021.08.025.

Philip N, Duraipandi S, Sreekumar A. 2022. Techno-economic analysis of greenhouse solar dryer for drying agricultural produce. Renewable Energy **199**:613–627. Elsevier Ltd.

Pires F de C, Pereira RGFA, Baqueta MR, Valderrama P, Alves da Rocha R. 2021. Near-infrared spectroscopy and multivariate calibration as an alternative to the Agtron to predict roasting degrees in coffee beans and ground coffees. Food Chemistry **365**:130471. Elsevier Ltd. Available from https://doi.org/10.1016/j.foodchem.2021.130471.

Prakash B, Siebenmorgen TJ. 2018. MATHEMATICAL MODELING OF A CROSS-FLOW RICE DRYER WITH GRAIN INVERTERS. Transactions of the ASAE **61**:1757–1765. Available from https://doi.org/10.13031/trans.12927.

Puerta GI. 1999. Influencia del proceso de beneficio en la calidad del cafe. Cenicafe **50**:78–88.

Ramirez-Gómez CA, Oliveros-Tascón CE, Roa-Mejía G. 2002. Construya El Secador Solar Parabólico. Cenicafé - Centro Nacional de Investigaciones de Café, Avances Técnicos:1–8.

Renaudo CA, Bertin DE, Bucalá V. 2019. Design Impact on Airflow Patterns in Fluidization Units. Chemical Engineering and Technology **42**:2365–2375.

Rendón JR. 2021. Producción de café variedad Castillo® en altas densidades de siembra con uno y dos tallos por sitio. Revista Cenicafé **72**:e72106.

Restrepo Victoria AH, Burbano Jaramillo JC. 2005. DISPONIBILIDAD TÉRMICA SOLAR Y SU APLICACIÓN EN EL SECADO DE GRANOS. Scientia Et Technica **1**.

Richardson CW. 1981. Stochastic simulation of daily precipitation, temperature, and solar radiation. Water Resources Research **17**:182–190.

Rodríguez-Robles F, Monroig-Saltar F. 2014. Parametric Thermodynamic Models of Parchment Coffee Beans during HARC2S Dehydration. Journal of Food Processing & Technology **05**:1–7.

Rodríguez Valencia N, Antonio D, Franco Z. 2010. Los subproductos del cafe: Fuente de energia renovable. Avances Técnicos Cenicafé **393**. Available from https://doi.org/10.38141/10779/0393.

Rueda X, Thomas NE, Lambin EF. 2014. Eco-certification and coffee cultivation enhance tree cover and forest connectivity in the Colombian coffee landscapes. Regional Environmental Change **15**:25–33.

Sandeep TN, Channabasamma BB, Gopinandhan TN, Nagaraja JS. 2021. The effect of drying temperature on cup quality of coffee subjected to mechanical drying. Journal of Plantation Crops **49**:35–41.

Sanghi A, Ambrose RPK, Maier D. 2018. CFD simulation of corn drying in a natural convection solar dryer. Drying Technology **36**:859–870. Taylor & Francis. Available from https://doi.org/10.1080/07373937.2017.1359622.

Siagian P, Setyawan EY, Gultom T, Napitupulu FH, Ambarita H. 2017. A field survey on coffee beans drying methods of Indonesian small holder farmers. IOP Conference Series: Materials Science and Engineering **237**.

Silva GM da, Ferreira AG, Coutinho RM, Maia CB. 2021. Energy and exergy analysis of the drying of corn grains. Renewable Energy **163**:1942–1950. Elsevier Ltd.

Simate I. 2003. Optimization of mixed-mode and indirect-mode natural convection solar dryers. Renewable Energy **28**:435–453. Available from https://linkinghub.elsevier.com/retrieve/pii/S0960148102000411.

Sonthikun S, Chairat P, Fardsin K, Kirirat P, Kumar A, Tekasakul P. 2016. Computational fluid dynamic analysis of innovative design of solar-biomass hybrid dryer: An experimental validation. Renewable Energy **92**:185–191. Elsevier Ltd.

Tarzia A, dos Santos Scholz MB, de Oliveira Petkowicz CL. 2010. Influence of the postharvest processing method on polysaccharides and coffee beverages. International Journal of Food Science and Technology **45**:2167–2175.

Tesfaye A, Workie F, Kumar VS. 2022. Production and Characterization of Coffee Husk Fuel Briquettes as an Alternative Energy Source. Advances in Materials Science and Engineering **2022**.

Trejos RA, Roa-Mejía G, Oliveros-Tascón CE. 1989. Humedad de equilibrio y calor latente de vaporización del café pergamino y del café verde. Revista Cenicafé **40**:5–15. Available from https://biblioteca.cenicafe.org/handle/10778/841.

Tun MM, Raclavská H, Juchelková D, Růžičková J, Šafář M, Štrbová K, Gikas P. 2020. Spent coffee ground as renewable energy source: Evaluation of the drying processes. Journal of Environmental Management **275**.

Udomkun P, Romuli S, Schock S, Mahayothee B, Sartas M, Wossen T, Njukwe E, Vanlauwe B, Müller J. 2020. Review of solar dryers for agricultural products in Asia and Africa: An innovation landscape approach. Journal of Environmental Management **268**:110730. Elsevier Ltd. Available from https://doi.org/10.1016/j.jenvman.2020.110730.

Wahyuni NLE, Rispiandi R, Hariyadi T. 2020. Effect of bean maturity and roasting temperature on chemical content of robusta coffee. IOP Conference Series: Materials Science and Engineering **830**:022019. Available from https://iopscience.iop.org/article/10.1088/1757-899X/830/2/022019.

Weigler F, Scaar H, Mellmann J. 2012. Investigation of Particle and Air Flows in a Mixed-Flow Dryer. Drying Technology **30**:1730–1741.

List of Appendices

Annex A. Climatic Data During the Hybrid Solar Dryer's Evaluation.

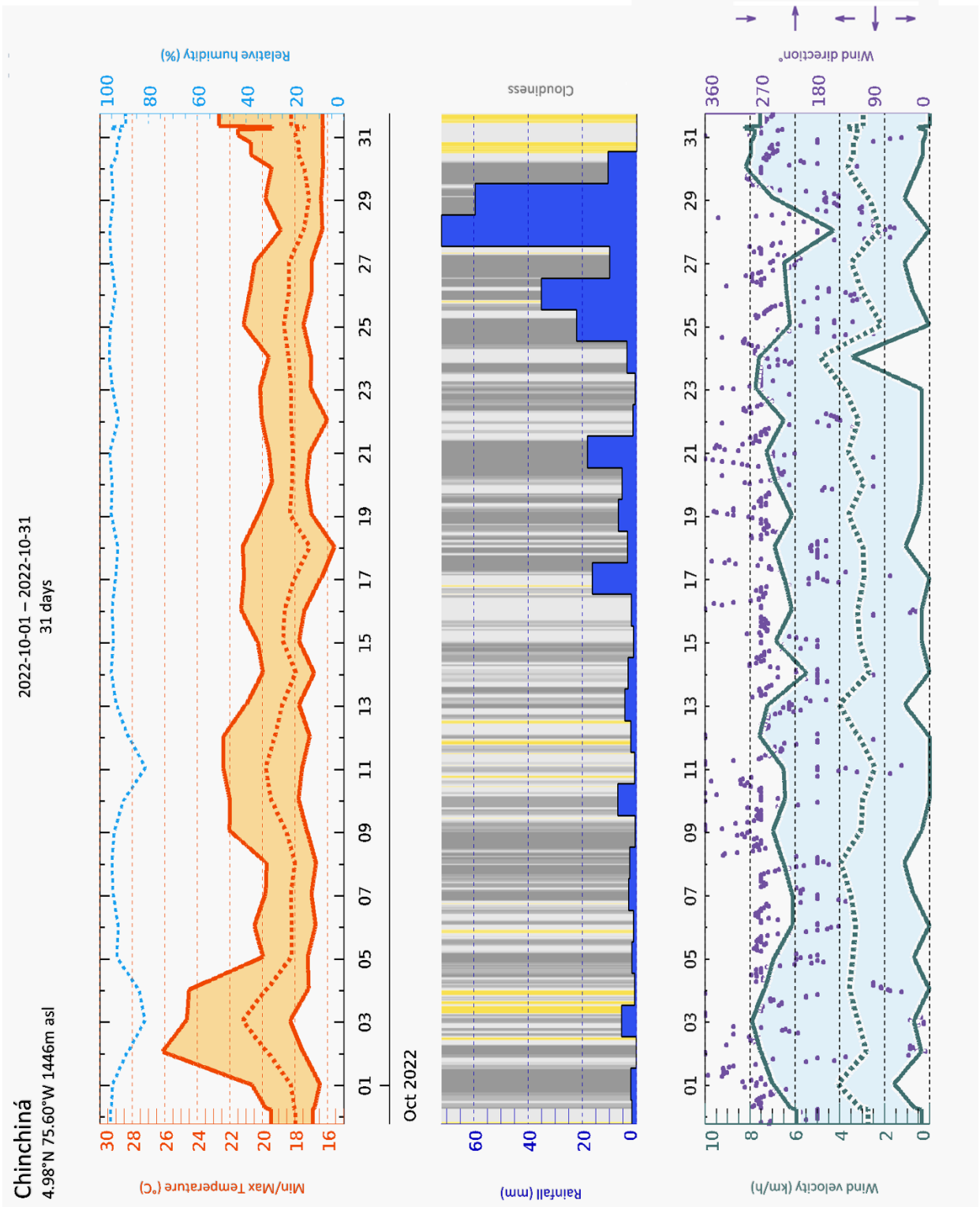

Figure 1. Climatic data in Chinchiná – October 2022.

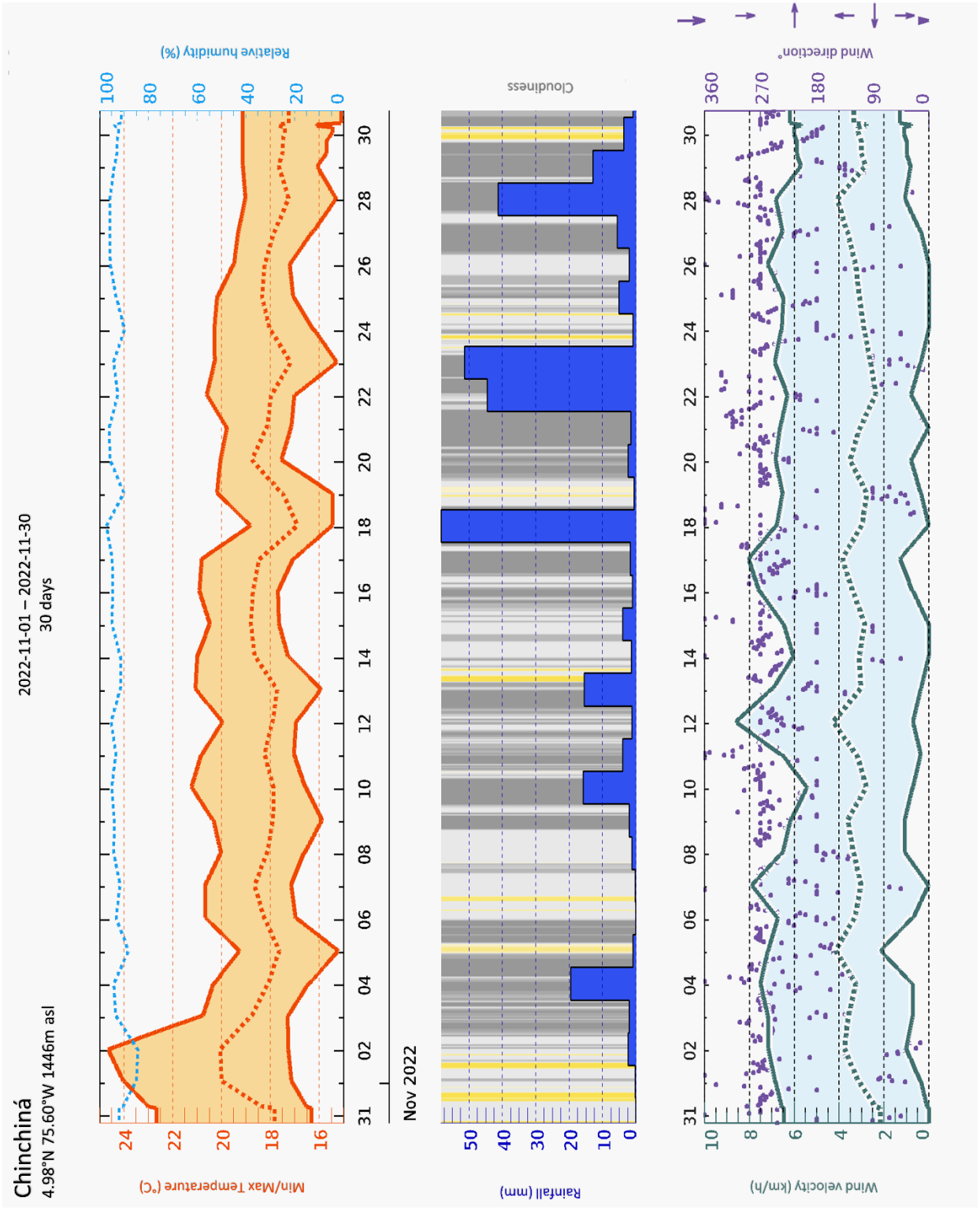

Figure 2. Climatic data in Chinchiná – November 2022.

Annex B. List of Publications.

Duque-Dussán, E., Figueroa-Varela, P.A., & Sanz-Uribe, J. R. (2023). Peaberry Shape and Size Influence on Different Coffee Postharvest Processes. Journal of Food Process Engineering, e14461. https://doi.org/10.1111/jfpe.14461

Duque-Dussán, E., Sanz-Uribe, J. R., & Banout, J. (2023). Design and evaluation of a hybrid solar dryer for postharvesting processing of parchment coffee. Renewable Energy, 215(March), 118961. https://doi.org/10.1016/j.renene.2023.118961

Duque-Dussán, E., Sanz-Uribe, J. R., Dussán-Lubert, C., & Banout, J. (2023). Thermophysical properties of parchment coffee: New Colombian varieties. Journal of Food Process Engineering, December 2022, 1–13. https://doi.org/10.1111/jfpe.14300

Duque-Dussán, E., & Banout, J. (2022). Improving the drying performance of parchment coffee due to the newly redesigned drying chamber. Journal of Food Process Engineering, 45(12). https://doi.org/10.1111/jfpe.14161

Duque-Dussán, E., Villada-Dussán, A., Roubík, H., & Banout, J. (2022). Modeling of Forced and Natural Convection Drying Process of a Coffee Seed. Journal of the ASABE, 65(5), 1061–1070. https://doi.org/10.13031/ja.15156

Cardona, C. I., Tinoco, H. A., Perdomo-Hurtado, L., Duque-Dussan, E., & Banout, J. (2022). Computational Fluid Dynamics Modeling of a Pneumatic Air Jet Nozzle for an application in Coffee Fruit Harvesting. 2022 International Conference on Electrical, Computer and Energy Technologies (ICECET), July, 1–7. https://doi.org/10.1109/ICECET55527.2022.9872877

Eduardo Duque Dussán

MECHANICAL AND CHEMICAL ENGINEER

Details

K Dolum 73/95, Prague, Czech Republic
725516314
eduardo.duque.dussan@gmail.com

Links

ResearchGate

LinkedIn

Website

Software

Solidworks

Ansys

COMSOL Multiphysics

Microsoft Office

Matlab

AutoCAD

Languages

Spanish

English

Czech

Portuguese

German

Hobbies

Reading, writing, art, football, scuba diving, trekking, judo, and gardening.

Employment History

Scientific Researcher at Faculty of Tropical AgriSciences CZU, Prague

SEPTEMBER 2020 — PRESENT

- Research and science in waste management technology design.
- Mechanical engineering with technical drawings and documentation.
- Development projects and teaching.
- Expertise in food drying technologies and food characterization.

Catedratic Lecturer at Universidad de Caldas, Manizales

NOVEMBER 2019 — NOVEMBER 2022

Lecturer of Fluid Mechanics, Mechanical Design, Mechanisms and Dynamics in the Mechatronics Engineering programme.

Discipline Engineer at Bilfinger Tebodin, Prague

AUGUST 2020 — AUGUST 2022

- Piping design for different industries (food, chemical automotive, petrochemical, etc.) and plant layout generation.
- Planning and monitoring engineering and other design activities.
- Advise internal and external customers regarding design, costs, and planning to achieve a better design.
- Projects: Clariant Sunliquid (Bioethanol plant – Romania); Umicore (Cathode materials plant – Poland); Net4Gas (Gasoduct – Czech Republic); Viterra (Canola Oil Plant – Czech Republic); Doosan ECube (Copper thin foil plant – Hungary); Huntsman Falcon (Biorefinery – Hungary); Mondelez - Bosch (Milka Production line Re-Design – Germany, Austria, and Switzerland).

Senior Design Engineer at Herragro S.A., Manizales

AUGUST 2019 — AUGUST 2020

- Design of dies, stamps, and press parts for the hot forging process.
- Design and develop new products and projects in R&D.
- Precision parts design for the automotive and military industries.
- Design of processes, equipment and machinery aimed at the efficiency and economic savings of the company.
- Perform the finite element analysis of the forging process on new or redesigned products.

Discipline Designer at Bilfinger Tebodin, Prague

JULY 2018 — JULY 2019

- Support the mechanical department in all the projects from the mechanical engineering and process engineering point of view.
- Perform specific tasks related to process engineering, such as equipment design, PFD and P&ID creation, process design, etc.

Design Engineer at TOTPEC S.A., Manizales

JUNE 2016 — SEPTEMBER 2017

- Responsible for developing new projects to improve the fibre cement sheet production process.
- Support the maintenance department by redesigning machinery and drawing technical blueprints of equipment for fabrication.
- Responsible for generating projects (over $10M) and executing them by the means of the PMI standards and PMBOK.

Services Engineer at Buencafé Liofilizado de Colombia, Chinchiná

JANUARY 2016 — JUNE 2023

- Develop innovative processes in the service area of the freeze-dried coffee plant.
- In charge of the service area, including the Wastewater treatment plant, steam generation plant, absorption and compression refrigeration plants, toaster, and green coffee silos.

- In charge of executing projects willing to increase the energy efficiency in the whole steam line of the factory.

Design and Maintenance Engineer at Básculas y Suministros S.A.S, Manizales

JULY 2015 — JANUARY 2016

- In charge of the mechanical design area: design new weighing and dosing elements such as scales, gauges, hoppers, and machinery in general for related applications in the industry.
- Supervise the assembly, installation and maintenance of the equipment requested by the client.

Maintenance Chief at Constructora CGM, Manizales

FEBRUARY 2014 — MARCH 2015

- Design maintenance routines for construction equipment and keep them up to date as well for supervising maintenance procedures.
- Direct the construction schedule for civil works and the design, execution, and control of projects.
- Advise, inspect, and verify the installation and maintenance of equipment for civil construction in the construction of the building "Portal de Campo Hermoso".

Education

PhD Sustainable Technologies, Czech University of Life Sciences, Prague

SEPTEMBER 2020 — NOVEMBER 2023

Thesis: Design and Evaluation of a Hybrid Solar Tunnel Dryer for Parchment Coffee in Colombia

MBA, ESNECA Business School, Madrid

JANUARY 2020 — OCTOBER 2021

MSc Process Engineering, Czech Technical University, Prague

SEPTEMBER 2017 — JUNE 2019

Thesis: Coffee Beans Dryer for Decentralized Purposes

Mechanical Engineer, Universidad Autónoma de Manizales, Manizales

JULY 2010 — JUNE 2016

Thesis: Energy Efficiency Evaluation of the Manufacturing Companies from Central-Southern Caldas.

Certifications

- Mechanical Design Professional (CSWP)- Solidworks.
- Professional: Advanced Surfaces, Weldments, Drawing Tools, Sheet Metal - Solidworks.
- Project Management - International Business Management Institute, Berlin.

Scientific Activities

Publications

Duque - Dussán, E., Figueroa-Varela, P.A., & Sanz-Uribe, J. R. (2023). *Peaberry Shape and Size Influence on Different Coffee Postharvest Processes. Journal of Food Process Engineering*, Accepted on 10.09.2023: in press.

Duque - Dussán, E., Sanz-Uribe, J. R., & Banout, J. (2023). *Design and evaluation of a hybrid solar dryer for postharvesting processing of parchment coffee.* Renewable Energy, 215(March), 118961. https://doi.org/10.1016/j.renene.2023.118961

Duque - Dussán, E., Sanz-Uribe, J. R., Dussán-Lubert, C., & Banout, J. (2023). *Thermophysical properties of parchment coffee: New Colombian varieties.* Journal of Food Process Engineering, December 2022, 1–13. https://doi.org/10.1111/jfpe.14300

Duque - Dussán, E., & Banout, J. (2022). *Improving the drying performance of parchment coffee due to the newly redesigned drying chamber.* Journal of Food Process Engineering, 45(12). https://doi.org/10.1111/jfpe.14161

Duque - Dussán, E., Villada-Dussán, A., Roubík, H., & Banout, J. (2022). *Modeling of Forced and Natural Convection Drying Process of a Coffee Seed.* Journal of the ASABE, 65(5), 1061–1070. https://doi.org/10.13031/ja.15156

Cardona, C. I., Tinoco, H. A., Perdomo-Hurtado, L., **Duque - Dussan, E.**, & Banout, J. (2022). *Computational Fluid Dynamics Modeling of a Pneumatic Air Jet Nozzle for an application in Coffee Fruit Harvesting.* 2022 International Conference on Electrical, Computer and Energy Technologies (ICECET), July, 1–7. https://doi.org/10.1109/ICECET55527.2022.9872877

Conferences

Thermophysical properties of Coffee: New Colombian Varieties. Scientific Seminars, National Coffee Research Center of Colombia (Cenicafé). April 24, 2023, Manizales, Colombia.

Using Image Analysis and Finite Element Methods to Study the Linear Heat Transfer in Parchment Coffee Drying. ELLS Conference. Sept 2022. Prague, Czech Republic.

Coffee Bean Drying Shrinkage Comparison by Finite Element Simulations and Real Image Processing. Tropentag Conference September 22, 2022. Prague, Czech Republic.

Computational Fluid Dynamics Modeling of a Pneumatic Air Jet Nozzle for an Application in Coffee Fruit Harvesting. International Conference on Electrical, Computer and Energy. 20-22 July 2022, Prague, Czech Republic.

Using Vetiver Grass Wetlands for Improved Coffee Wet Processing Wastewater Treatment. International Scientific and Advanced Conference: "PROSPECTS OF BIOENERGY CROPS FEEDSTOCK PRODUCTION ON RECLAIMED MINE LANDS" 23-24 June 2022, Dnipro, Ukraine.

Drying Process Improvement of a Cacao Beans Hybrid Solar Dryer. CASEE Conference "Sustainable agriculture in the context of climate change and digitalization" 22-24 June 2022, Prague, Czech Republic.

Effects of Different Drying Methods on Organoleptic Properties of Traditional Vietnemese Beef and Buffalo Jerky. 2nd MULTIDISCIPLINARY CONFERENCE "Sustainable Development Trends and Challenges under COVID-19" 29-30 November 2021, Sumy, Ukraine.

Coffee Seed Drying Predictive Finite Element Model. 2nd MULTIDISCIPLINARY CONFERENCE "Sustainable Development Trends and Challenges under COVID-19" 29-30 November 2021, Sumy, Ukraine.

Solar Drying Applications in Conventional Vietnamese Beef Jerky Preparation. Green (r)evolution: from molecules to ecosystems. ELLS Conference 2021. 19-20 November 2021, Warsaw, Poland.

A Review about Induced Polyploidization in the Medicinal Species of the Lamiaceae Family. IX COLAPLAMED Latin American Congress of Medicinal Plants. 13-15 October 2021, Quito, Ecuador.

Operational Improvement of a Convective Coffee Dryer by Numerical Methods and Computational Fluid Dynamics. Tropentag 2021 Conference. 15-17 September 2021, Hohenheim, Germany.

Development Projects

Novel Systemic Advisory Tool to Reduce Food Loss and Waste in Cambodia (NOSATOR-FLOW). Target country: Cambodia. Responsibilities: Machine design for food processing, chemical engineering expert, project manager.

Higher Himalaya*.* Target country: Nepal. Responsibilities: YCRAC Scientific Mentor, IAAS – FAO.

Through Biogas Technology towards Higher Resilience of Communities in Western Province of Zambia*.* Target country: Zambia. Responsibilities: Mechanical design and chemical engineering expert.

Strengthening scientific capacities and cooperation of Ukrainian universities in AgriSciences. Target country: Ukraine. Website www.agrisci-ua.com. Responsibilities: Mechanical design and chemical engineering expert.

Research Groups

Biogas Research Team – Faculty of Tropical AgriSciences, Czech University of Life Sciences.

Food Security - Faculty of Tropical AgriSciences, Czech University of Life Sciences.

Postharvest Technologies – National Coffee Research Centre (Cenicafé), Colombia.